BLAST EFFECTS ON PRESTRESSED CONCRETE BRIDGES

By

DEBRA SUE MATTHEWS

A thesis submitted in partial fulfillment of the requirements for the degree of

MASTER OF SCIENCE IN CIVIL ENGINEERING

WASHINGTON STATE UNIVERSITY
Department of Civil and Environmental Engineering

August 2008

To the Faculty of Washington State University:

The members of the Committee appointed to examine the thesis of DEBRA SUE MATTHEWS find it satisfactory and recommend that it be accepted.

_____
Chair

_____

_____

ACKNOWLEDGEMENTS

Thank you to the Federal Highway Administration
and Washington State Department of Transportation
for providing funding for this research.

Thank you to all the individuals at the Army Corps of Engineers
and the Transportation Technology Center
for all their hard work, especially
James Ray,
Chuck Ertle,
Sharon Garner,
and Ruben Peña.

Thanks to Karl Olsen and Harish Radhakrishnan
for their help with developing the model.

For all their patience and guidance, a gigantic thanks to
Dr. David McLean,
and Dr. William Cofer.

And of course, thanks to my family for tolerating
me through this stressful time.

BLAST EFFECTS ON PRESTRESSED CONCRETE BRIDGES

Abstract

Debra Sue Matthews, M. S.
Washington State University
August 2008

Chair: David I. McLean

Since the events of September 11th, more attention has been given to the effects of blast on structures. Bridges are especially important in this area due to their potentially critical role in the economy and for emergency response. Prestressed concrete bridges are very common, representing 40% of Washington's state bridges and 11% of state bridges nationwide. Despite this, very little is known about how prestressed concrete bridges respond to blast loading. A finite element model of a precast, prestressed girder was created and validated with two empirical tests. It was found that for an explosive event above or below the girder, analytical and empirical results were consistent.

The girder model was expanded to a four-girder, simple-span bridge model. Four different scenarios were examined at the midspan of the bridge: a blast between two girders both above and below the deck, and a blast centered on a girder both above and below the deck. For the two load cases from above, a TNT equivalent of 250 pounds at a four-foot standoff distance was investigated. This load resulted in highly localized damage with the possibility for other sections of the bridge to be immediately reopened after the event. For the two load cases from below, a TNT equivalent of 500 pounds at a ten-foot standoff distance was investigated. Results indicate that the slab will be heavily damaged but the girders will remain intact.

TABLE OF CONTENTS

TABLE OF FIGURES

CONVERSION FACTORS

ENGLISH TO SI (METRIC) UNITS OF MEASUREMENT

MULTIPLY	BY	TO OBTAIN
Pounds	0.454	Kilograms
Inches	2.54	Centimeters
Feet	0.3048	Meters
Pounds (force) per square inch	0.006895	Megapascals

CHAPTER 1: INTRODUCTION

Since the events of September 11th 2001, engineers have focused more attention on blast resistant design strategies. Where this consideration has previously been reserved for military structures or buildings subject to accidental explosion, it is now being applied to more common structures. Since infrastructure can be critical to the economy and for emergency response, bridges especially are receiving more attention in this area.

Because blast effects on structures have only recently hit mainstream interest, there is still much to learn in this field. Also, because of the many variables involved in a blast event, it is difficult to conduct research that is widely applicable. Blast charge shape, size, standoff, and orientation all have significant effects on the load applied to the structure. Most of the existing research is targeted towards buildings. Within that research very little information exists for prestressed concrete specifically.

Prestressed concrete bridges are very common. In Washington, nearly 3000 of the state-owned bridges are of this construction type. This represents nearly 40% of the bridges. Across the nation, about 11% of bridges are prestressed concrete. This makes understanding the effects of blast on prestressed concrete a priority for the Federal Highway Administration and the Washington State Department of Transportation.

1.1 OBJECTIVES

The overall goals of this study are to investigate the effects of blast loadings on prestressed girder bridges using finite element analyses and to provide guidance for the

design and interpretation of explosive tests of prestressed girders. The explosive tests were performed in a separate study coordinated by the Washington State Department of Transportation through the national pooled-fund program. The specific objectives of the research at Washington State University in support of the overall project are as follows:

1. Evaluate the state of the art for blast analysis of precast, prestressed concrete girders and develop and validate modeling techniques for the blast analysis of bridge systems.
2. Characterize the expected response of precast, prestressed girder bridges to blast loadings.
3. Provide guidance on the expected level of damage for precast, prestressed girder bridges subjected to blast loadings.

CHAPTER 2: LITERATURE REVIEW

Traditionally blast resistant design strategies were reserved for military and government buildings. However, with recent events many engineers are now incorporating anti-terrorism measures into the design of a much wider variety of structures. Bridges especially require special consideration because the condition of transportation infrastructure can significantly affect the economy. The loss of a critical bridge could result in economic damage not only on a local level, but possibly on a national or global level. Much of the knowledge about blast effects on structures is based on buildings. In the past, focus was placed on protecting government and military facilities from blast as well as designing for accidental explosions in chemical facilities. Thus, there is a need to understand how bridges respond to blast loads. In particular, very little is known about the blast response of prestressed concrete.

Work has been done by Marchand, Williamson and Winget to develop new design procedures for bridges to assess and mitigate terrorism risks (Marchand, Williamson & Winget, 2004; Winget, Marchand & Williamson, 2005). Using BlastX and uncoupled single-degree-of-freedom (SDOF) dynamic analysis, they analyzed a prestressed concrete, multiple span bridge. BlastX calculates pressures due to blast load, accounting for blast size, standoff distance, and wave reflection. They concluded that bridge geometry and blast standoff and location significantly affect response. Explosions below the deck may result in more damage due to the reflection of blast waves in confined spaces between girders or near abutments. As waves are reflected in these confined areas, pressures are magnified. Also peak pressures are greatly reduced as standoff is increased. However, there is a region for a blast scenario from below where decreasing the standoff results in less damage. This is due to a

phenomenon known as a Mach front. If an explosive charge is detonated below a bridge, the blast wave will reflect off the ground. Since the explosive event heats and compresses the air as it propagates, the reflected wave now traveling through this heated air travels faster than the incident wave. Thus, there is a region in which the reflected wave will merge with the incident wave and create pressures nearly twice as great. Moving the blast closer to the underside of the bridge then may allow the incident wave to hit the bridge before the reflected wave is able to merge with it.

An effective approach to bridge design would be to first assess the risks to a bridge and determine what is acceptable (Williamson & Winget, 2005). Once unacceptable risks are identified, a variety of methods may be used to reduce risk. In addition to hardening a structure, there are some less expensive options to reduce risk. These include restricting access, increasing standoff with barriers, controlling undergrowth to ensure clear line of sight, and using security cameras. Even more inexpensive would be placing fake cameras or an abandoned police vehicle in strategic locations.

Although there are no great works available describing the response of prestressed concrete to blast loads, there is some information on its response to impact. Ishikawa, et al. studied prestressed concrete beams used as rock-shed structures (Ishikawa, Enrin, Katsuki & Ohta, 1998; Ishikawa, Katsuki & Takemoto, 2000; Ishikawa, Katsuki & Takemoto, 2002). Bonded and unbonded prestressed beams were tested experimentally and analytically. It was found that while static loading resulted in failure of the compression concrete for both the bonded and unbonded specimens, the higher load rate induced by impact resulted in the breaking of the prestressed tendon. The change in failure mode was attributed to concrete's increased strength with increased load rate. In addition it was found that while both beams

had nearly the same static capacity, the ultimate displacement of the unbonded beam was twice that of the bonded beam. Lastly, the unbonded beam is able to absorb 2.4 times as much dynamic energy as the bonded beam. The breaking of the unbonded tendon occurred over a longer time than that of the bonded tendon. These experimental results were reproduced with simple models combining the sectional discrete element method and the rigid body spring method.

Compared to prestressed concrete, reinforced concrete has received much more attention from researchers over the years. Magnusson and Hallgren (2004) subjected 49 high strength reinforced concrete beams to air blast loading. Their study revealed that concrete beams show an increased load capacity for blast loading relative to static loading. The failure mechanism also changed for some beams between static and dynamic loading. Whereas all of the beams subjected to static loading failed in flexure, some of the beams subjected to air blast loading failed in shear. It was observed that high ratios of flexural reinforcement resulted in shear failures whereas beams with lower ratios of reinforcement failed in flexure. Thus it was seen that by reducing the flexural reinforcement or by increasing the shear strength, ductility was improved for air blast scenarios.

Watson, Hobbs, and Wright (1989) conducted experiments on T-beams and slabs. Since the wave speed perpendicular to the cylinder axis is greater than the wave speed along the axis, the orientation of the charge has an effect on damage. It was shown that shallow inclinations caused more damage than steeper ones. Greater contact area between the charge and the beam was also shown to result in greater damage.

Several different methods have been used to model reinforced concrete beams subjected to blast loads. Van Wees and Weerheijm (1989) found that finite element analysis

resulted in a good match to empirical results as long as strain rate effects are incorporated for concrete. Although finite element modeling takes more time and effort over a simpler and quicker SDOF analysis, it ultimately yields far more accurate results. Incorporating an accurate material model is crucial.

Fang, Qian, and Shi (1996) report that strain rate effects can have a significant impact on reinforced concrete beam capacities. Two analyses were conducted utilizing Timoshenko beam theory. The first utilized amplification of static properties to account for load rate while the second used a rate-sensitive material model. It was shown that amplification of static properties results in over-conservatism. It was concluded that strain-rate effects are significant and should be included with any model.

In contrast, Stevens and Krauthammer (1989) propose the use of a rate-independent material model for use with finite element analysis. Using a continuum Damage/Plasticity model with a Timoshenko beam element was found to yield results matching empirical data. The damage model accounted for strain softening and stiffness degradation due to micro-cracking. The plasticity model accounted for the pre-peak nonlinearity from frictional slip. Although creating a 3-D representation of micro-cracking requires a higher order damage variable, it is acceptable to treat damage as a scalar since its directionality is not a dominant feature in beams.

CHAPTER 3: MODELING TECHNIQUES

To investigate blast effects on precast, prestressed concrete girders, two finite element models were created: a simple-span single girder and a 4-girder, simple-span bridge. The single girder was created primarily for verification of the modeling technique while the full bridge model was used to extrapolate predictions of bridge response. Both models utilized solid elements, modeling the concrete and each individual piece of prestressing and mild reinforcement.

3.1 ELEMENTS

The girder section used for modeling was a Colorado Department of Transportation section. The bulb-tee section measured 3'-6" high with a 3'-7" wide top flange. Twenty 0.6 inch grade 270 strands provided the prestressing for the girder. Figure 3-1 shows a cross-section of the girder at midspan. Complete details for the section can be found in APPENDIX A. A span of 68'-4" was used for the model and experiments.

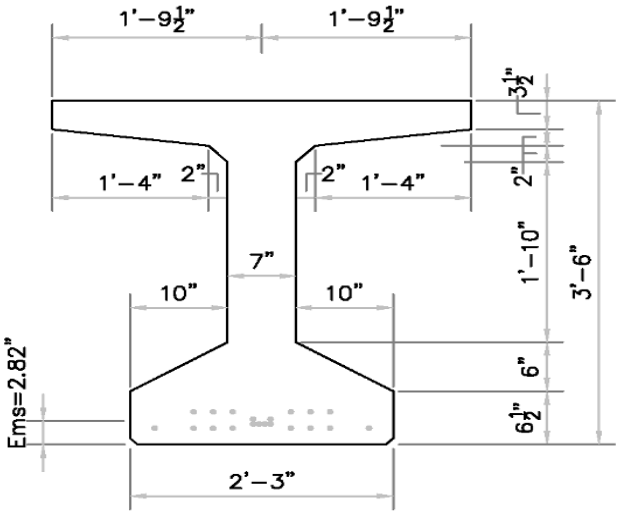

Figure 3-1: Girder Cross-Section at Midspan

The single girder, shown in Figure 3-2, was modeled in its entirety. A typical concrete element at the location of the blast was a 3 inch cube. Due to its capabilities, ABAQUS was selected as the best program in which to create and analyze the model. ABAQUS/Standard was used to determine the initial state of equilibrium due to prestressing. ABAQUS/Explicit was then used for all of the dynamic analyses. The model utilized 8-node continuum elements with reduced integration for the modeling of all concrete. Since hourglassing is a problem with this element, the built-in hourglass control was used. The reinforcing was modeled with 2-node, 3-D stress and displacement truss elements. These were constrained within the concrete elements.

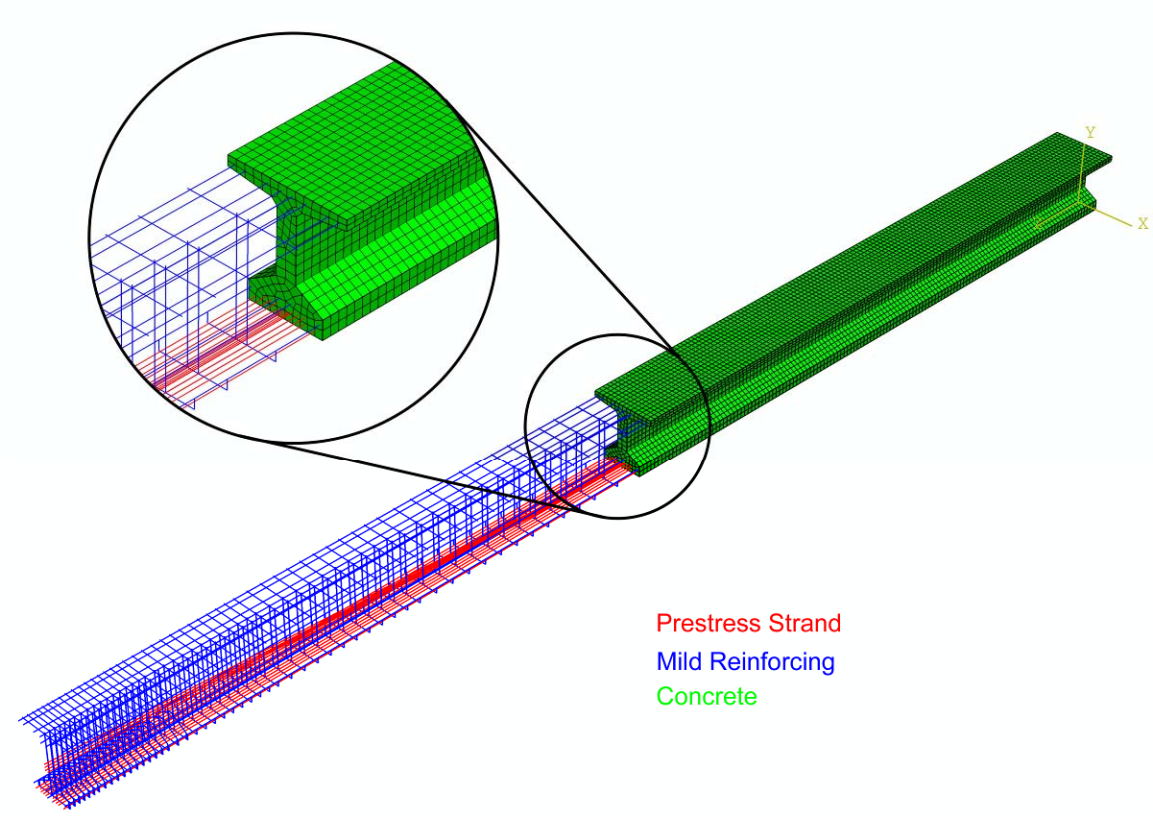

Figure 3-2: Single Girder Model

3.2 MATERIALS

Since ABAQUS/Standard and ABAQUS/Explicit include established and proven material models, these were used for the analysis. ABAQUS' concrete damaged plasticity model was used for all concrete. This model "is designed for applications in which concrete is subjected to monotonic, cyclic, and/or dynamic loading under low confining pressures." (Abaqus Analysis User's Manual, 18.5.3) Since the section is essentially completely unconfined, this material model is applicable. The plasticity model allows concrete's nonlinear properties to be described, while the damage model describes irreversible damage caused by crushing and cracking. Figure 3-3 shows the concrete properties programmed into ABAQUS. The dashed lines show the damaged modulus of elasticity.

The ends of the girder model were pin- and roller-supported effectively on a knife edge. This was simpler than modeling the actual bearing of the concrete on a polyurethane pad. As a result of this simplification, the material properties at the supports were adjusted to allow for elastic behavior. This is acceptable since the area of interest is at midspan.

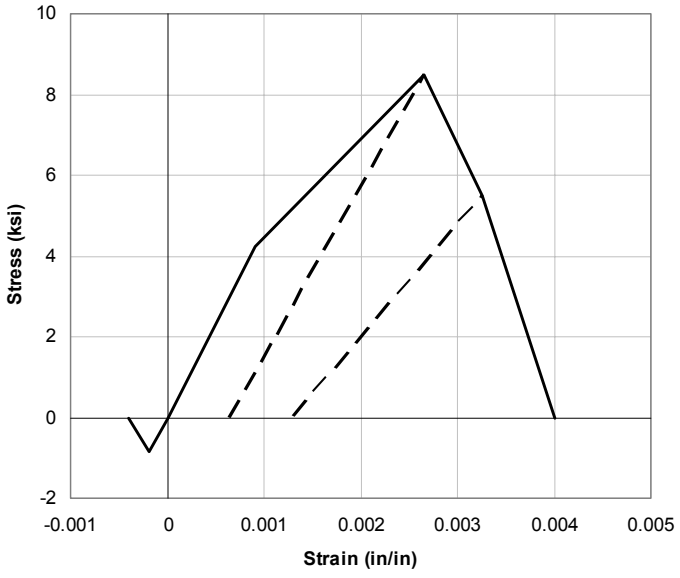

Figure 3-3: High-Strength Concrete Material Properties

The prestressing and mild reinforcement were modeled with simple elastic-plastic models. A damage parameter was also introduced to account for breaking of the strands or bars. Figure 3-4 and Figure 3-5 show the material properties used for the mild reinforcing and prestressing, respectively.

Although both of these material models allow for the introduction of strain rate effects, their properties are not well defined and including them caused severe numerical difficulties. Thus, it was determined that the model was sufficiently accurate without this. Model validation is discussed in the next chapter.

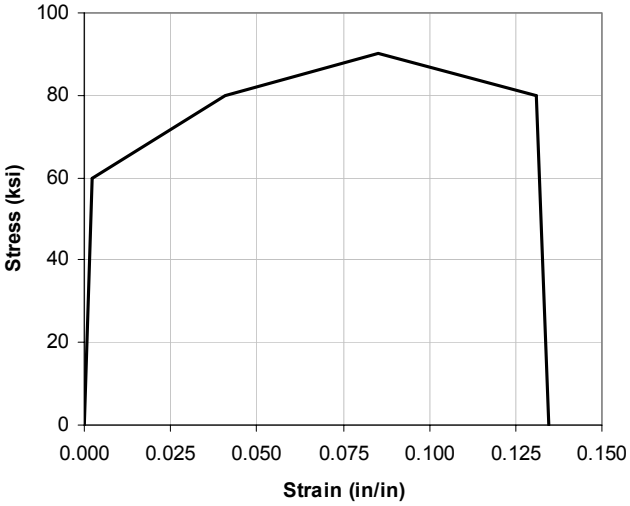

Figure 3-4: Mild Reinforcing Material Properties

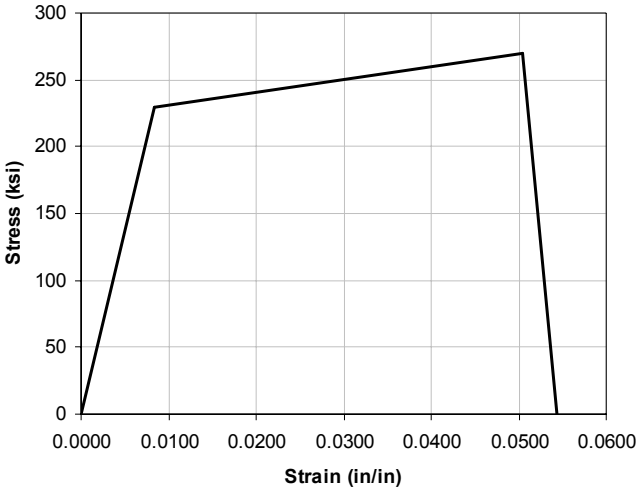

Figure 3-5: Prestressing Steel Material Properties

3.3 LOADING

To determine the pressures to be applied to the girder, Bridge Explosion Loading (BEL) was used. BEL is a software program developed by the US Army Corps of Engineers. Among other things, the program outputs pressure-time histories for a given

surface area, charge, and standoff. The pressures obtained from BEL were then applied to the model.

Within ABAQUS there is a feature that allows the user to input a peak pressure and then prescribe its spatial and temporal decay. Figure 3-6 shows the peak pressure over the girder as described by BEL and as applied in ABAQUS. Figure 3-7 shows the decay of pressure over time.

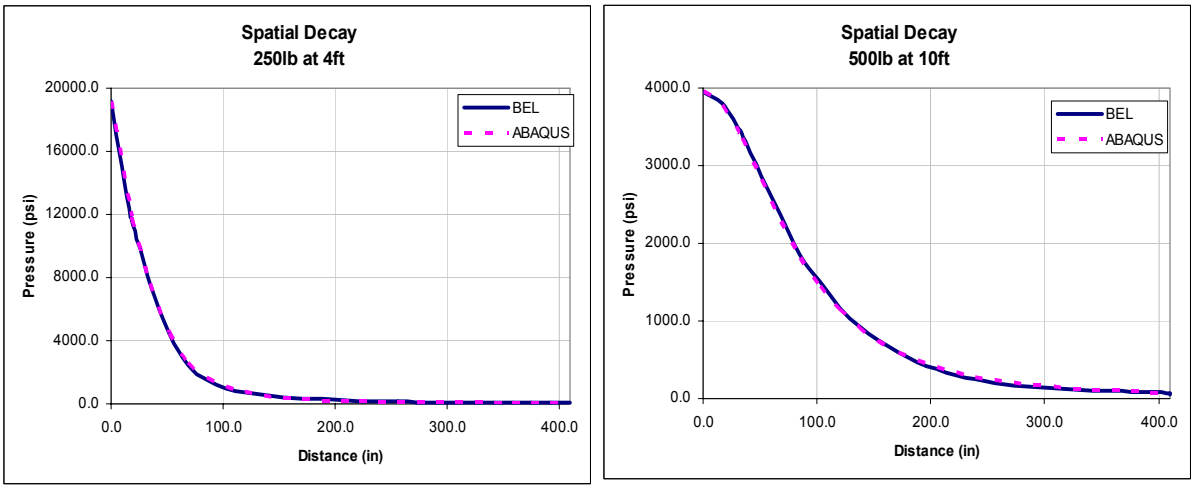

Figure 3-6: Peak Pressure

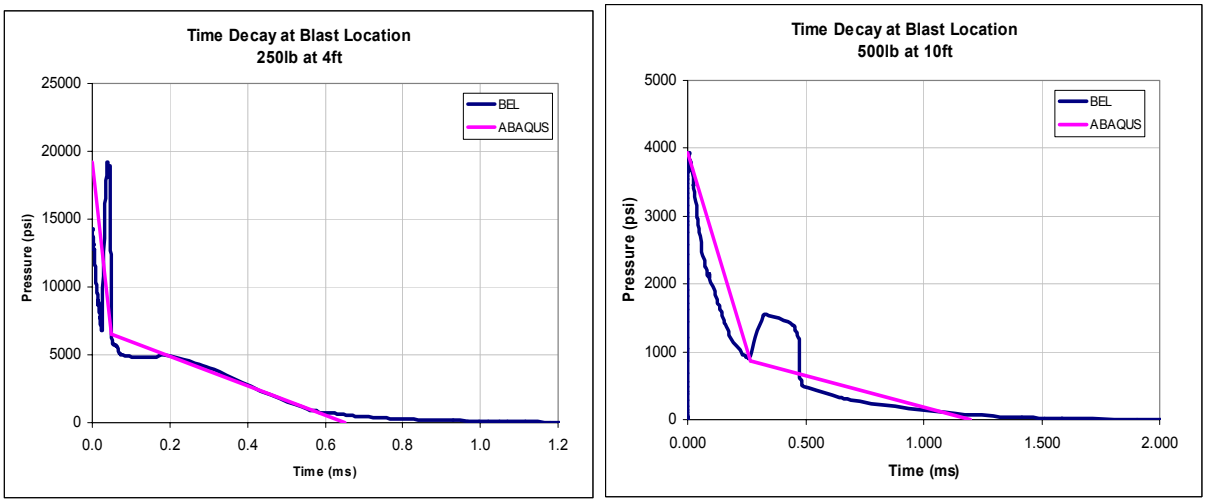

Figure 3-7: Pressure-Time History

3.4 BRIDGE MODEL

In contrast to the single girder, the bridge model utilized symmetry and included only half of the span in the model. The use of symmetry limited loading scenarios to blast events at the midspan of the bridge. This was necessary, however, due to the demand on the computer's memory. In addition to utilizing symmetry, it was also necessary to coarsen the meshing of the concrete. Elements near the location of the blast measured approximately 5.5x5x3.5 inches. These elements were kept as close to cubes as possible. Since no edge exceeded twice that of another edge, the mesh was deemed appropriate. The mesh was further optimized near the supports, resulting in elements measuring approximately 5.5x10x3.5 inches. Although these elements were not as ideally proportioned, they were far enough away from the area of interest that they were satisfactory. The bridge model is shown in Figure 3-8.

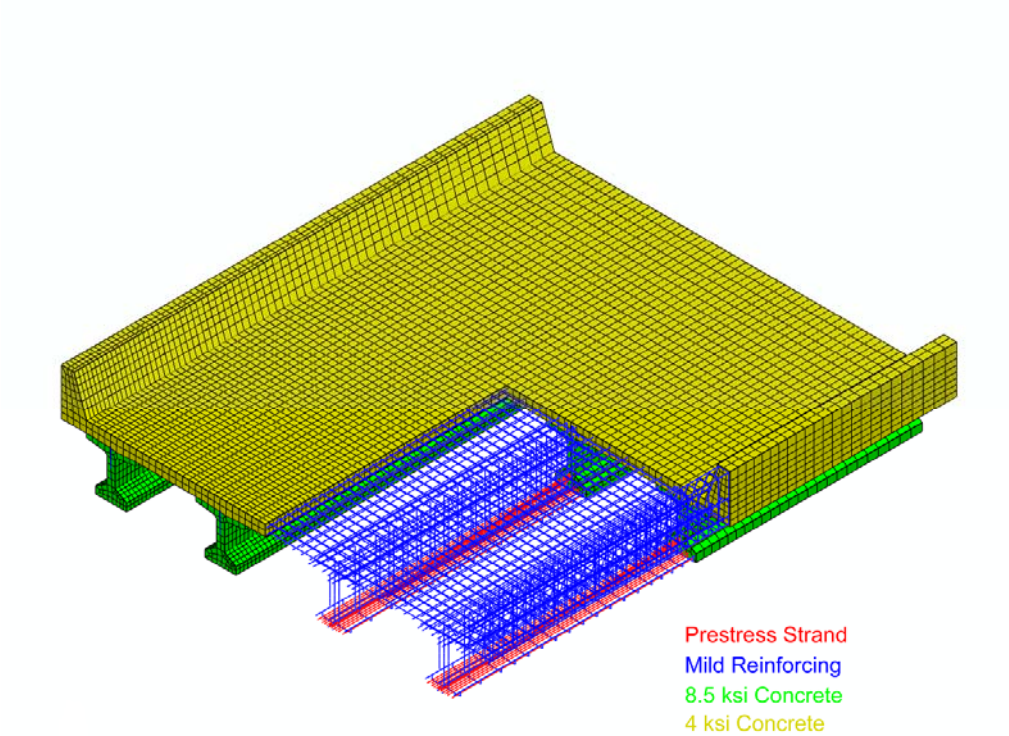

Figure 3-8: Bridge Model

No changes were necessary in the materials, although a lower strength concrete material was created for the deck. This material model is shown in Figure 3-9. Along the mirrored surface at midspan, all nodes were fixed out of plane. Since the reaction at this surface was evenly distributed over the cross-section, no stress concentrations were developed and so the correct material properties were used. The outer end of the bridge model remained roller-supported on a theoretical knife edge. Along with the appropriate increases in material strength to allow for elastic behavior at the supports, this avoided unwanted computational effort.

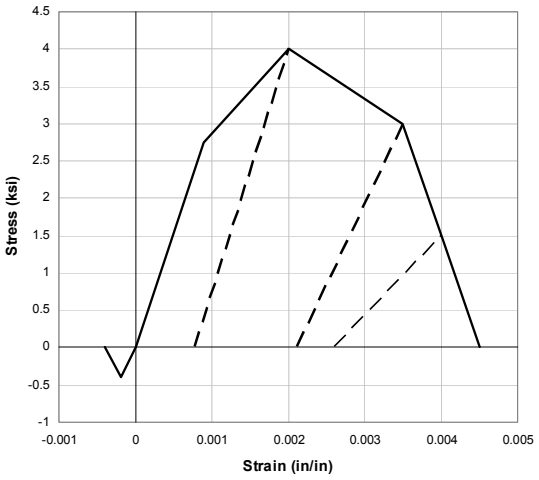

Figure 3-9: Slab Concrete Material Properties

Computer memory issues prevented the slab from being free of the prestressing force. The girder and bridge are both modeled as a mass of concrete and embedded prestressing strands with a given force. Difficulties arose when attempting to apply the prestressing to the girders alone, and then adding the slab afterward. Thus, the bridge model effectively has some prestressing in the slab. Acknowledging this effect, it is believed that the results derived from the model are reasonable.

Finally, the analysis time was set at 5 milliseconds with a prescribed step of 50 nanoseconds. The small time step was necessary to capture all of the behavior at the time of the blast. The 5 millisecond run time was the time it took for the blast wave to move across the bridge.

CHAPTER 4: MODEL VERIFICATION

To validate the model, two full-sized girders were exposed to blast loads. The experimental and analytical results were compared. Overall, the model was found to be adequate.

4.1 ANALYTICAL RESULTS

After completing the model, it was checked for reasonable results. First, the initial stress in the prestressing strand was examined. The girder was designed to have an initial prestressing force of 878.9 kips and a final force of 738.0 kips. It was discovered that inputting 878.9 kips as an initial force resulted in a final force that was too high. Therefore, the initial force in the prestressing strands was reduced such that the correct level of force was present after the girder settled into static equilibrium. This change is reasonable. In reality, there is some slippage and settling when prestressing is applied to a beam, resulting in some loss. Since ABAQUS treats the prestressing as in an ideal world, it makes sense that some prestressing loss must be manually included.

Next, deflections were examined. The static analysis resulted in an initial upward deflection at midspan of 0.958 in. The prescribed initial deflection given on the drawings for the girder was 2-1/8 inches at 90 days. Taking creep into account, the results from the model were determined to be acceptable.

4.2 EXPERIMENTAL RESULTS

On October 10th and 11th of 2007, two full-sized girders were exposed to blast loading at the Transportation Technology Center, Inc. in Pueblo, Colorado. Under the direction of personnel from the Engineer Research and Development Center of the US Army Corps of Engineers (Ertle, Ray, Walker & Johnson, 2008), two loading scenarios were executed: an explosion above the girder and an explosion below the girder.

Explosive charges and standoff distances were selected based on preliminary analytical results. The goal was to damage the girders enough to cause total failure, but not to destroy them to the point that little would remain for observation.

4.2.1 EXPLOSION ABOVE

For the loading from above scenario, the equivalent of 257 pounds of TNT was used. The analytical model was approximated as 250 pounds. The bottom of the charge was placed three feet above the girder. Accounting for the size of the charge, a standoff distance of four feet was used for the analysis. The container for the explosive fuel resulted in an approximately spherical blast wave, as was modeled in ABAQUS. Figure 4-1 shows the test setup for the girder.

Figure 4-1: Test Setup

Examination of the girder after the test indicated that a little over 3.5 feet of the top flange and web had been rubblized. Additionally, heavy cracking could be seen for about four or five feet on either side of the destroyed web. Figure 4-2 shows the damaged girder.

Figure 4-2: Damage from Blast Above, Experimental

Near the location of the blast, large 45° cracks were observed. There was also longitudinal cracking on the underside of the flange where it intersected with the web.

This cracking pattern is consistent with shear failure at the location of the blast. Due to the high pressures and rapid application, the pressure wave essentially punched through the girder. The longitudinal cracking also indicates localized flexure of the flange.

These observations are consistent with the finite element model. To determine areas of significant cracking, the maximum principal plastic strain parameter was examined. Strains exceeding 0.004 are associated with heavy cracking. This limit is equivalent to ten times the tensile cracking strain and thus represents large, highly visible cracks. To determine the extent of damaged concrete, minimum principal plastic strain was examined. A strain limit of -0.004 is associated with crushing of the concrete. The model shows about ten feet of damaged concrete. The extent of heavy cracking is similar. Localized bending of the flange is also observed in the model.

Figure 4-3 shows the model at the end of the pressure wave application (5 milliseconds). All material shown in grey indicates heavily cracked concrete (maximum principal plastic strain greater than 0.004). The removed elements are associated with rubblized concrete (equivalent plastic strain greater than 0.02). This limit was derived

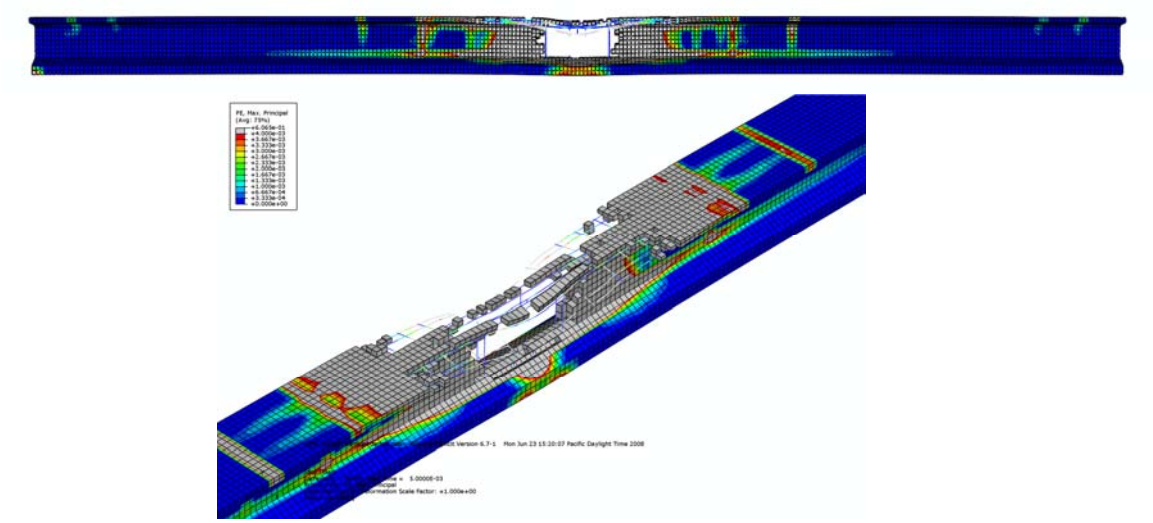

Figure 4-3: Maximum Principal Plastic Strain-Girder Blast Above

from observations of the actual blast tests.

Similarly, Figure 4-4 shows damaged concrete in black. The removed elements are based off of the same parameters as the previous figure.

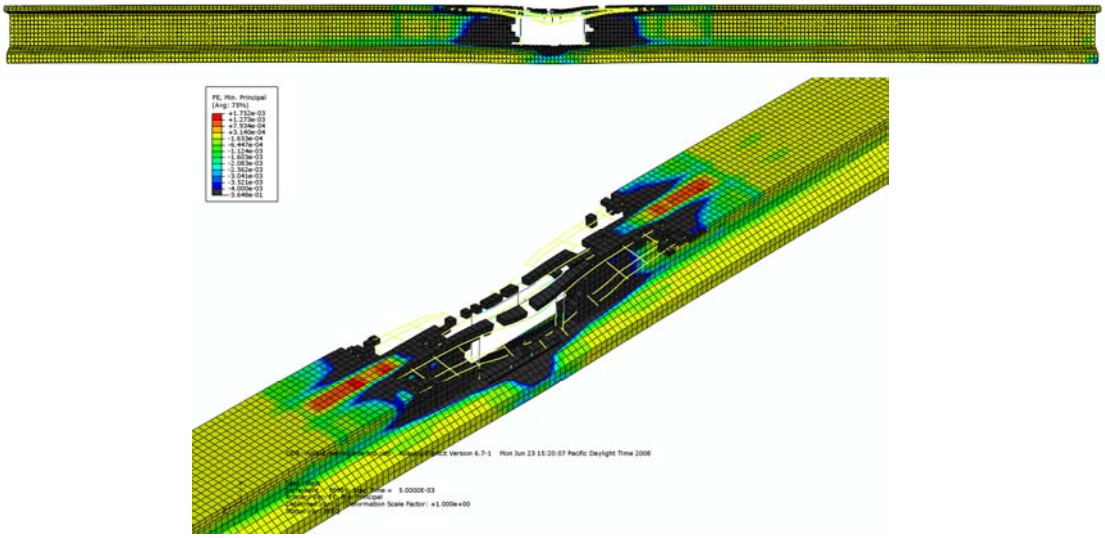

Figure 4-4: Minimum Principal Plastic Strain-Girder Blast Above

Examination of the damaged cross section revealed vertical cracks within the web (shown in Figure 4-5). Investigation of the direction of principal plastic strain within the model revealed the same type of cracking (shown in Figure 4-6).

Figure 4-5: Web Cracking-Blast Above, Experimental

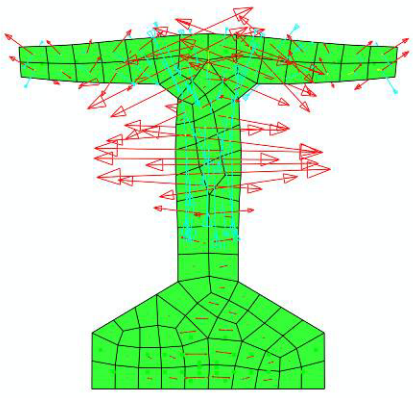

Figure 4-6: Web Cracking-Blast Above, Analytical

Thus, through similar levels of damage and similar directions of stress, the finite element model was deemed to be a reasonable match. Additionally, pressure sensors placed on top of the flange indicate that the pressure predictions from BEL are in good agreement with actual pressures (Ertle, et al., 2008). Figure 4-7 shows predicted and measured values from the test.

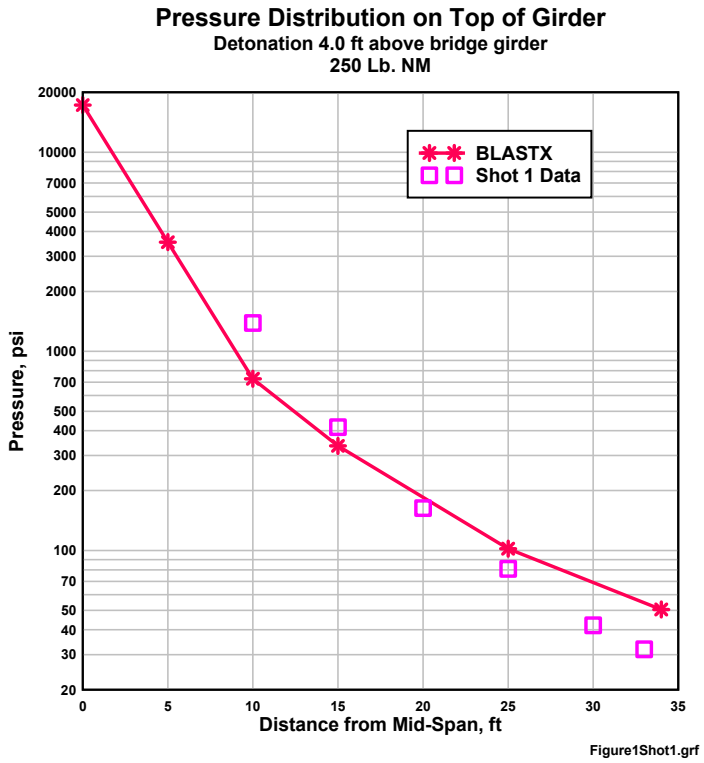

Figure 4-7: Pressure-Girder Blast Above (Ertle, et al., 2008)

Accelerometers were also placed on the test specimen. A peak acceleration of approximately 6.5e5 in/sec^2 was measured at ten feet from midspan. Within the finite element model, a peak acceleration of approximately 6.0e5 in/sec^2 was seen at the same location. These are very consistent results.

4.2.2 EXPLOSION BELOW

For the loading below scenario, the equivalent of 530 pounds of TNT at a standoff of about ten feet was used. The analytical model was approximated as 500 pounds. The container for the explosive fuel again resulted in an approximately spherical blast wave, as was modeled in ABAQUS. The girder setup was similar to the loading from above scenario except that additional plates were welded to the supports to hold the girder down. This is shown in Figure 4-8.

Figure 4-8: Explosion Below-End Support

Pressure sensors located on the girder once again measured the blast wave. This time however, there was a notable difference between predicted pressures and measured values. It was seen that the pressures obtained from BEL may be two or three times the actual value (Ertle, et al., 2008). This is shown in Figure 4-9. Thus, it is expected that the damage and cracking in the model should be greater than observed. It is noted here that BEL is intended for predicting

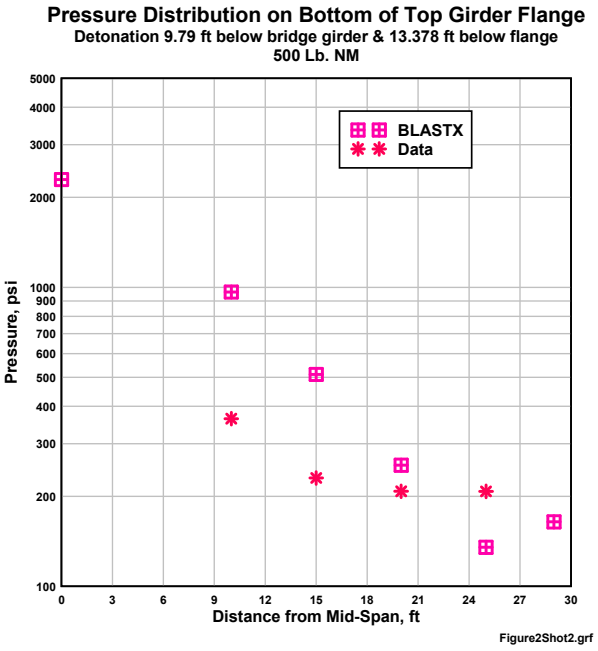

Figure 4-9: Pressure-Girder Blast Below (Ertle, et al., 2008)

pressures on the top of flat bridge decks. It does not have the capability to account for wave reflection off the ground. In addition, it cannot account for the complicated geometry below the bridge deck. Thus, it is not well suited to predicting pressures on anything other than a flat surface. However, it is the best tool available for this research.

Examination of the girder after the test indicated that less than a foot of the web had been rubblized, although a length of about nine feet was missing from the top flange. It is noted that the detached top flange may have been a result of the girder falling rather than an exclusive result of the blast wave. Additionally, heavy cracking could be seen for about 10 feet on either side of the destroyed web. Figure 4-10 shows the damaged girder.

Figure 4-10: Damage from Blast Below, Experimental

Near the location of the blast, large 45° cracks were again observed. These were oriented in the opposite direction of the blast from above scenario, as would be expected. This cracking pattern is consistent with shear failure at the location of the blast, similar to the first scenario. Longitudinal cracking was also observed in this case, but to a much larger degree than before. Figure 4-11 shows this cracking pattern.

Figure 4-11: Longitudinal Cracking at Web-Flange Intersection

These observations are consistent with the finite element model which shows heavy cracking through the middle third of the girder. Figure 4-12 shows maximum principal plastic strain. Figure 4-13 shows minimum principal plastic strain. Once again the grey is associated with heavy cracking while the black is associated with damaged concrete, respectively.

The damage in the model compares reasonably well to observed results, considering the difference between actual and predicted pressure. It is noted, however,

that in addition to the difference in pressure, ABAQUS/Explicit does not appear to be able to account for shadowing effects and wave reflection without modeling the fluid surrounding the girder. The pattern and amount of damage is still informative, however. It can be seen that the cracking at the web-flange intersection is shown all along the

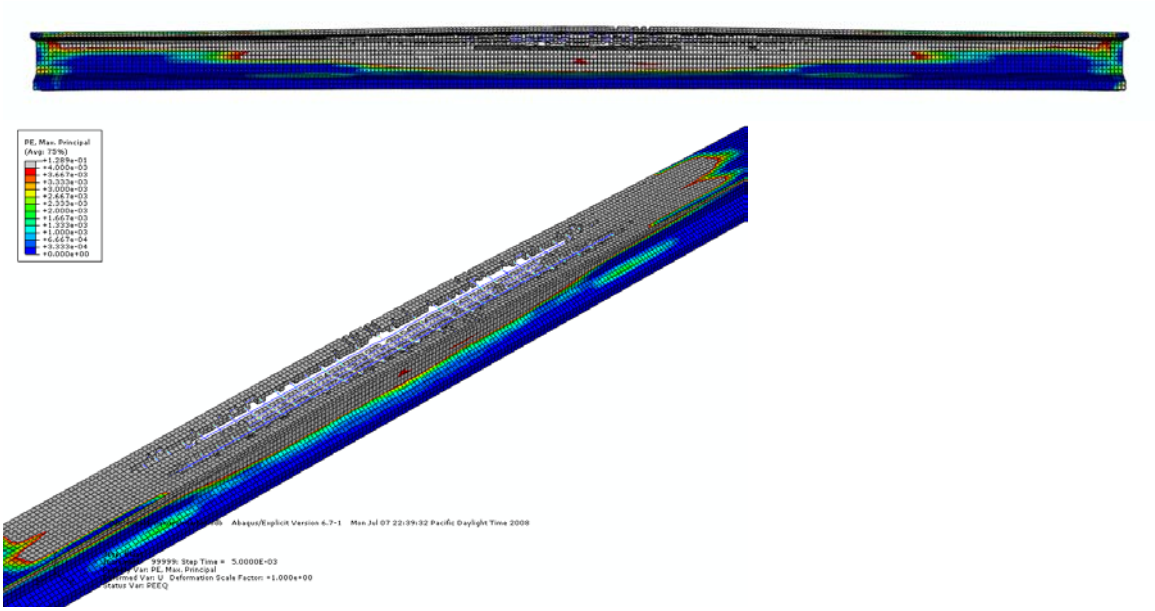

Figure 4-12: Maximum Principal Plastic Strain-Girder Blast Below

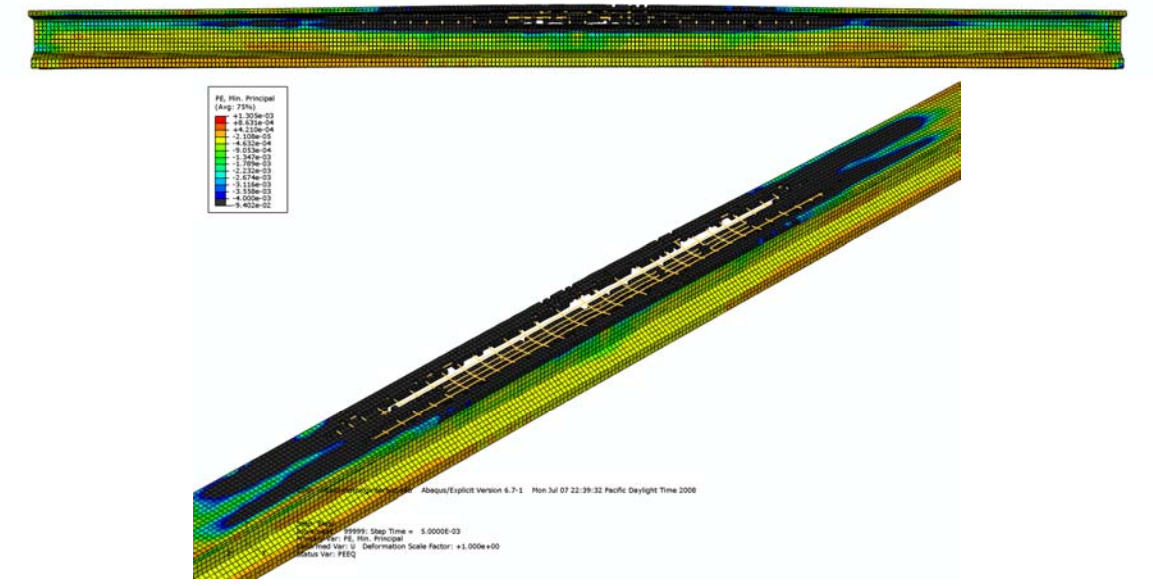

Figure 4-13: Minimum Principal Plastic Strain-Girder Blast Below

length of the girder. Although, the model shows rubblized concrete at this location, the results are acceptable considering the greater pressures applied to the model. The cracking all along the top of the web is consistent with the tests. Also, approximately 25 feet of cracking in the web can be seen in the model, similar to the 20 feet observed in the full-scale test.

Accelerometers were also placed on this specimen. Acceleration of the girder at ten feet from midspan was measured as approximately 7.5e6 in/sec^2. The finite element model shows a peak acceleration of 3.0e6 in/sec^2 at the same location. These values are not as consistent as the blast from above case, but they are of the same order of magnitude and thus reasonable. Overall, the model is acceptable.

CHAPTER 5: BRIDGE MODEL

Four different blast event scenarios were investigated using finite element analysis. The technique for applying pressure loading from the girder model was also used for the bridge investigation. Thus, using BEL to calculate the equivalent of 250 pounds of TNT at a standoff of four feet, a pressure wave was applied at midspan directly above the centerline between the two interior girders and at midspan directly above an interior girder. Then, using the equivalent of 500 pounds of TNT at a standoff of ten feet, a pressure wave was applied at midspan directly below the centerline between the two interior girders and at midspan directly below an interior girder.

5.1 BLAST ABOVE, BETWEEN GIRDERS

For the blast applied above the deck, centered between the interior girders, the model shows that the blast punches a hole in the deck slab but leaves the girders relatively undamaged. The exterior girders and traffic barriers show no significant damage. The interior girders show a small region of cracking along the girder web near the bulb. The slab itself is left with a hole measuring approximately four feet transversely and eight feet longitudinally. Heavy cracking is seen in an area spanning approximately eight feet transversely between the girders and about 16 feet longitudinally. This is shown in Figure 5-1.

Examining minimum principal plastic strain reveals that damaged concrete is limited to the slab. See Figure 5-2. Therefore, the girders should not see any significant reduction in strength, even the ones adjacent to the blast.

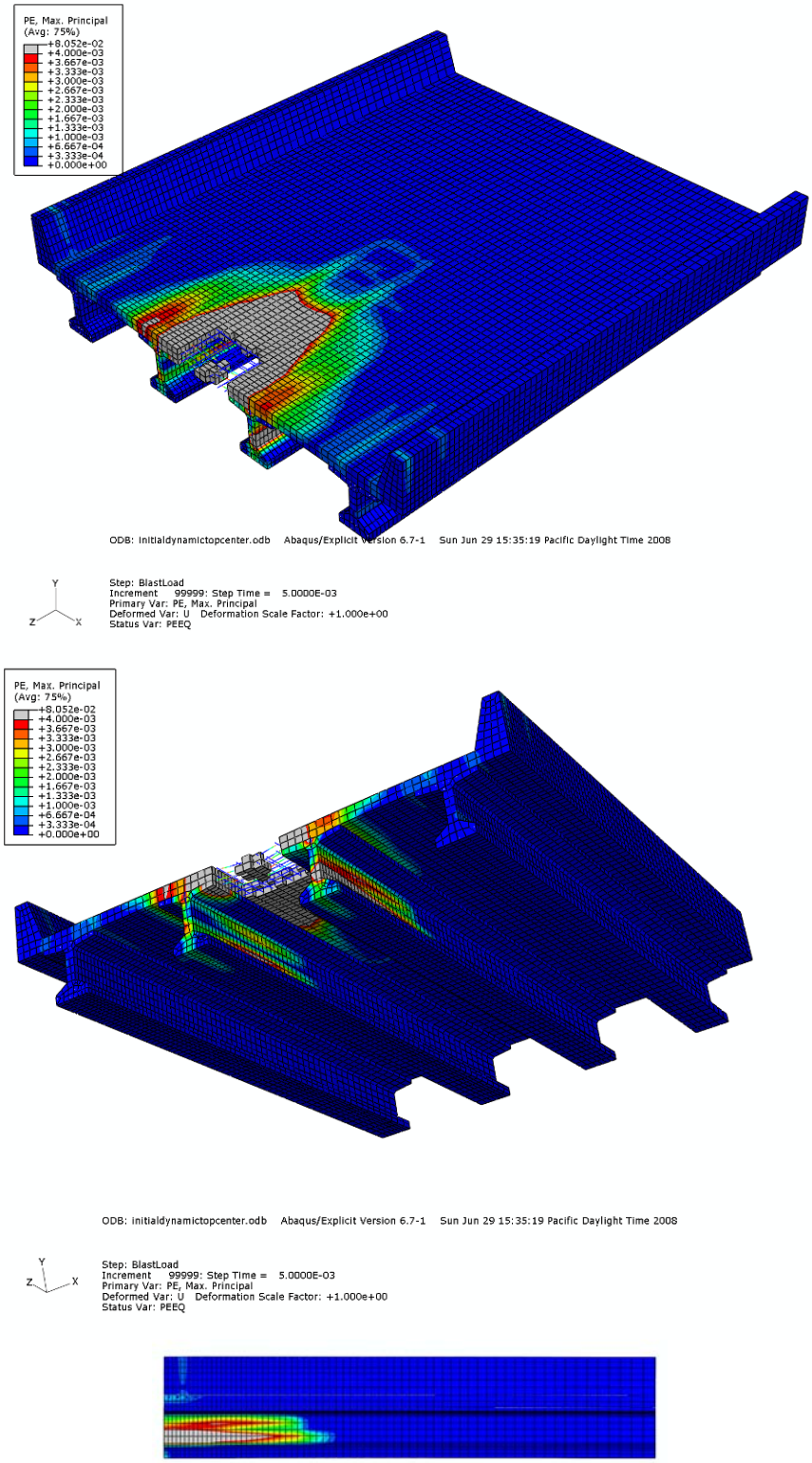

Figure 5-1: Maximum Principal Plastic Strain-Blast Above, Between Girders (Top View, Bottom View, Side View of Interior Girder)

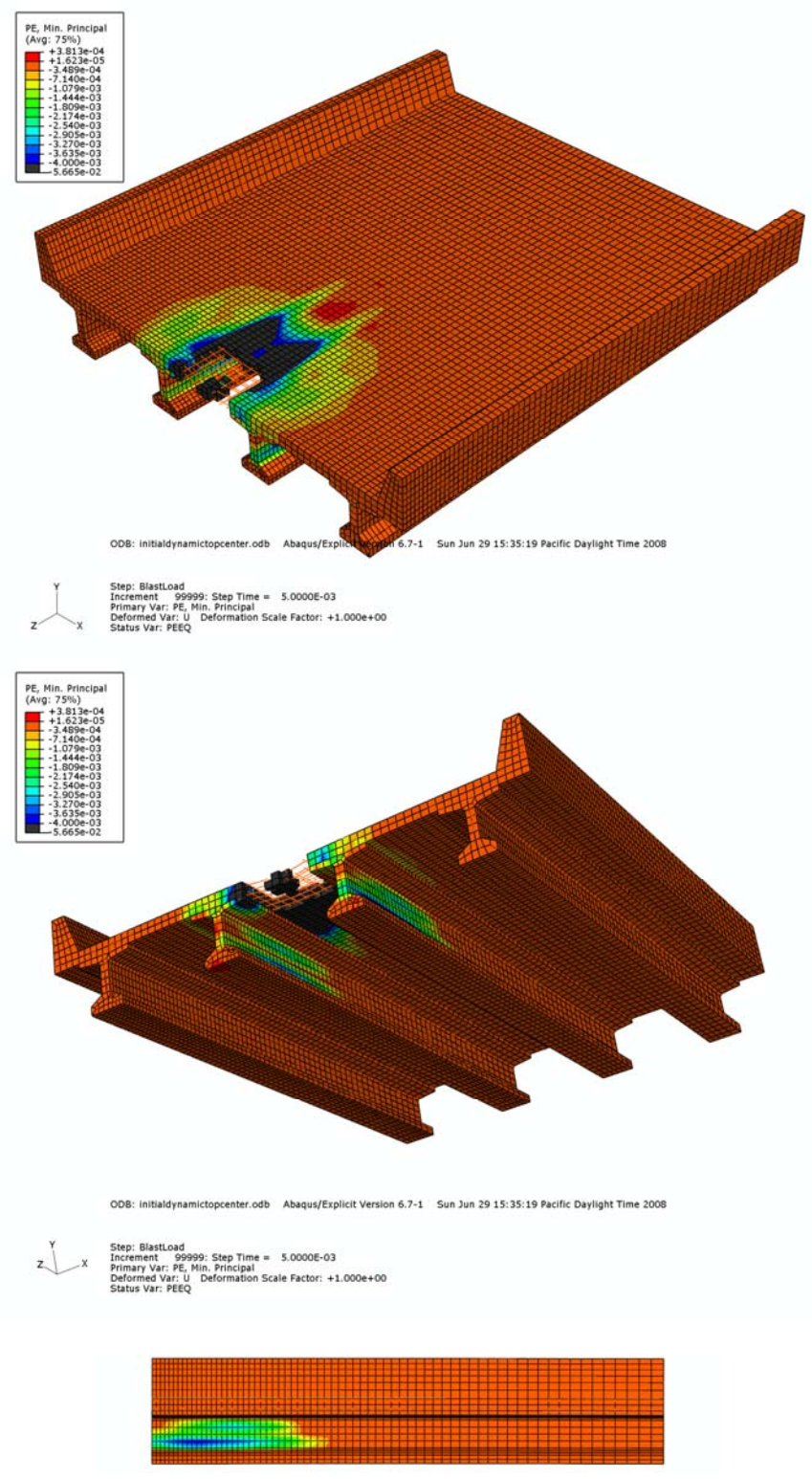

Figure 5-2: Minimum Principal Plastic Strain-Blast Above, Between Girders (Top View, Bottom View, Side View of Interior Girder)

Examining the direction of principal plastic strain illustrates again that shear is the predominant form of failure. At less than one millisecond into the analysis, when the pressure wave is still being applied, the strong tendency to punch through the deck can be seen. This is shown in Figure 5-3.

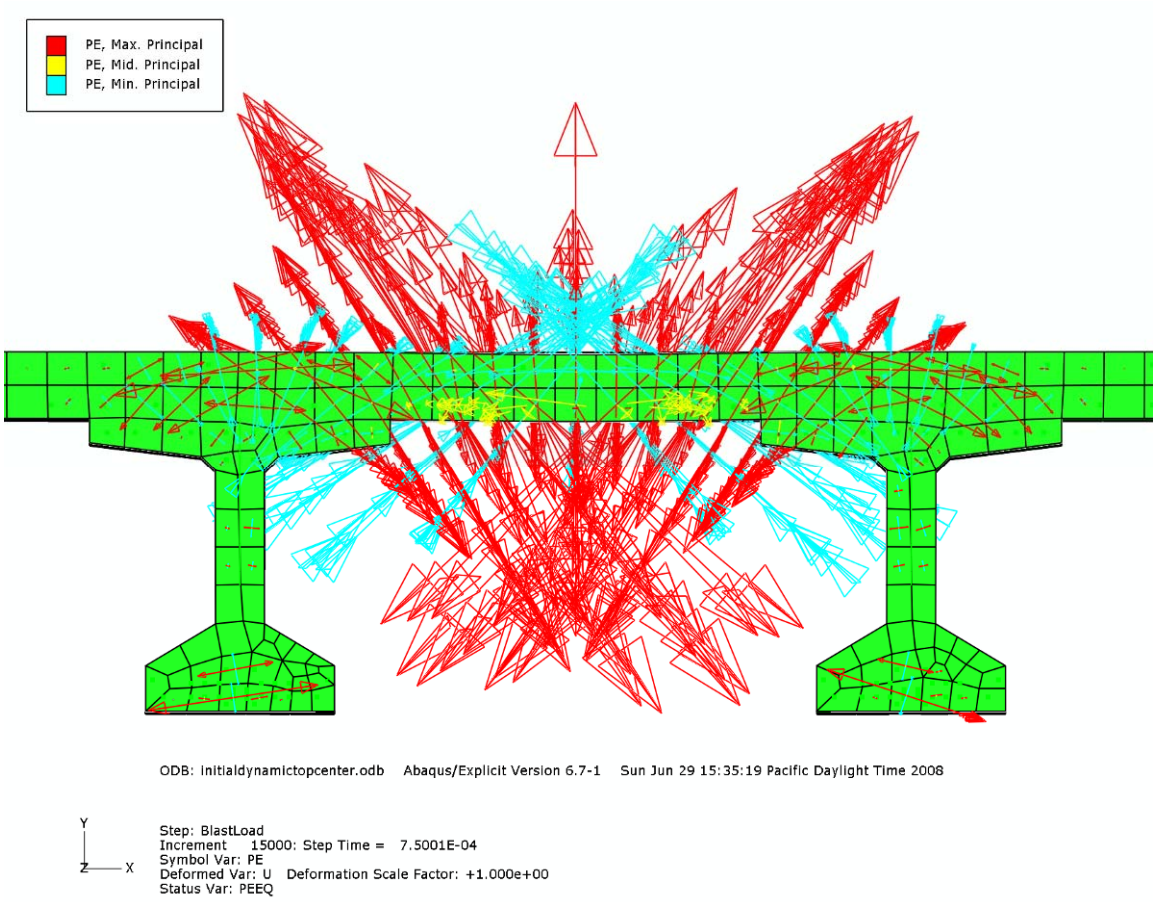

Figure 5-3: Cracking Direction-Blast Above, Between Girders

These results imply that at this level of blast, the bridge would not be destroyed. If the bridge was wide enough, the area with the damaged slab could even be blocked off and the rest of the lanes of traffic could be immediately reopened.

5.2 BLAST ABOVE, CENTERED ON GIRDER

For the blast applied above the deck, centered over an interior girder, it is observed that very little if any concrete is rubblized, although there is significant cracking. It would appear that having the girder immediately under the center of the blast is enough to stiffen the slab to the point that a punching failure does not occur. Additionally, the slab provides enough protection to the girder to prevent total demolition.

The extent of cracking for this loading scenario is similar to the case above the deck and between the girders. We see that the cracking extends longitudinally about sixteen feet. In the transverse direction, heavy cracking extends to the adjacent girders on either side of the blast event, resulting in a width of about sixteen feet. The girder immediately below the blast source shows heavy cracking all the way through its depth. The girders adjacent to this one, however, show no significant cracking. See Figure 5-4.

The extent of damage is similar to the extent of cracking. It is seen that the girder beneath the blast has damage through its web, indicating a decrease in capacity. The other girders have no significant damage. See Figure 5-5.

Examination of the direction of cracking at the end of the analysis shows a slight difference in the failure pattern. Instead of seeing a single cone-shaped failure surface where the blast load punches through the deck, it is observed that there is a cone-shaped failure surface on either side of the girder. This trend is illustrated in Figure 5-6. This is just further confirmation that the girders offer stiffening and protection to the slab.

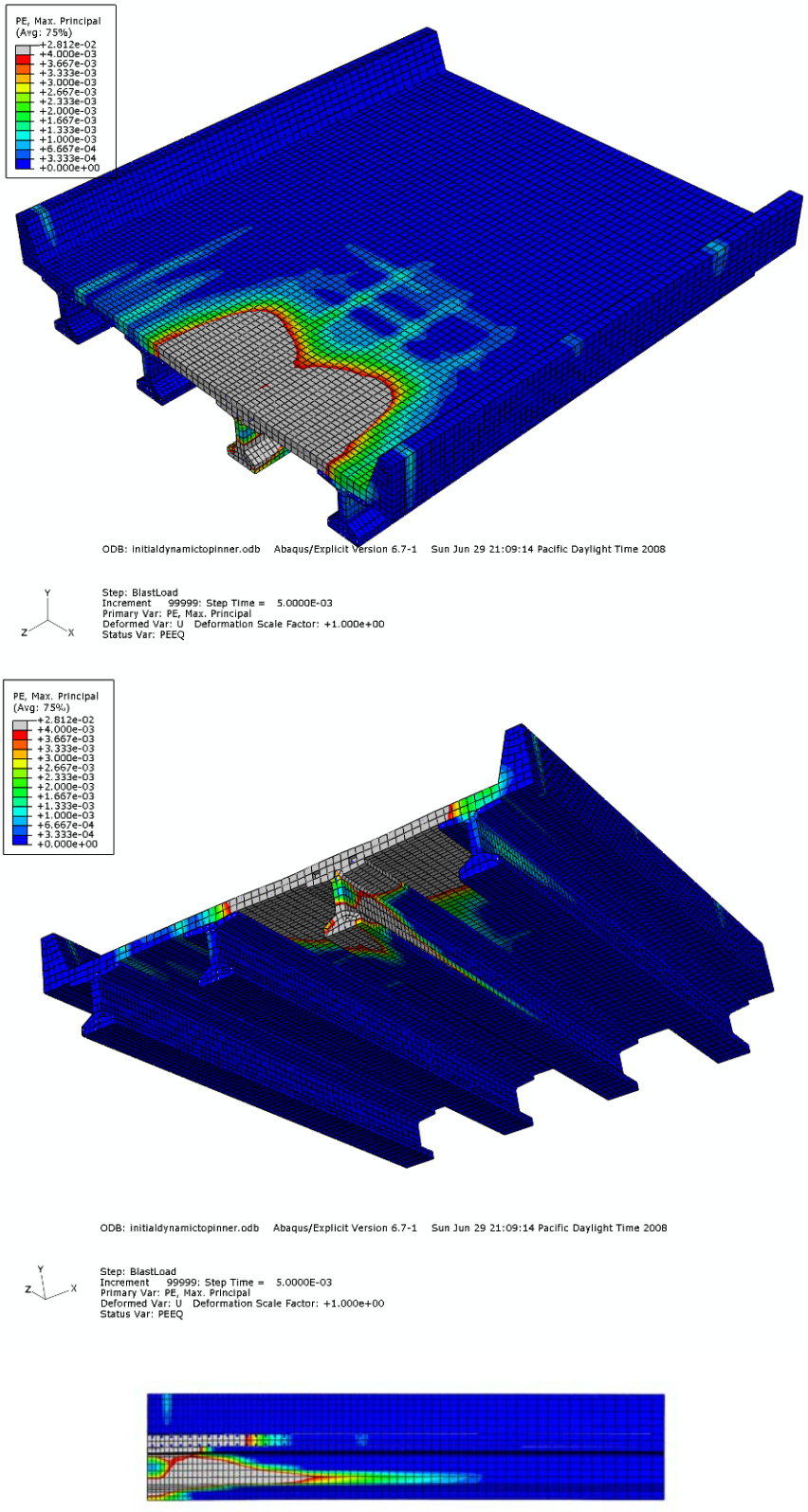

Figure 5-4: Maximum Principal Plastic Strain-Blast Above, Centered on Girder (Top View, Bottom View, Side View of Interior Girder)

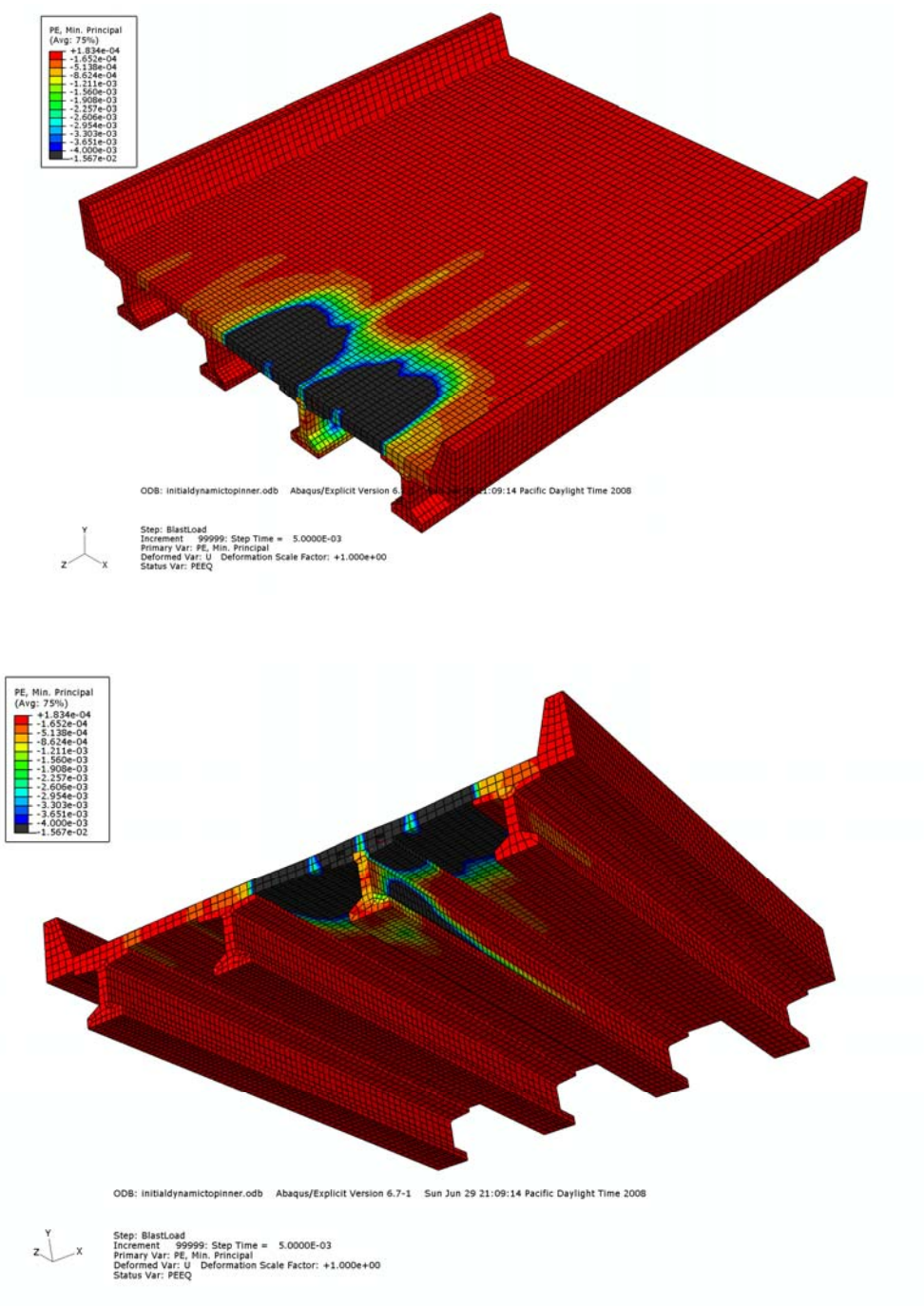

Figure 5-5: Minimum Principal Plastic Strain-Blast Above, Centered on Girder (Top View, Bottom View, Side View of Interior Girder)

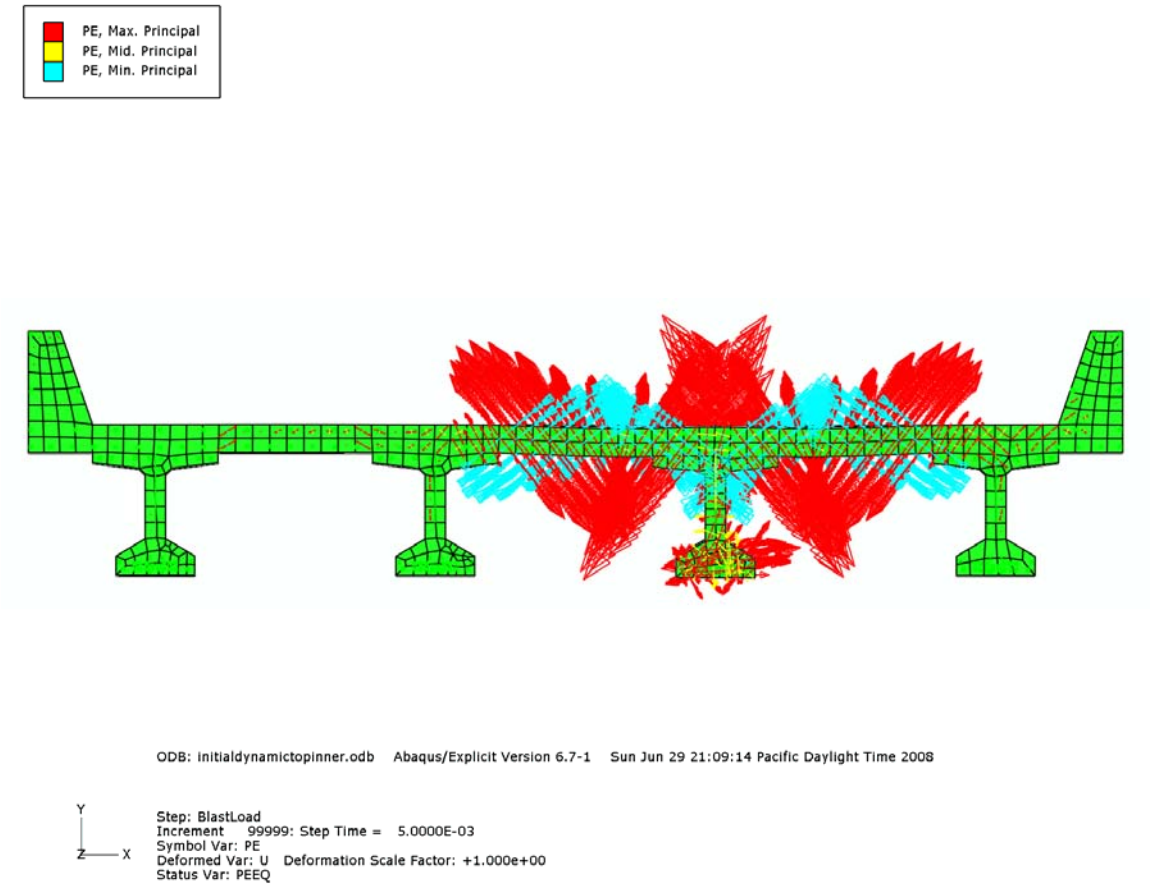

Figure 5-6: Cracking Direction-Blast Above, Centered on Girder

For both explosive events above the deck, it is seen that except for the area immediately below the blast source, the presence of a girder is effective for stiffening the slab and stopping the propagation of heavy cracking. Once again, it can be concluded that for a wide enough bridge, some lanes may be reopened immediately after the event. Even if a single lane can remain open, this would allow emergency vehicles to be uninterrupted in their service. Allowing emergency vehicles to get to their destinations in the quickest way possible is critical following a terrorist attack. In fact, it is critical at all times.

5.3 BLAST BELOW, BETWEEN GIRDERS

For the blast applied below the deck, centered between the interior girders, it is once again seen that very little if any concrete is rubblized. However, the extent of cracking is much greater than for either of the blast scenarios from above. All four girders show heavy cracking through the full depths of their webs. The deck also shows cracking along its full width, and extending longitudinally for about half the total bridge span. This is shown in Figure 5-7.

Figure 5-8 shows the extent of damage. Since damage does not extend through the webs of the girders, it is concluded that they would not see a significant decrease in capacity. However, the extent of damage on the slab indicates that it would need to be replaced after such an event.

It must be noted that for these load cases below the bridge, wave reflection can have significant effects. As the wave reflects off the sides of the girders, they may see increased pressures as multiple reflected waves intersect and merge. There is also the effect of wave reflection off the ground to consider. As noted in the literature review, there is a range of standoff distances where the reflected wave from the ground can combine with the incident wave, effectively doubling the pressures. However, it is known from the experiments that the incident wave pressure applied to the girder is less than that used in the model, so this is likely not a concern for the current setup.

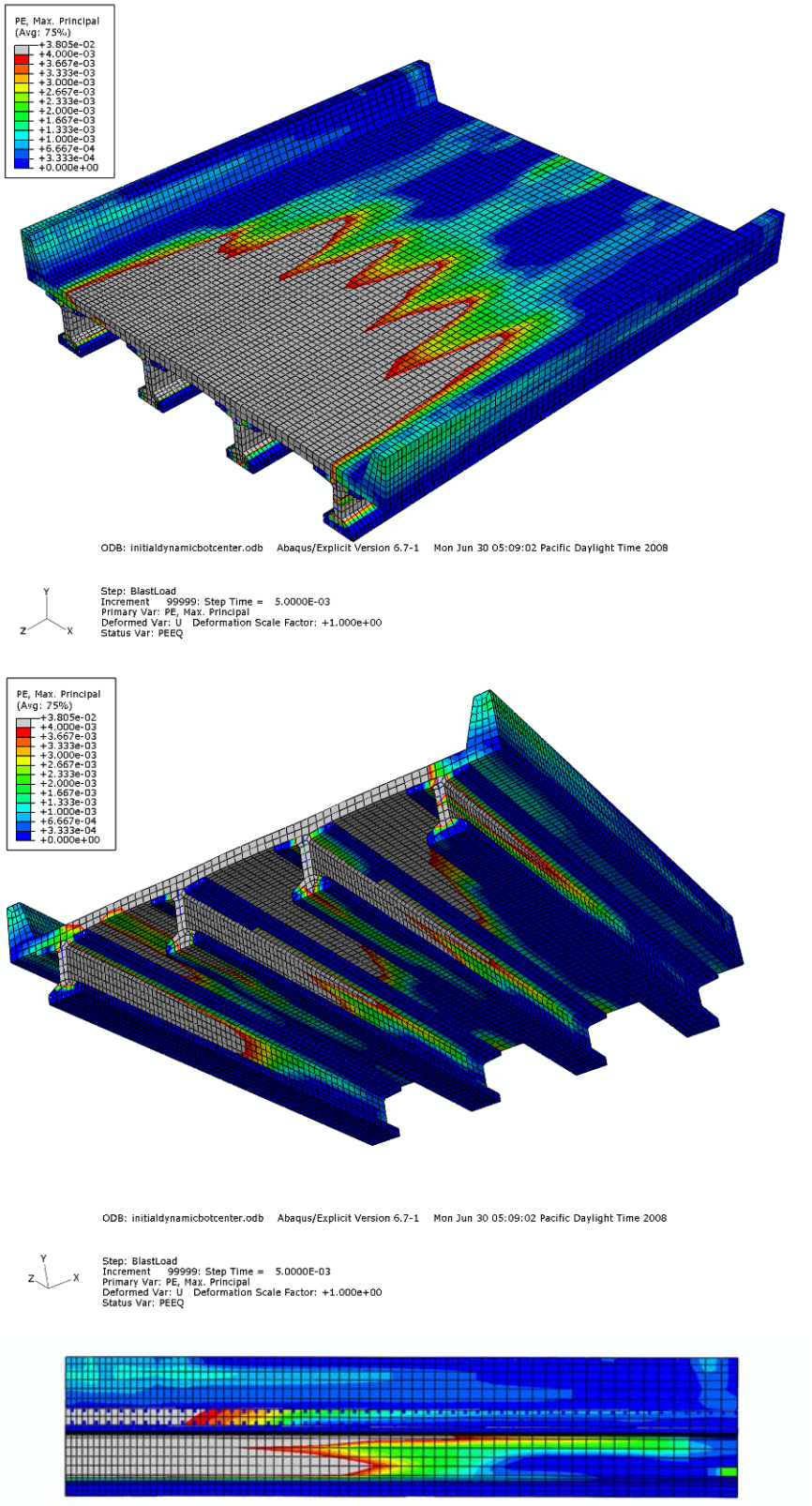

Figure 5-7: Maximum Principal Plastic Strain-Blast Below, Between Girders (Top View, Bottom View, Side View of Interior Girder)

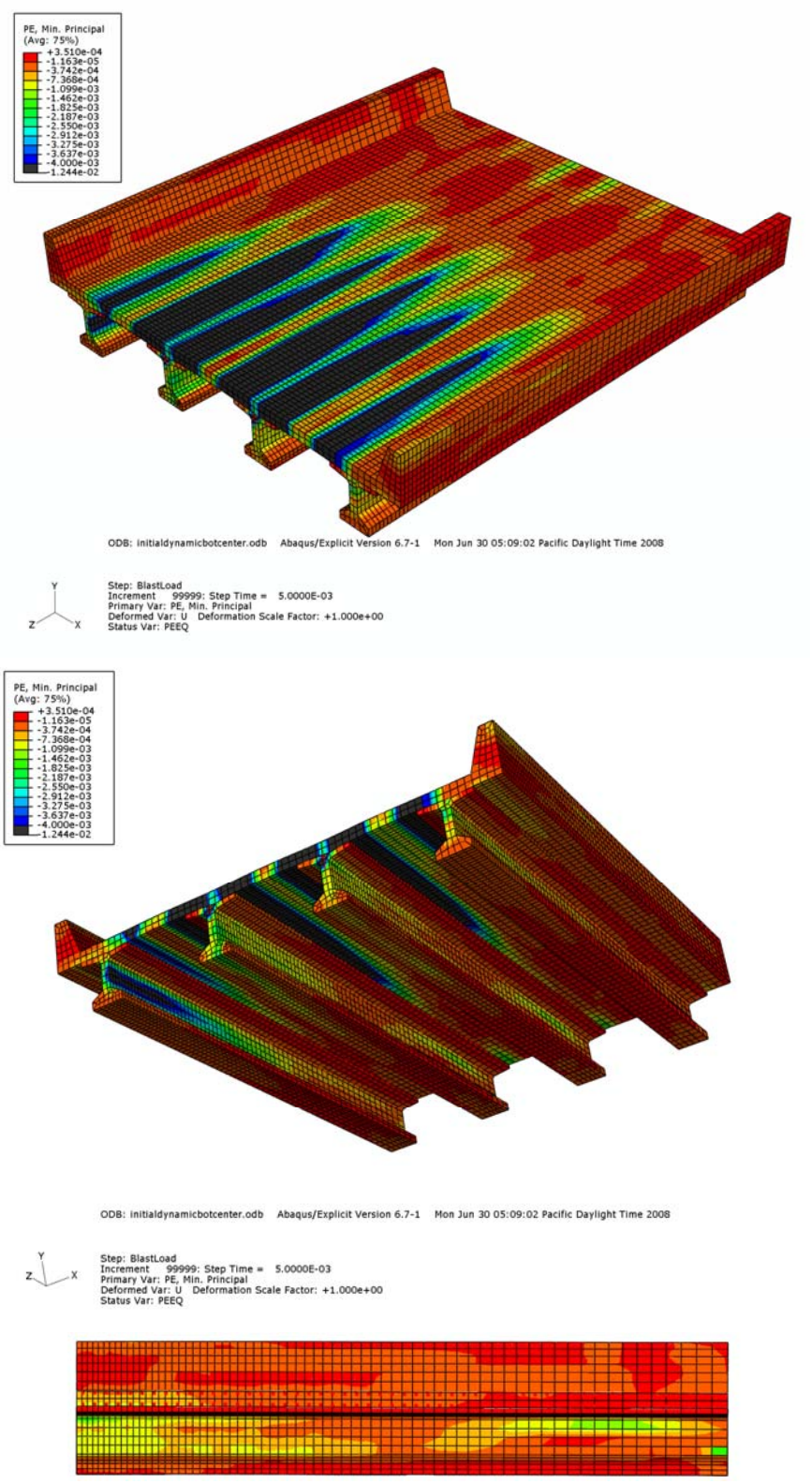

Figure 5-8: Minimum Principal Plastic Strain-Blast Below, Between Girders (Top View, Bottom View, Side View of Interior Girder)

5.4 BLAST BELOW, CENTERED ON GIRDER

For the blast applied below the deck, centered under an interior girder, the level of cracking and damage was nearly identical to the other load case from below. These results are shown in Figure 5-9 and Figure 5-10.

The conclusions for this scenario are the same as for the other blast event from below. With a standoff distance of ten feet, blast pressures are much more even than for a standoff distance of just a few feet. Thus, shifting the blast source over by just four feet does not significantly change the loading on the bridge model. This is why the results are nearly the same.

The results achieved for both load cases from below are thought to be reasonable. It is reiterated, however, that to truly gain a full understanding of bridge response, it may be necessary to create a mesh of the fluid surrounding the bridge, to fully account for wave reflection and shadowing effects.

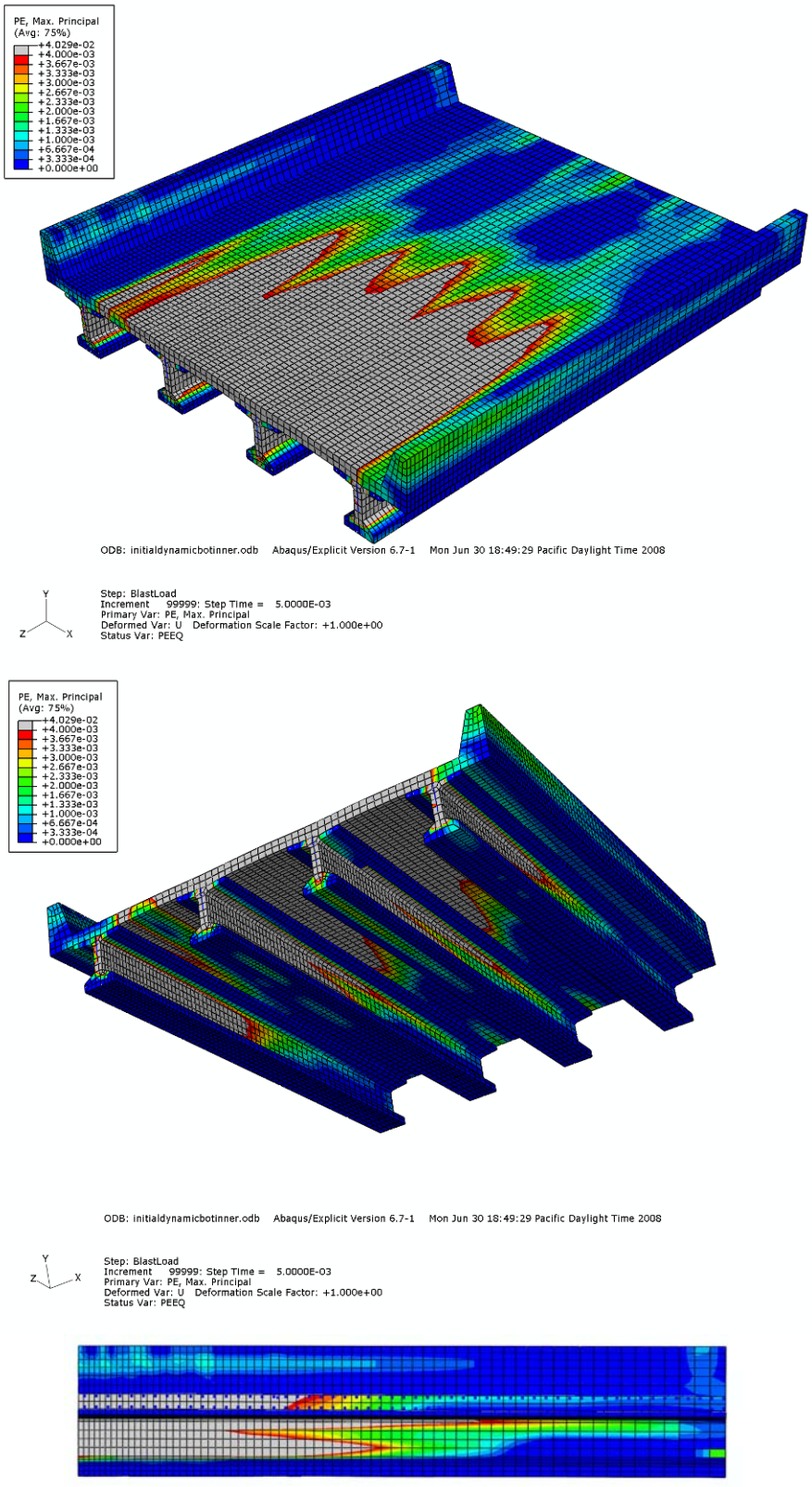

Figure 5-9: Maximum Principal Plastic Strain-Blast Below, Centered on Girder (Top View, Bottom View, Side View of Interior Girder)

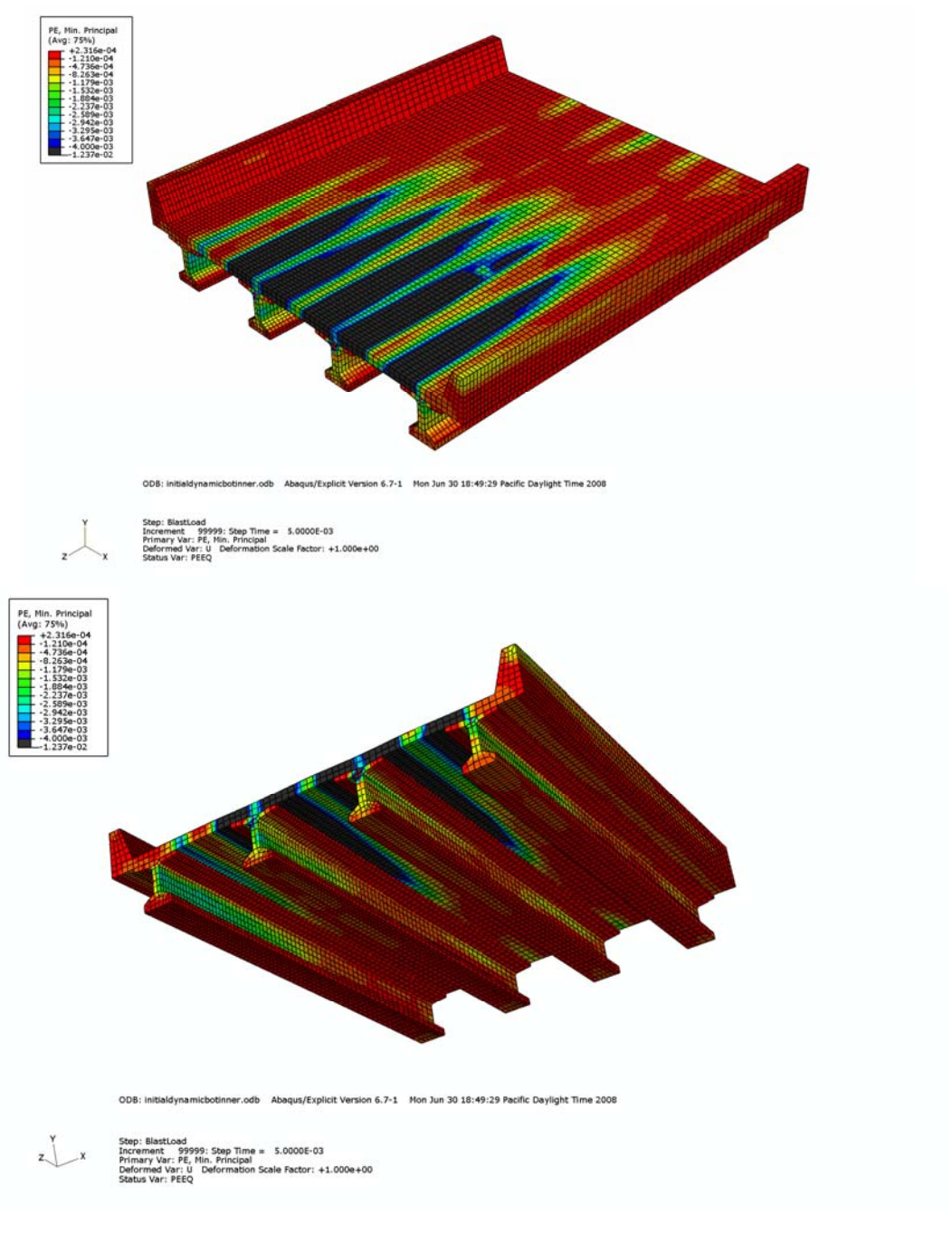

Figure 5-10: Minimum Principal Plastic Strain-Blast Below, Centered on Girder (Top View, Bottom View, Side View of Interior Girder)

CHAPTER 6: CONCLUSIONS

A finite element model of a precast, prestressed concrete girder was created using ABAQUS/Standard and ABAQUS/Explicit. The analytical girder was subjected to blast loading above and below. These results were compared to full-scale experiments. Close agreement was seen between analytical and empirical results. Thus, finite element analysis is an effective technique for capturing the actual behavior of prestressed concrete in response to blast. Continued utilization of this method should prove useful.

The blast tests conducted on full-scale girders revealed that the primary mode of failure for both scenarios was shear. This is consistent with previous research. Increasing shear strength could improve girder performance under blast loading.

The analytical models proved to be reliable in predicting girder response. Blast pressures predicted by BEL and applied to the top of the girder were nearly identical to those observed in the tests. Blast loads applied below were greater than those observed by a factor of two or three. Results, however, were still very good in that the location and type of damage and cracking were accurately predicted. A greater level of damage was observed in the analytical model than in the full-scale test, but this is to be expected considering the difference in pressures.

The model was then expanded into a four-girder, simple-span bridge. Four different loading scenarios were applied to the bridge model: a blast between two girders both above and below the deck, and a blast centered on a girder both above and below the deck.

For the blast load applied above the deck, between two girders, the pressure punched a hole through the slab, but left the girders relatively untouched. This scenario

indicates that the bridge would remain aloft and could even have a section of it immediately reopened after a blast event.

For the blast load applied above the deck, centered over a girder, the blast wave caused damage to the girder immediately below the blast source and to the surrounding slab. Once again, the bridge is expected to remain aloft and sections of it are expected to be immediately serviceable.

For both of the blast loads applied from below, results were essentially identical. Due to the even distribution of pressure for a ten-foot standoff compared to a four-foot standoff, moving the blast source by four feet did not create any significant changes in response. Heavy cracking is seen through the middle half of the bridge, but only the slab sees real damage. Thus, the bridge will remain aloft, but not be immediately serviceable.

The inherent inaccuracies of modeling blast loads from below are noted to be of significant interest. Since ABAQUS is not able to account for shadowing effects and wave reflection without including a mesh of the fluid surrounding the girder, including a mesh of the air would allow for more accurate analysis of blast loads on non-flat surfaces. This is an area for continued research.

Finite element analysis is a very good way to investigate the effects of blast on whole bridges. These same techniques can be used for any loading scenarios on the top of the bridge deck to achieve very accurate results. Applying blast loads to the underside of a bridge yields good results, but the modeling can be improved by including a mesh of the surrounding fluid.

APPENDIX A: SECTION DETAILS

The section used for the empirical and analytical study was a Colorado Department of Transportation standard section. The two girders actually used for the test were surplus girders that had been donated to the project. Both girders had been stored outdoors for approximately a year before being transported to the test site and used for testing. The following pages show the section details for the girder and the bridge layout.

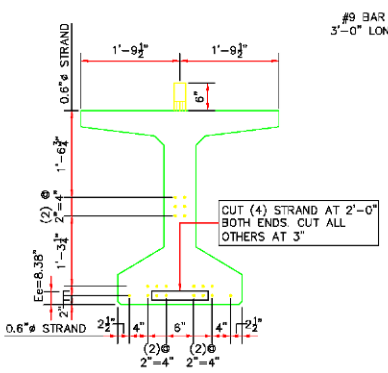

END DETAIL "A"

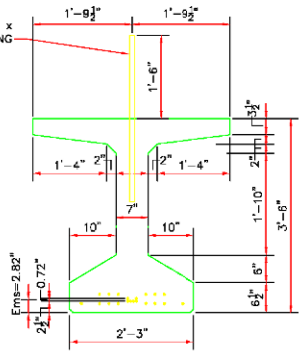

MIDSPAN DETAIL "B"

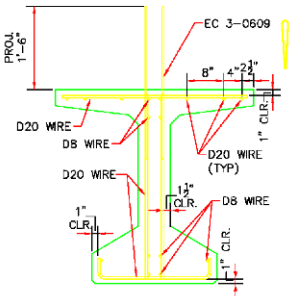

MIDSPAN REINFORCING DETAIL "C"

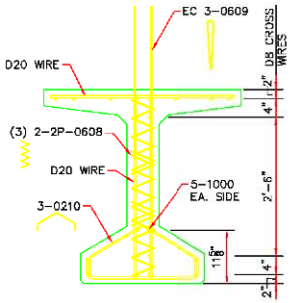

END REINFORCING DETAIL "D"

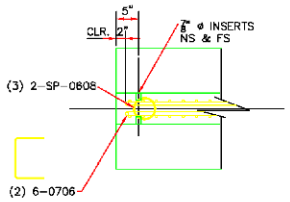

WEB END DETAIL "E"

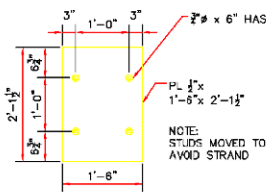

SG-1 GALVANIZED PLATE DETAIL

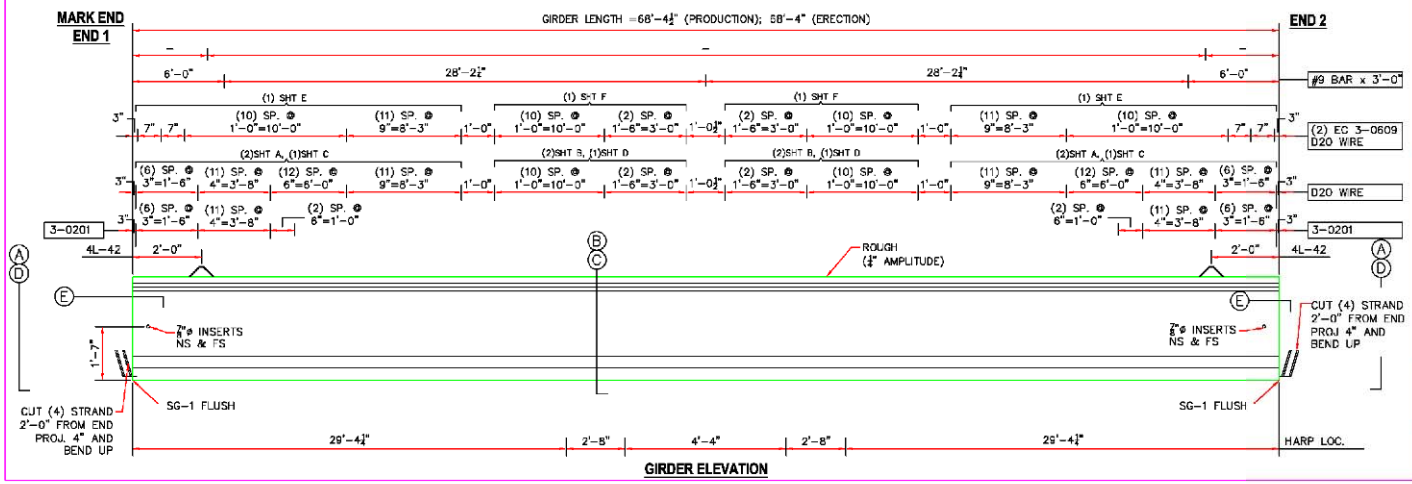

GIRDER ELEVATION

POUR #: LOCATION:

GENERAL NOTES

1. USE 0.6" SPECIAL LOW RELAX. STRAND (GRADE 270)
2. USE CLASS "S" CONCRETE
3. USE GRADE 60 REINFORCING STEEL
4. SLING ANGLE MUST EXCEED 60°

TOP FINISH: ROUGH (¼" AMPLITUDE)
END FINISH: FORM
SIDE FINISH: FORM

BILL OF MATERIALS

	MARK	DESCRIPTION	QTY.	WT.
EMBEDS	4L-42	LIFTERS	2	–
	SG-1	GALV. BRG. PLT.	2	–
	ø INS.	D-S F-42	4	–
	#9 BAR	BY OTHERS	3	–
	–	–	–	–
	–	–	–	–
	–	–	–	–
STANDARD REBAR	4-0500	SPLICE BARS	18	
	WWF	D20 x VAR	16	
	5-1000		4	
	–		–	
	–		–	
	6-0706	2'-3" 3'-0"	4	
	–		–	
	2-SP-0608	5"ø, 4" PITCH 1'-4"	8	
	3-0210	4" 7" 1'-11½"	40	
EPOXY REBAR	EC 3-0609	3'-3" 3"	148	

	CAMBER @ 90 DAYS (in.) =	2⅛"
	NO. OF STRAIGHT STRAND =	14
	NO. OF HARPED STRAND =	6
No. Req'd	f'ci (PSI) =	6500
	f'c (PSI) =	8500
	INITIAL TENSION (Fi)(k) =	878.9
	FINAL TENSION (Ff)(k) =	738.0
3	VOLUME (CY) =	11.5
	WEIGHT (TONS) =	25.6

8600 N. Welby Road, P.O. Box 29039, Denver, CO 80229
(303) 288-6477; Fax (303) 284-4234
1-800-783-7473 Rocky Mountain Region Only

Rinker MATERIALS
Hydro Conduit & Prestress
Denver Plant

DWG. STATUS	DATE
FOR APPROVAL	5/2/03
FOR PRODUCTION	6/9/03
REVISION 1	–
REVISION 2	–
REVISION 3	–

GIRDER G-7, 8, 9

DRAWN: MSH DATE: 4/30/03
OWNER: CDOT
PROJECT NO.: NH 0505-037 13547
STRUCTURE NO.: L-25-D, L-25-F
DESIGNER: CDOT
CONTRACTOR: NEATLINE STRUCTURES
PROJECT NAME: STATE HIGHWAY 50
LOCATION: LUBERS, CO

SHEET NUMBER 6

JOB NUMBER 304.A14

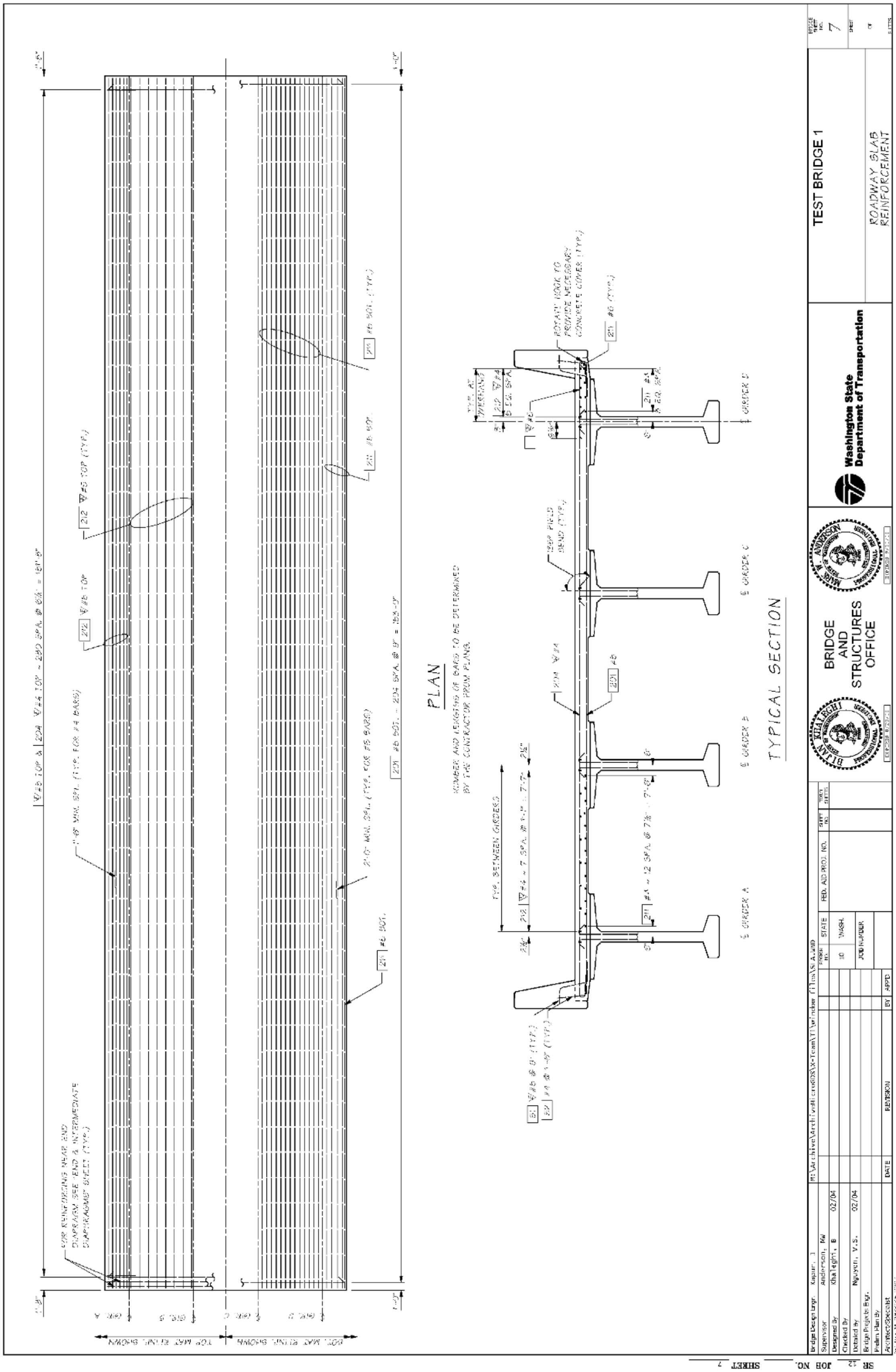
TEST BRIDGE 1
ROADWAY SLAB REINFORCEMENT
PLAN
TYPICAL SECTION
BRIDGE AND STRUCTURES OFFICE
Washington State Department of Transportation

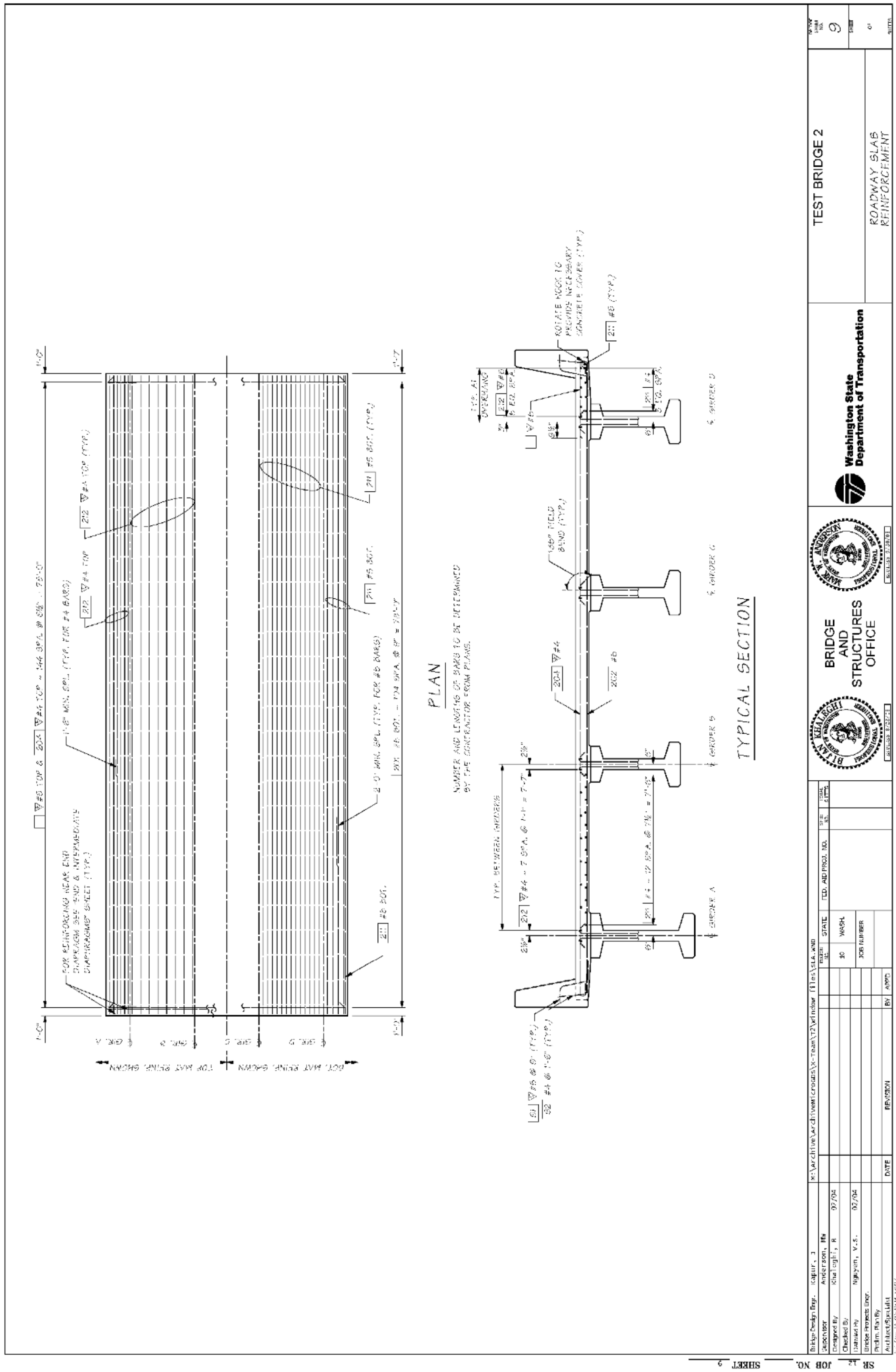
PLAN
TYPICAL SECTION
BRIDGE AND STRUCTURES OFFICE
Washington State Department of Transportation
TEST BRIDGE 2
ROADWAY SLAB REINFORCEMENT

APPENDIX B: MODELING DETAILS

```
*Heading
** Job name: InitialStatic Model name: InitialStatic
**
**----------------------------------------------------------
** GEOMETRY
**----------------------------------------------------------
**
**
**
***********
** PARTS **
***********
**
*Include, input=BLASTPOINTS.inp
**
**
**
**************
** ASSEMBLY **
**************
**
*Assembly, name=Assembly
**
*Include, input=INSTANCES-DYNAMIC.inp
**
*Include, input=SETS-DYNAMIC.inp
**
*Embedded Element, host elset=Set-2
Set-1
**
*End Assembly
**
**
**
***************
** MATERIALS **
***************
**
*Include, input=MATERIALS-DYNAMIC.inp
**
**
**
*************************
** BOUNDARY CONDITIONS **
*************************
**
** BOUNDARY CONDITIONS
*Boundary
_PickedSet435, 2, 2
*Boundary
_PickedSet436, 1, 1
_PickedSet436, 2, 2
```

```
_PickedSet436, 3, 3
**
**
**
**********************
** BLAST PROPERTIES **
**********************
**
*Amplitude, definition=tabular, name=blasttimedecay
0., 1., .00005, .34, .00065, 0
**
*Incident wave interaction property, name=centerblast, type=sphere
136244, 4e-5,   1.00, -0.73685, 0.
*Incident wave interaction property, name=blast, type=sphere
136244, 4e-5,   -0.2, -0.73685, 0.
**
*Acoustic Wave Formulation
**
**
**
**------------------------------------------------------------
** ANALYSIS
** STEP: Blast Load
**------------------------------------------------------------
**
**
**
*************************
** INITITAL CONDITIONS **
*************************
**
*Step, name=Blast, nlgeom=yes
*Dynamic, Explicit, direct user control
5.0e-8, 0.005
*Bulk Viscosity
0.06, 1.2
**
**
**
***********
** LOADS **
***********
**
*Dload
, GRAV, 386., 0., -1., 0.
**
*Incident wave interaction, property=centerblast, pressure amplitude =
blasttimedecay
"Blast Surface Center", SOURCE, STANDOFF, 19180.
*Incident wave interaction, property=blast, pressure amplitude =
blasttimedecay
"Blast Surface", SOURCE, STANDOFF, 14208.85
**
**
********************
** OUTPUT REQUESTS **
********************
```

```
**
*Output, field, number interval=100, variable=PRESELECT
*Output, history, frequency=100, variable=PRESELECT
*End Step
```

APPENDIX C: EXPERIMENTAL RESULTS

C.1: EXPLOSION ABOVE

C.2: EXPLOSION BELOW

APPENDIX D: ANALYTICAL RESULTS

In order to illustrate the progression of cracking, pictures from different time steps within each bridge analysis are included in this appendix. Also displayed here are the variations of several model parameters, such as kinetic energy, and strand stress.

D.1: BLAST ABOVE, SINGLE GIRDER

D.1.1. MAXIMUM PRINCIPAL PLASTIC STRAIN

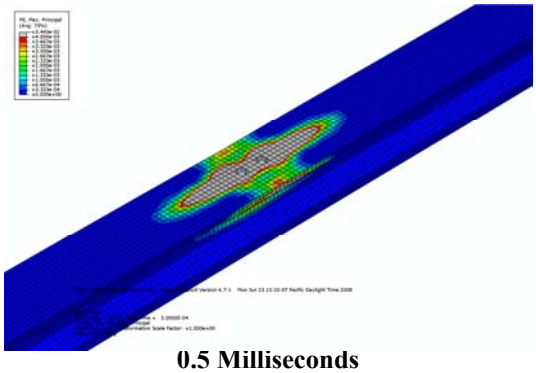

0.5 Milliseconds

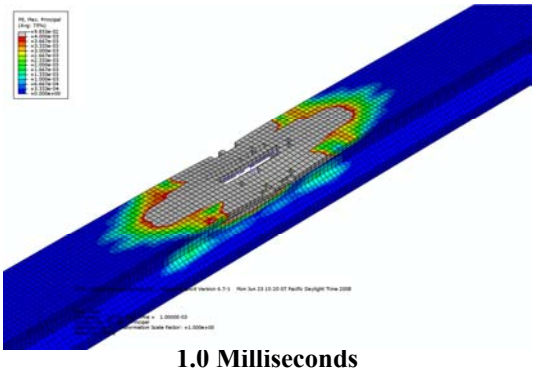

1.0 Milliseconds

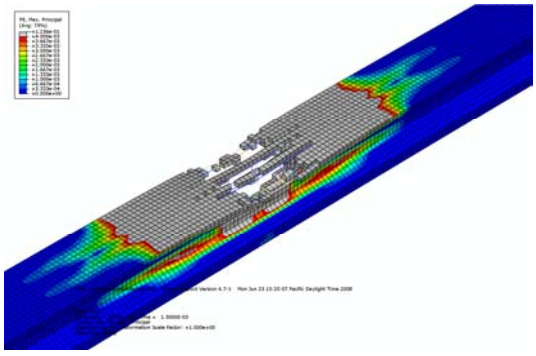

1.5 Milliseconds

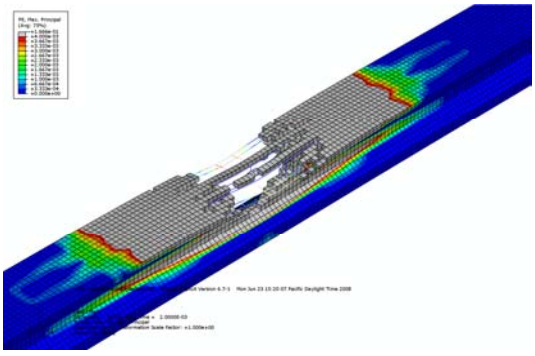

2.0 Milliseconds

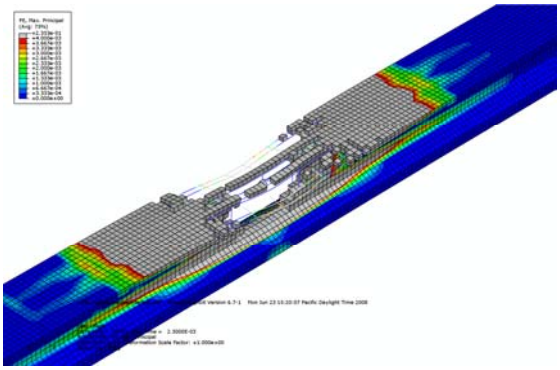

2.5 Milliseconds

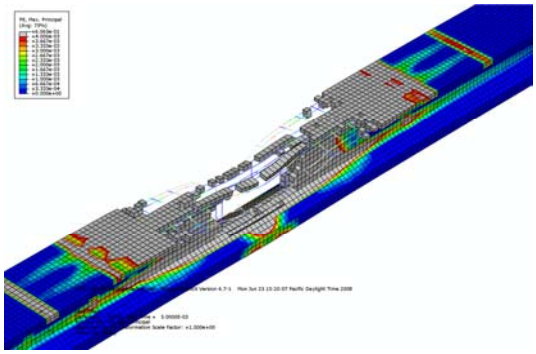

5.0 Millisecond

D.1.2. STRAND STRESS, BLAST ABOVE

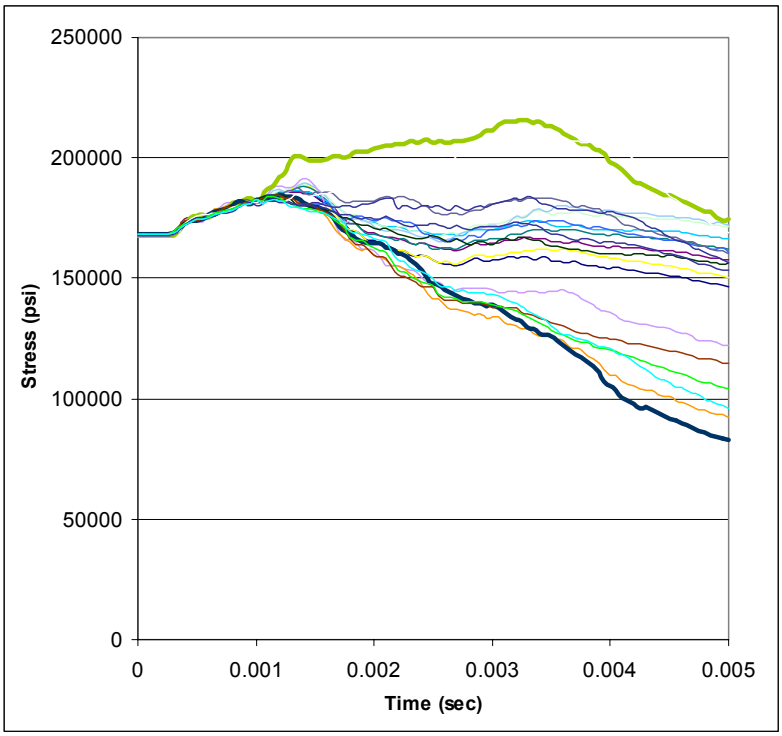

D.1.3. MODEL PARAMETERS

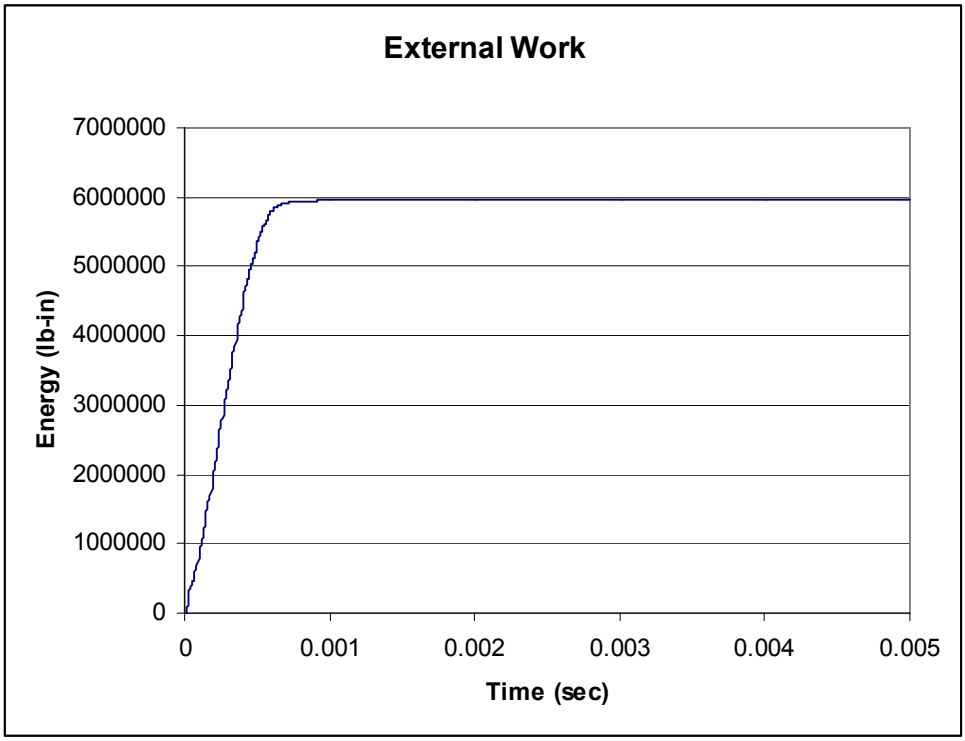

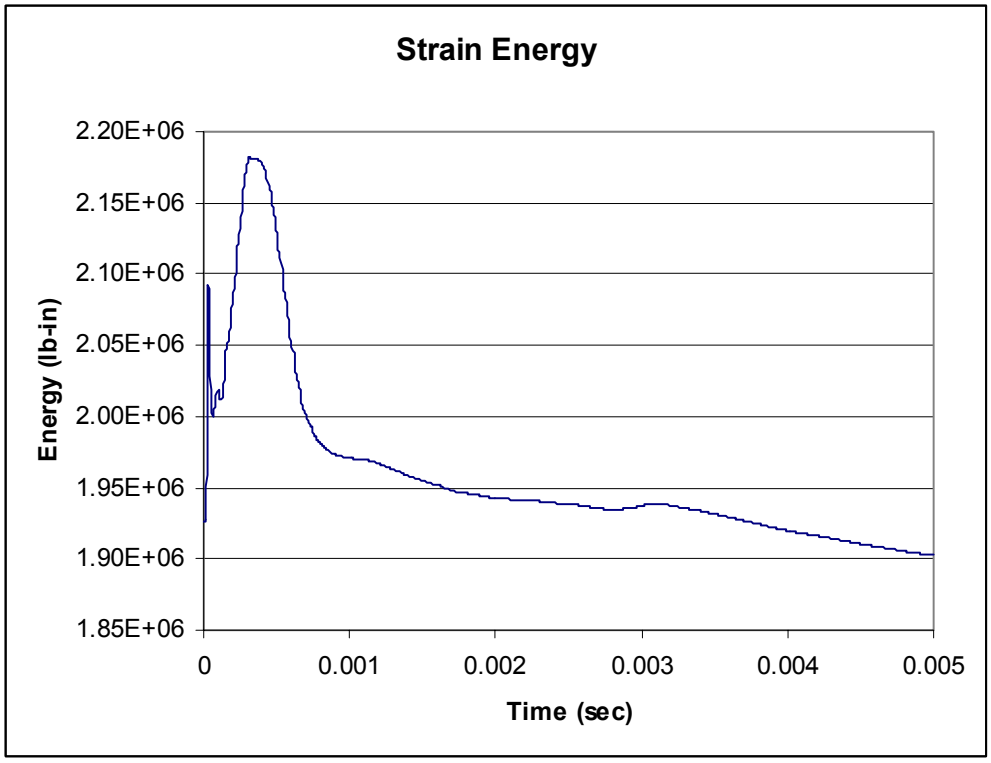
Strain Energy
2.20E+06
2.15E+06
2.10E+06
2.05E+06
2.00E+06
1.95E+06
1.90E+06
1.85E+06
Energy (lb-in)
0
0.001
0.002
0.003
0.004
0.005
Time (sec)

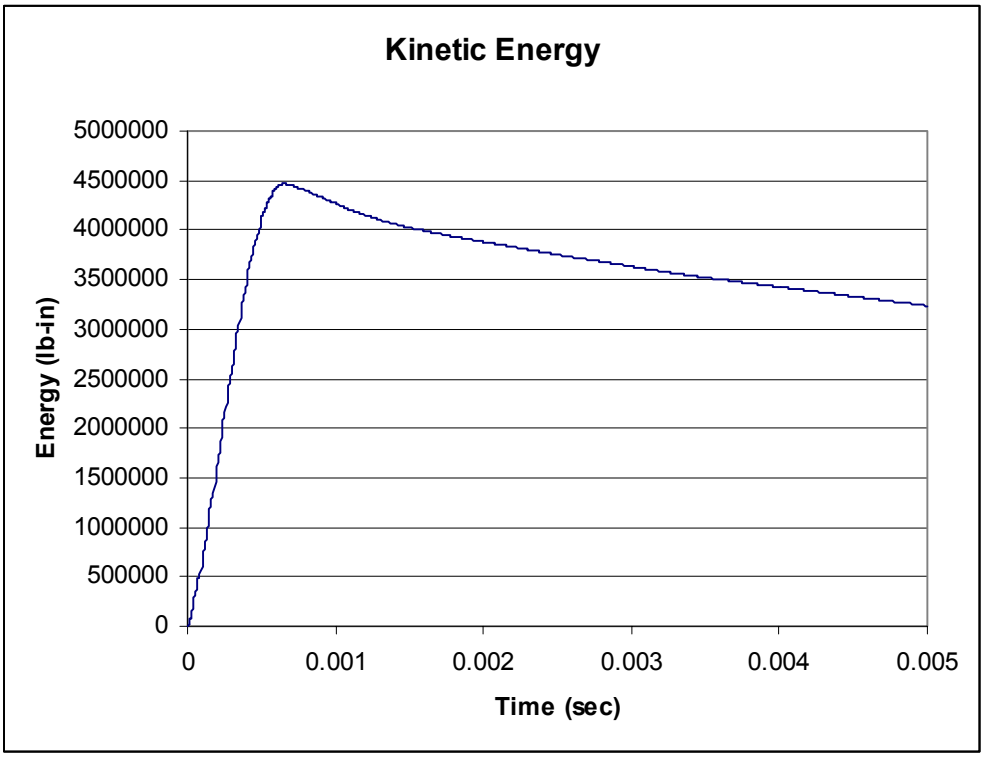
Kinetic Energy
5000000
4500000
4000000
3500000
3000000
2500000
2000000
1500000
1000000
500000
0
Energy (lb-in)
0
0.001
0.002
0.003
0.004
0.005
Time (sec)

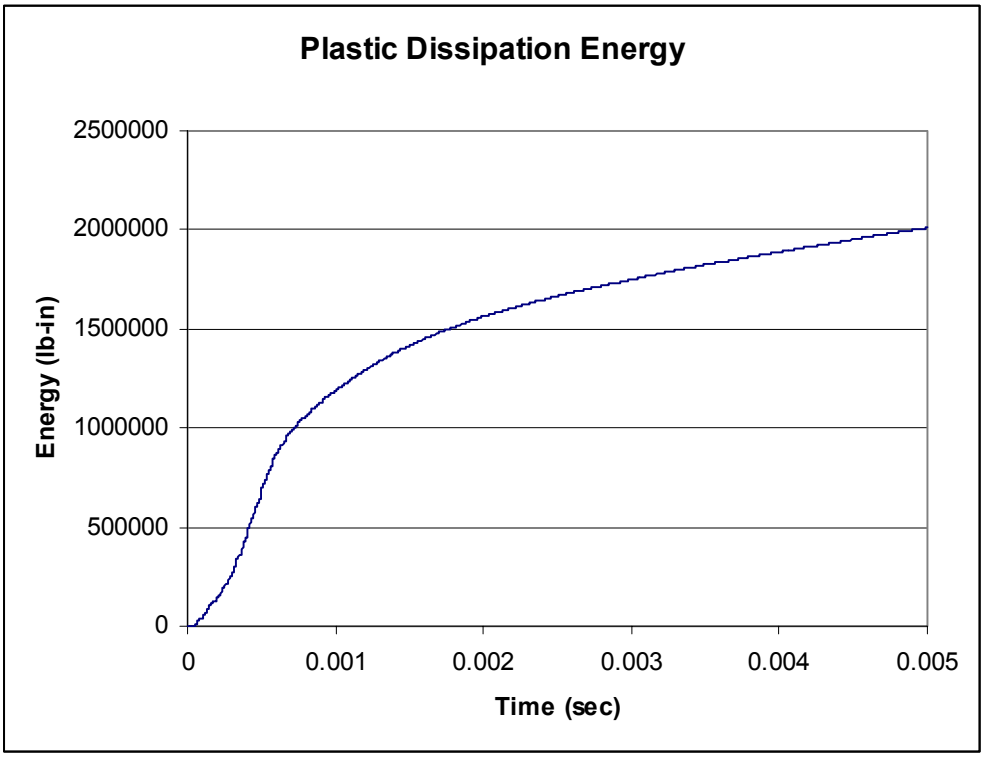
Plastic Dissipation Energy
2500000
2000000
1500000
1000000
500000
0
Energy (lb-in)
0
0.001
0.002
0.003
0.004
0.005
Time (sec)

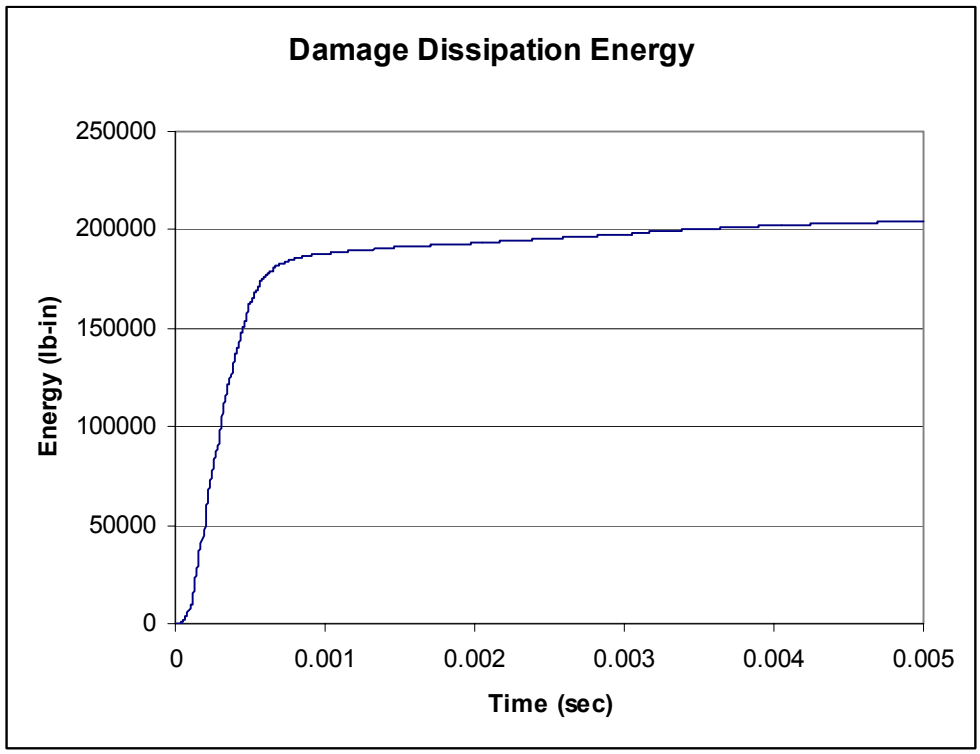
Damage Dissipation Energy
250000
200000
150000
100000
50000
0
Energy (lb-in)
0
0.001
0.002
0.003
0.004
0.005
Time (sec)

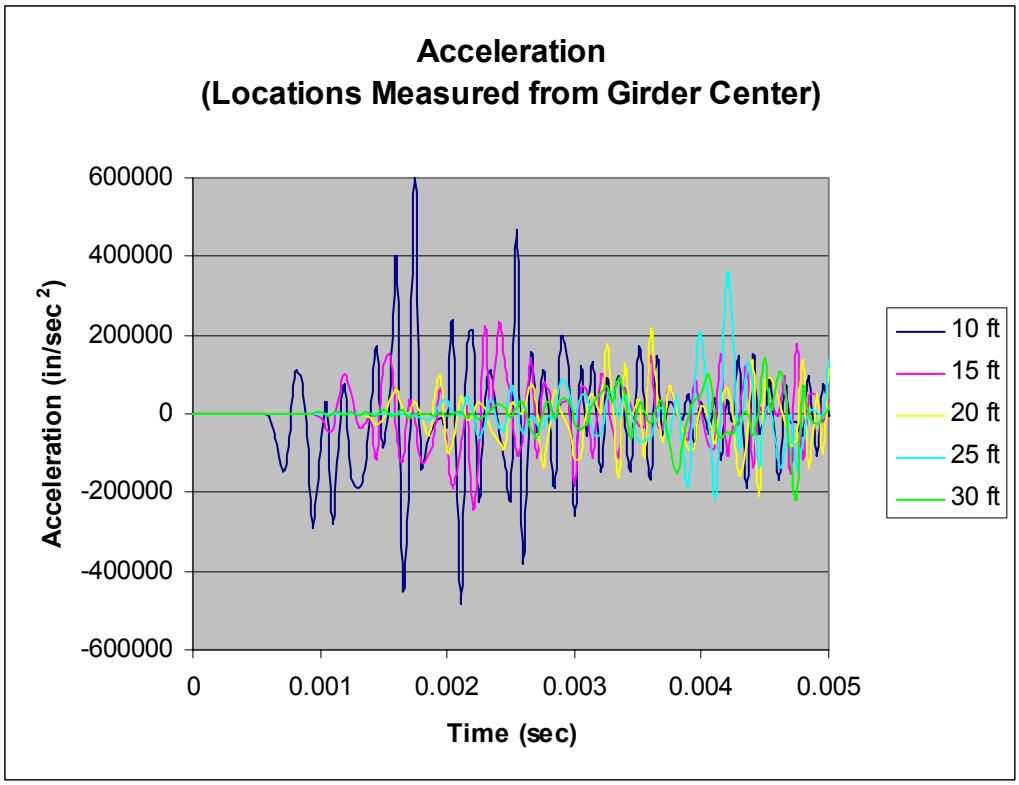
Acceleration
(Locations Measured from Girder Center)
600000
400000
200000
0
-200000
-400000
-600000
Acceleration (in/sec 2)
0
0.001
0.002
0.003
0.004
0.005
Time (sec)
10 ft
15 ft
20 ft
25 ft
30 ft

D.2: BLAST BELOW, SINGLE GIRDER

D.2.1. MAXIMUM PRINCIPAL PLASTIC STRAIN

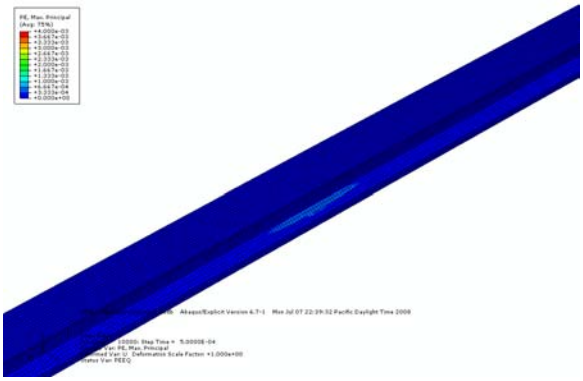

0.5 Milliseconds

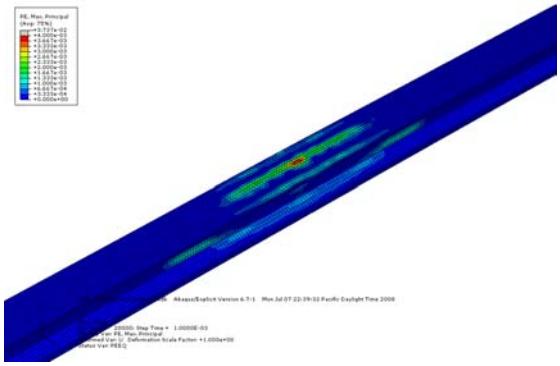

1.0 Milliseconds

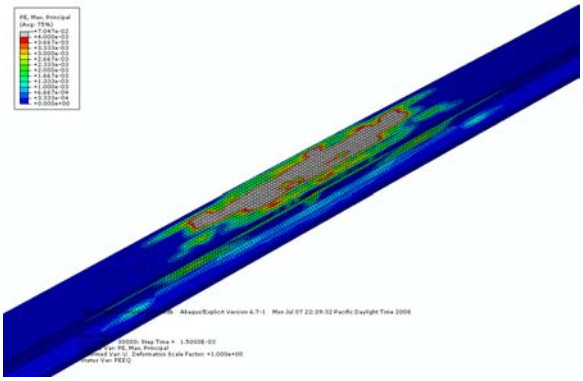

1.5 Milliseconds

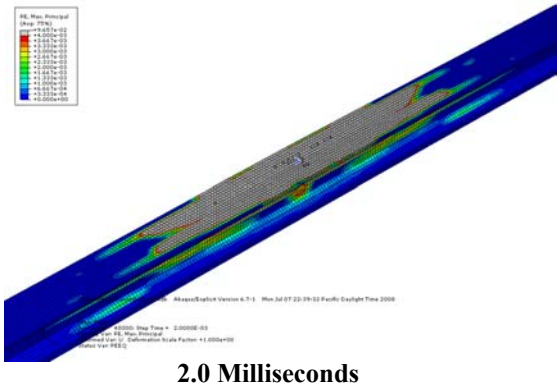

2.0 Milliseconds

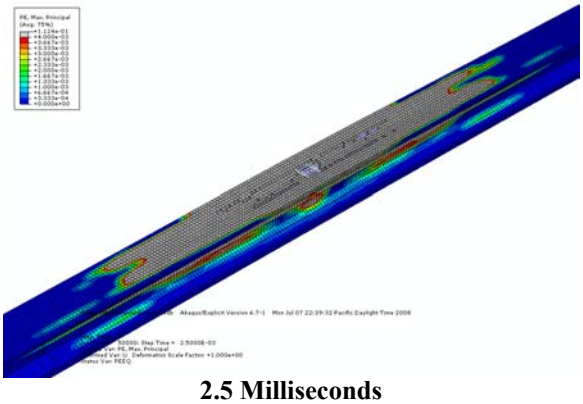

2.5 Milliseconds

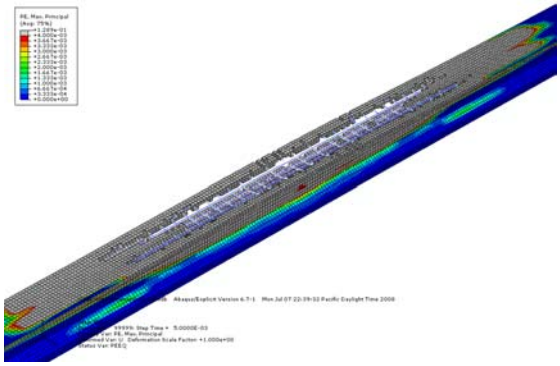

5.0 Millisecond

D.2.2. STRAND STRESS, BLAST BELOW

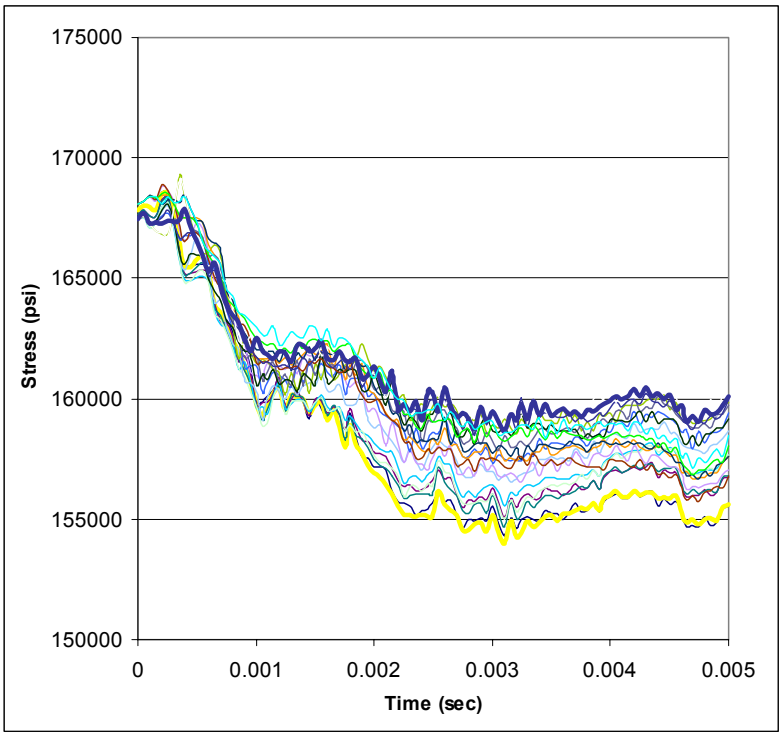

D.2.3. MODEL PARAMETERS

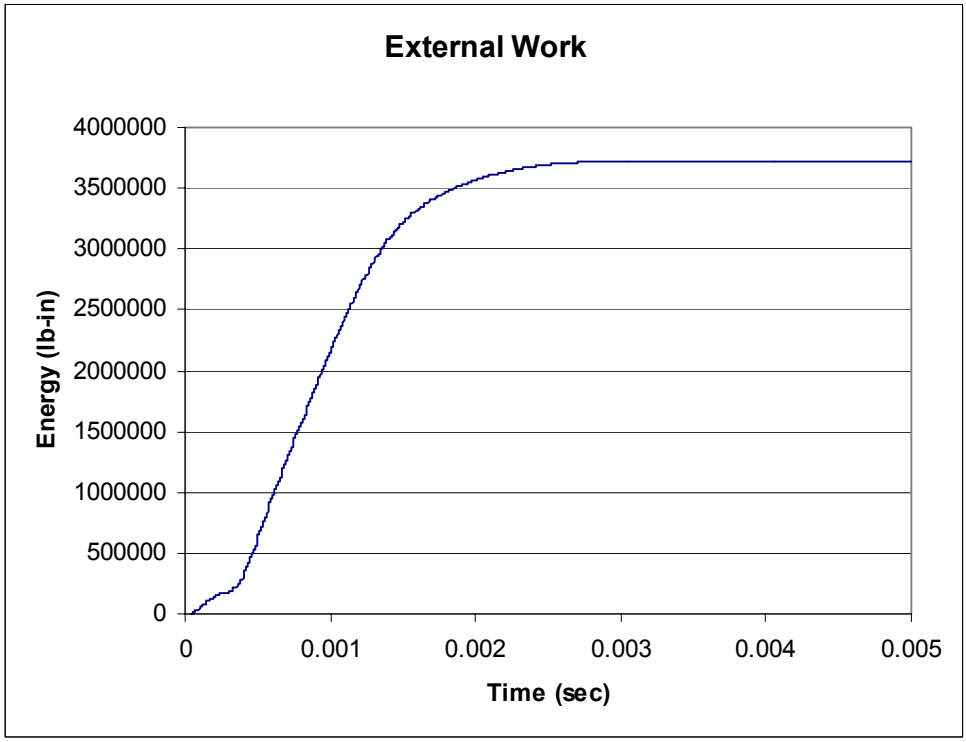

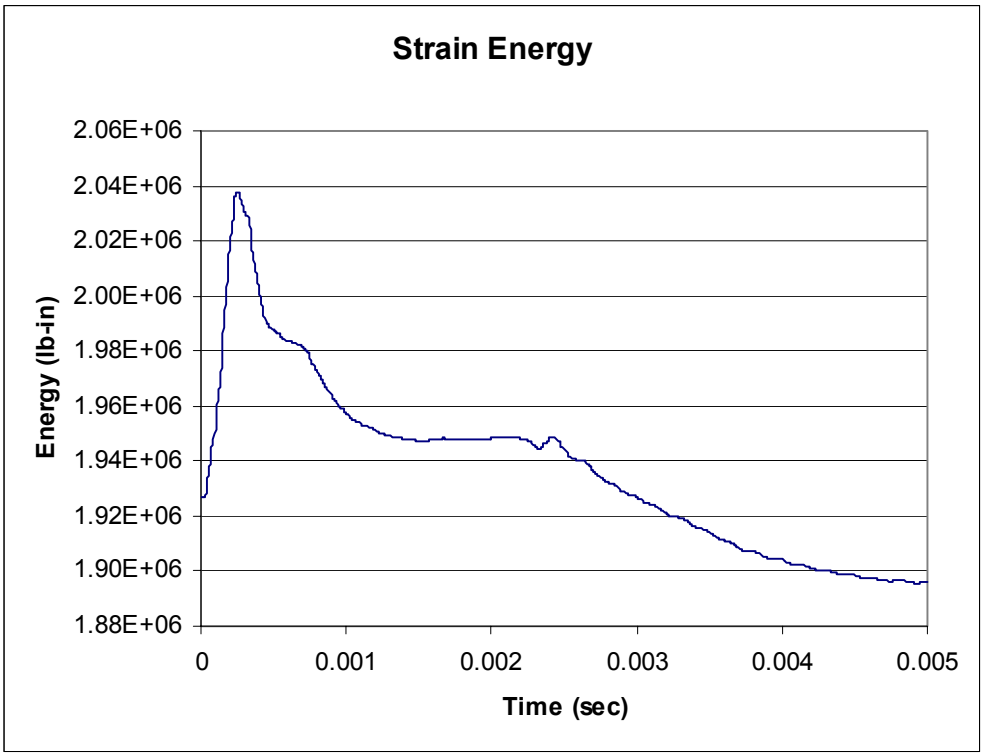
Strain Energy
2.06E+06
2.04E+06
2.02E+06
2.00E+06
1.98E+06
1.96E+06
1.94E+06
1.92E+06
1.90E+06
1.88E+06
Energy (lb-in)
0
0.001
0.002
0.003
0.004
0.005
Time (sec)

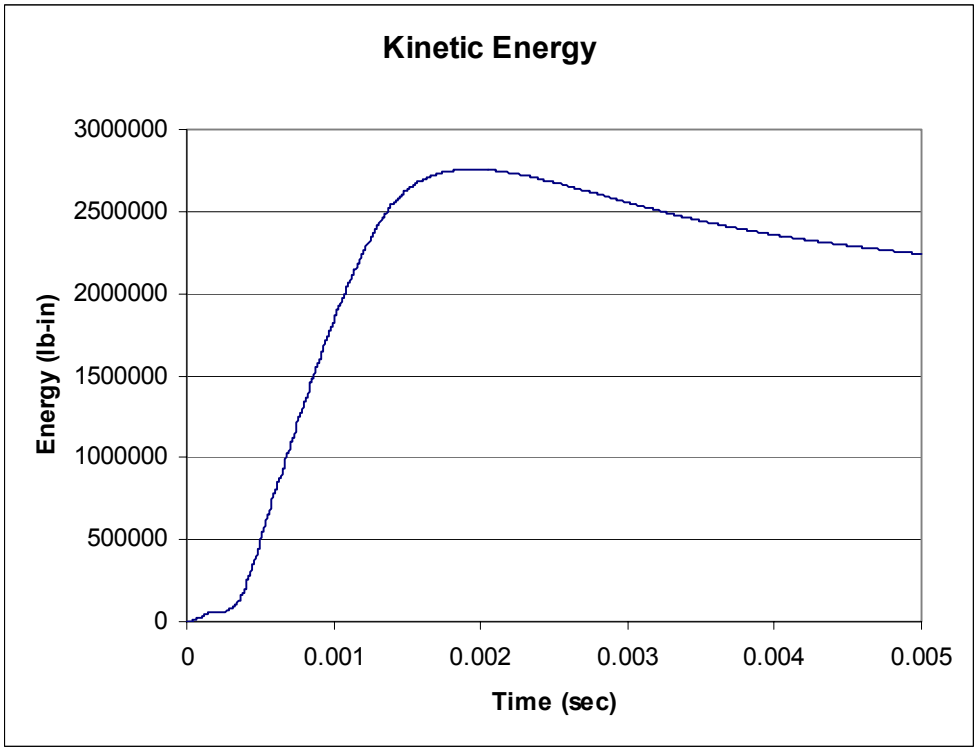
Kinetic Energy
3000000
2500000
2000000
1500000
1000000
500000
0
Energy (lb-in)
0
0.001
0.002
0.003
0.004
0.005
Time (sec)

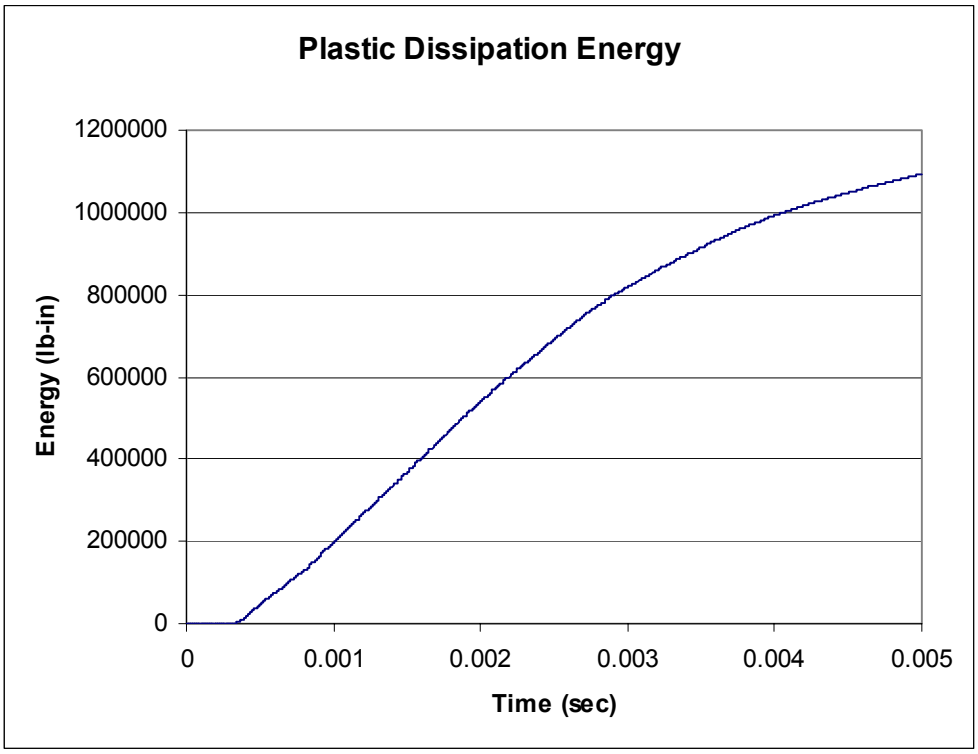
Plastic Dissipation Energy
1200000
1000000
800000
600000
400000
200000
0
Energy (lb-in)
0
0.001
0.002
0.003
0.004
0.005
Time (sec)

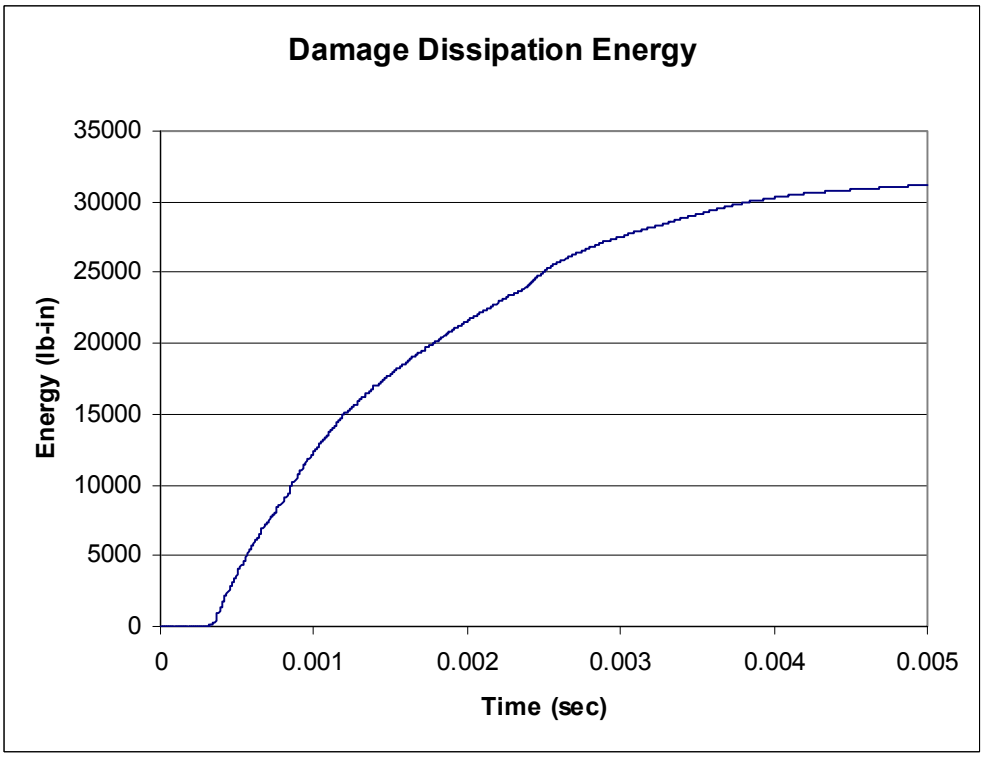
Damage Dissipation Energy
35000
30000
25000
20000
15000
10000
5000
0
Energy (lb-in)
0
0.001
0.002
0.003
0.004
0.005
Time (sec)

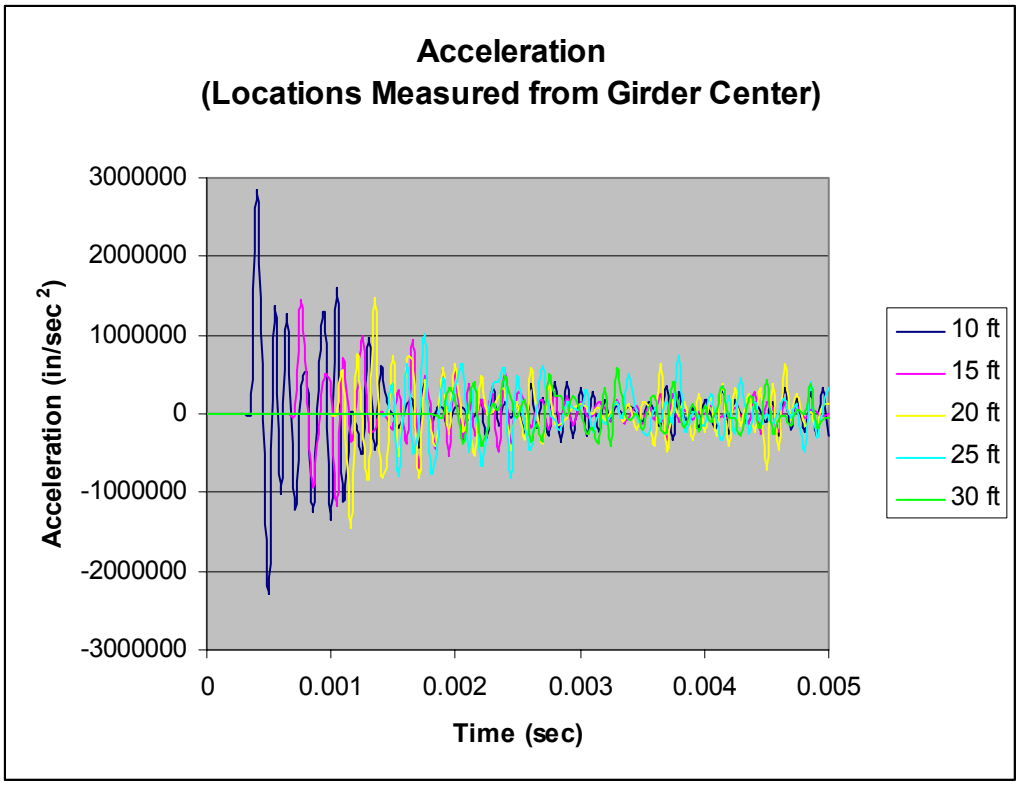
Acceleration
(Locations Measured from Girder Center)
Acceleration (in/sec 2)
3000000
2000000
1000000
0
-1000000
-2000000
-3000000
0
0.001
0.002
0.003
0.004
0.005
Time (sec)
10 ft
15 ft
20 ft
25 ft
30 ft

D.3: BLAST ABOVE, BETWEEN GIRDERS

D.3.1. MAXIMUM PRINCIPAL PLASTIC STRAIN

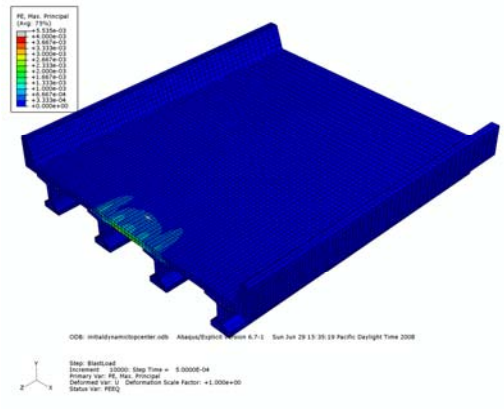

0.5 Milliseconds

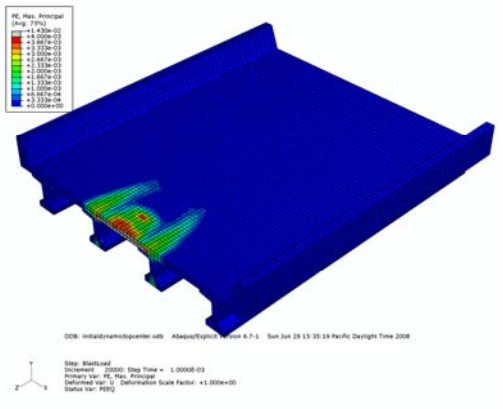

1.0 Milliseconds

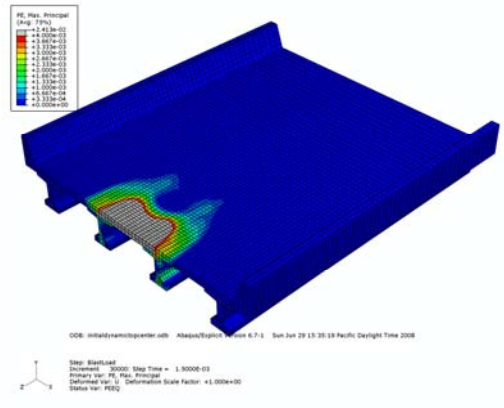

1.5 Milliseconds

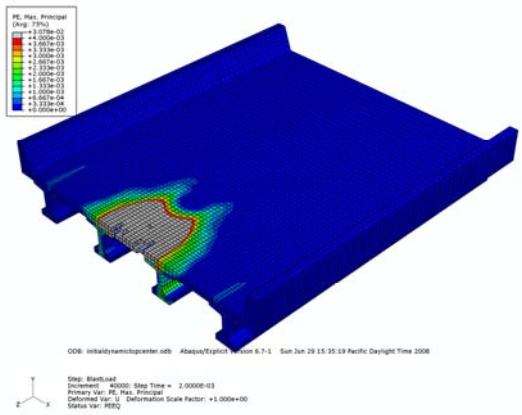

2.0 Milliseconds

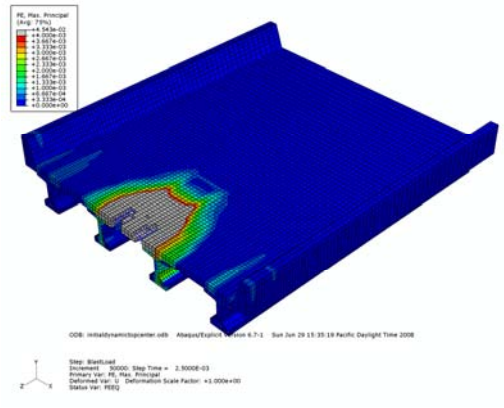

2.5 Milliseconds

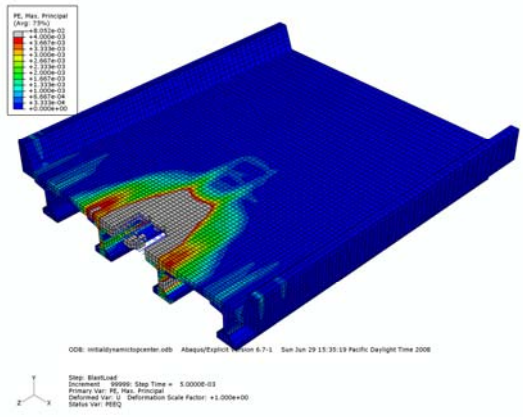

5.0 Milliseconds

D.3.2. STRAND STRESS, GIRDER ADJACENT TO BLAST

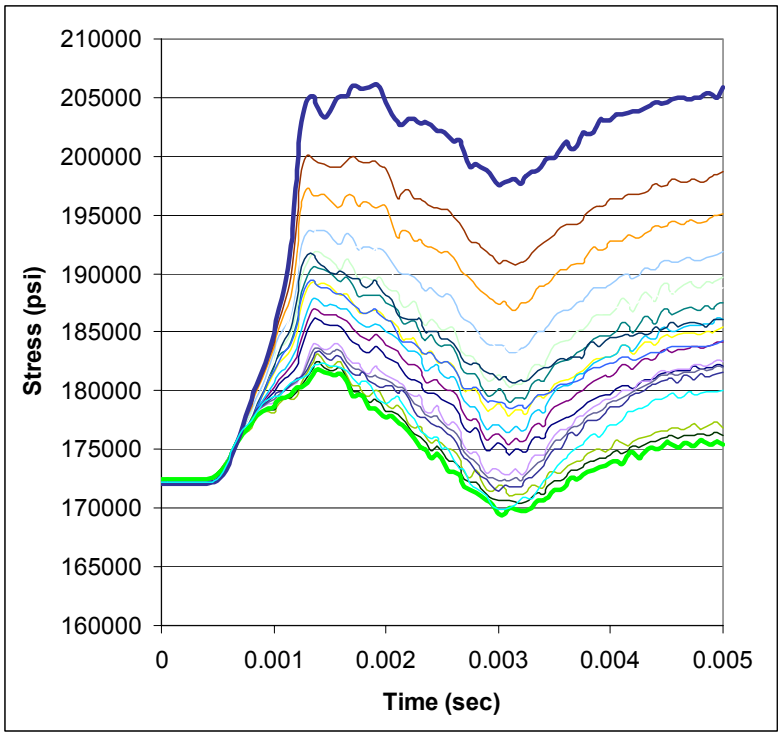

D.3.3. MODEL PARAMETERS

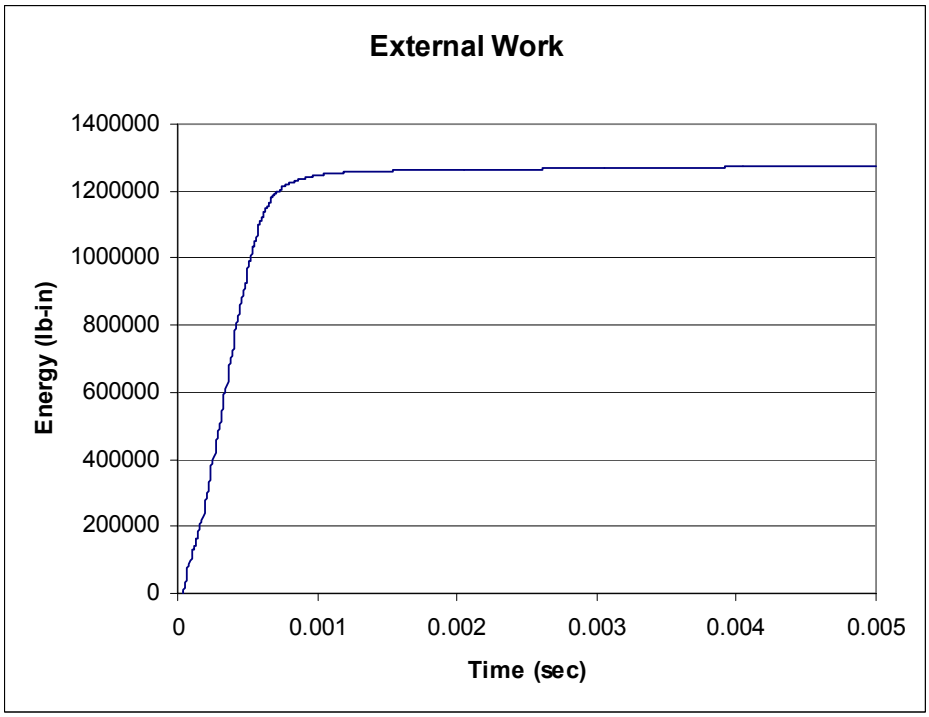

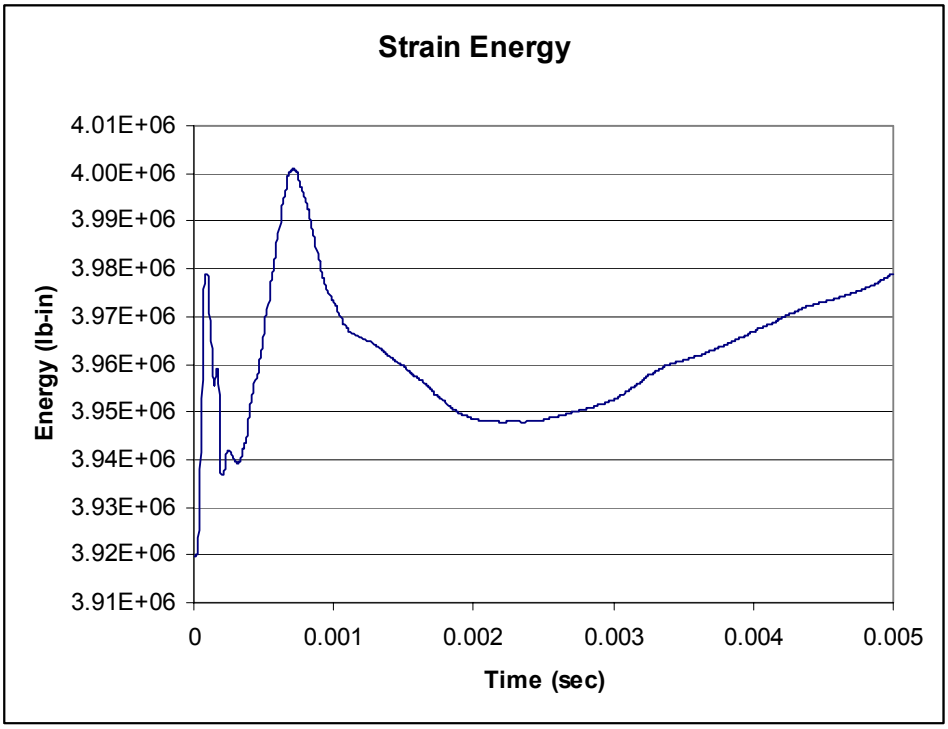
Strain Energy
4.01E+06
4.00E+06
3.99E+06
3.98E+06
3.97E+06
3.96E+06
3.95E+06
3.94E+06
3.93E+06
3.92E+06
3.91E+06
Energy (lb-in)
0
0.001
0.002
0.003
0.004
0.005
Time (sec)

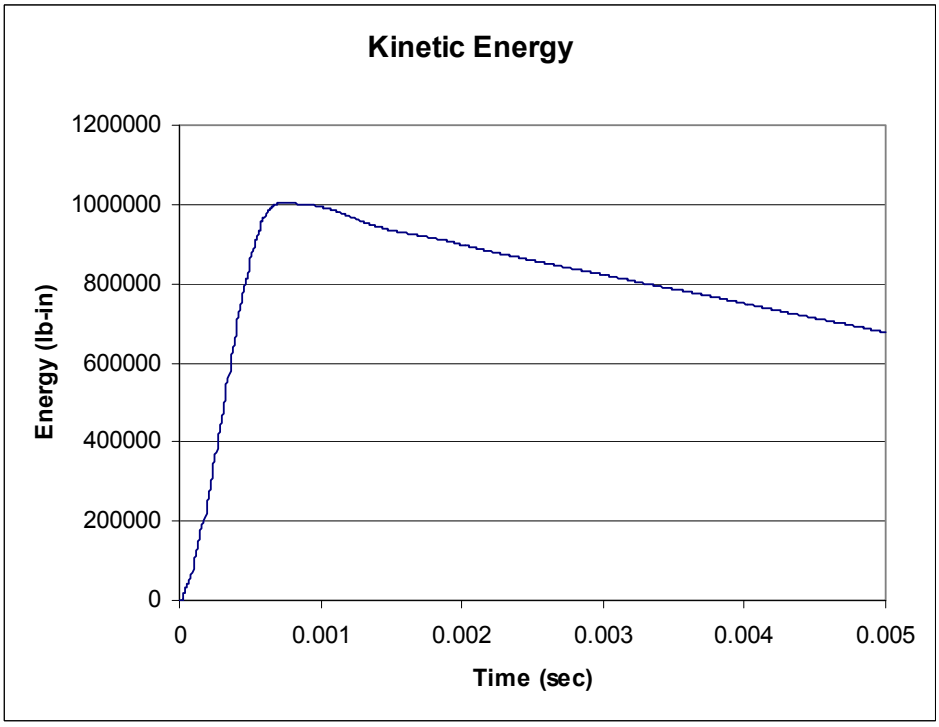
Kinetic Energy
1200000
1000000
800000
600000
400000
200000
0
Energy (lb-in)
0
0.001
0.002
0.003
0.004
0.005
Time (sec)

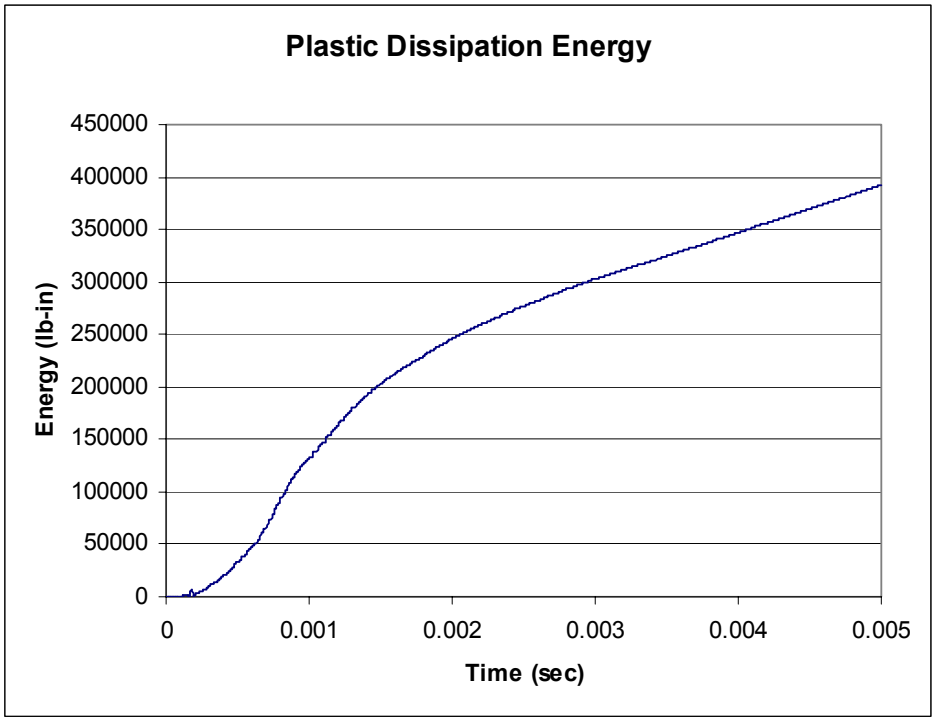
Plastic Dissipation Energy
Energy (lb-in)
450000
400000
350000
300000
250000
200000
150000
100000
50000
0
0
0.001
0.002
0.003
0.004
0.005
Time (sec)

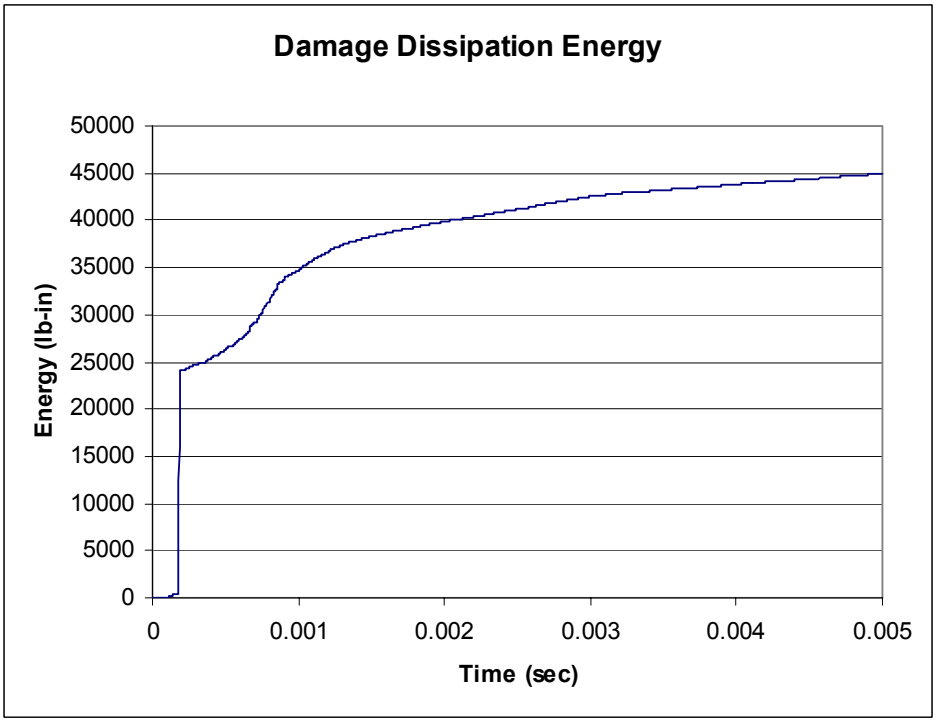
Damage Dissipation Energy
Energy (lb-in)
50000
45000
40000
35000
30000
25000
20000
15000
10000
5000
0
0
0.001
0.002
0.003
0.004
0.005
Time (sec)

D.4: BLAST ABOVE, CENTERED ON GIRDER

D.4.1. MAXIMUM PRINCIPAL PLASTIC STRAIN

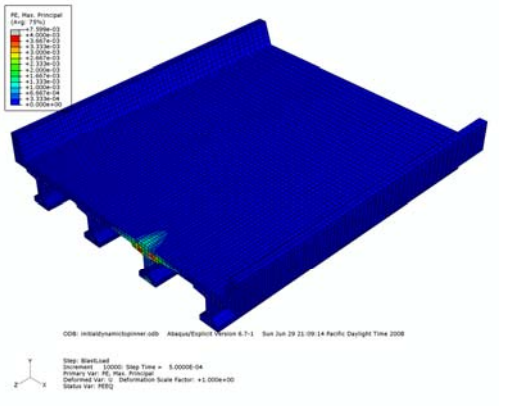

0.5 Milliseconds

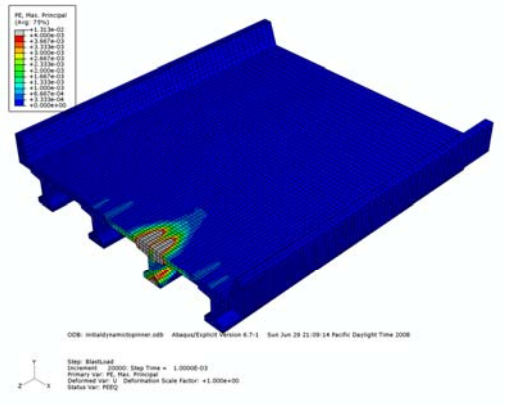

1.0 Milliseconds

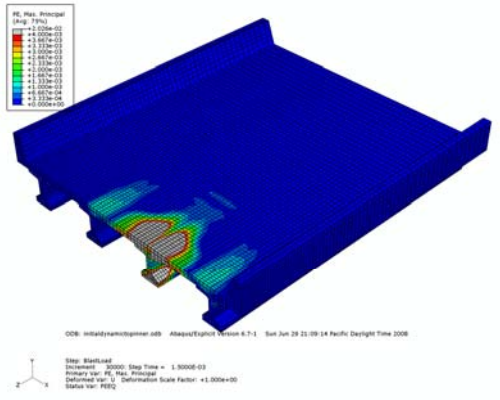

1.5 Milliseconds

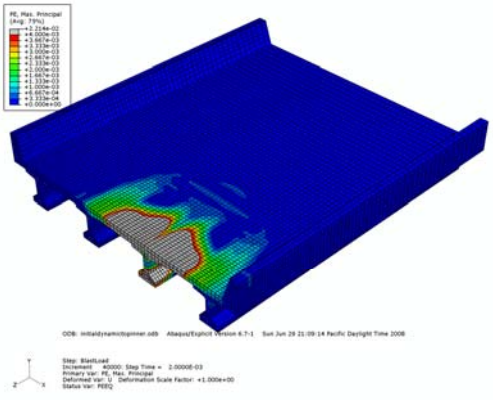

2.0 Milliseconds

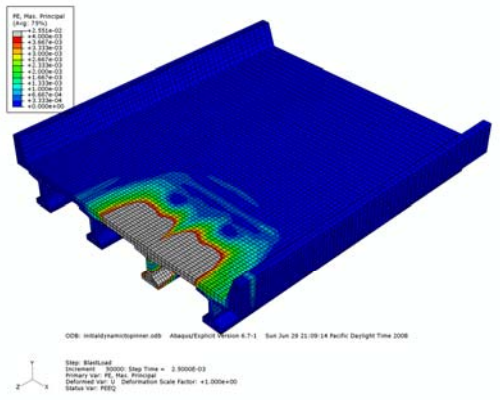

2.5 Milliseconds

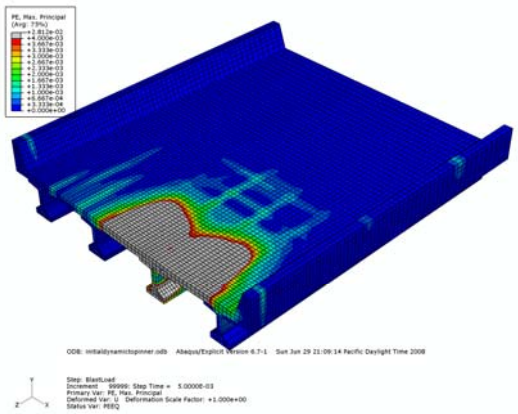

5.0 Milliseconds

D.4.2. STRAND STRESS, GIRDER BENEATH BLAST

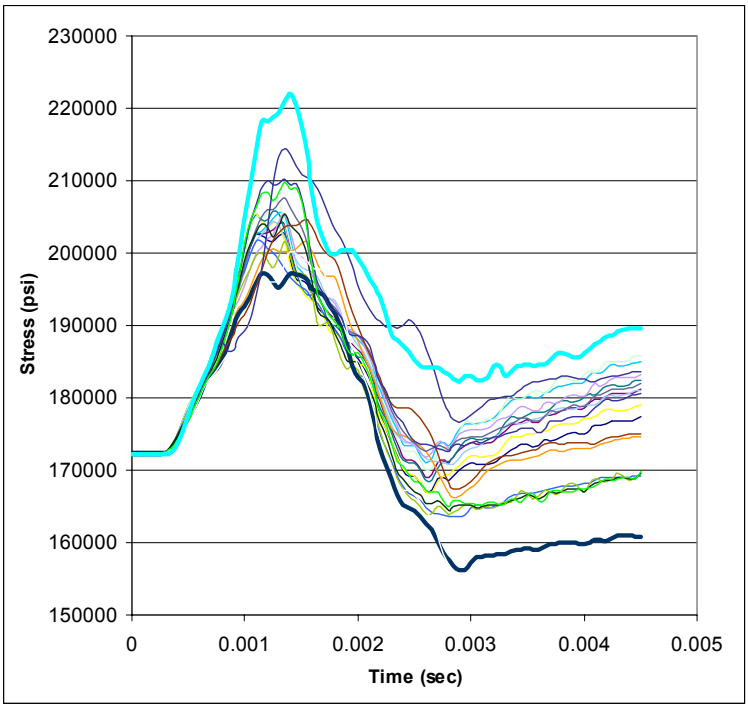

D.4.3. MODEL PARAMETERS

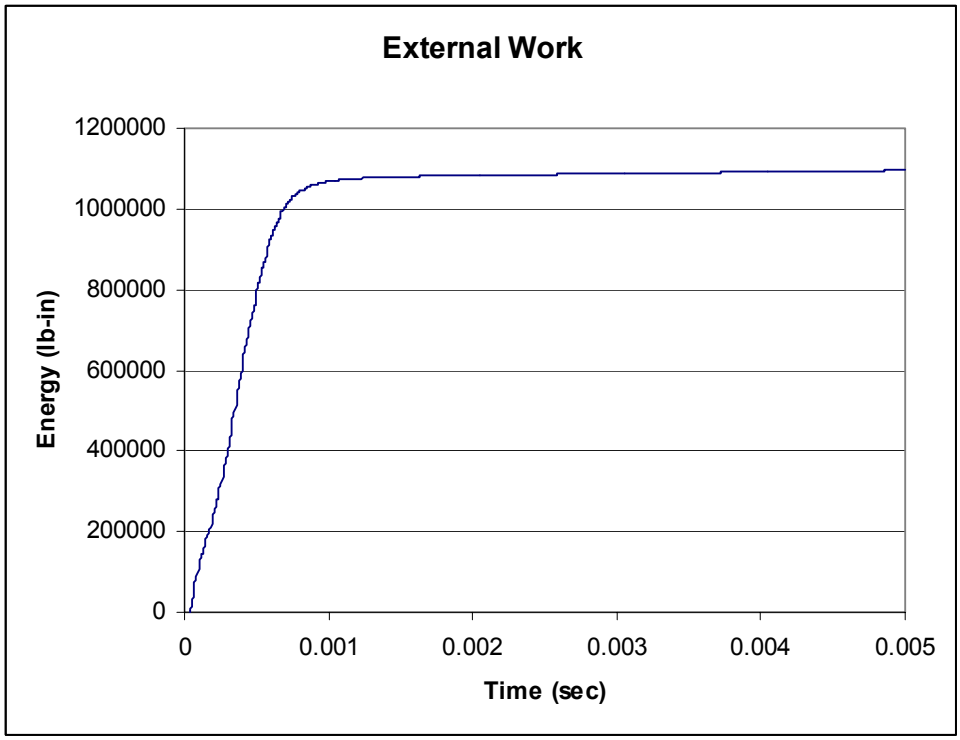

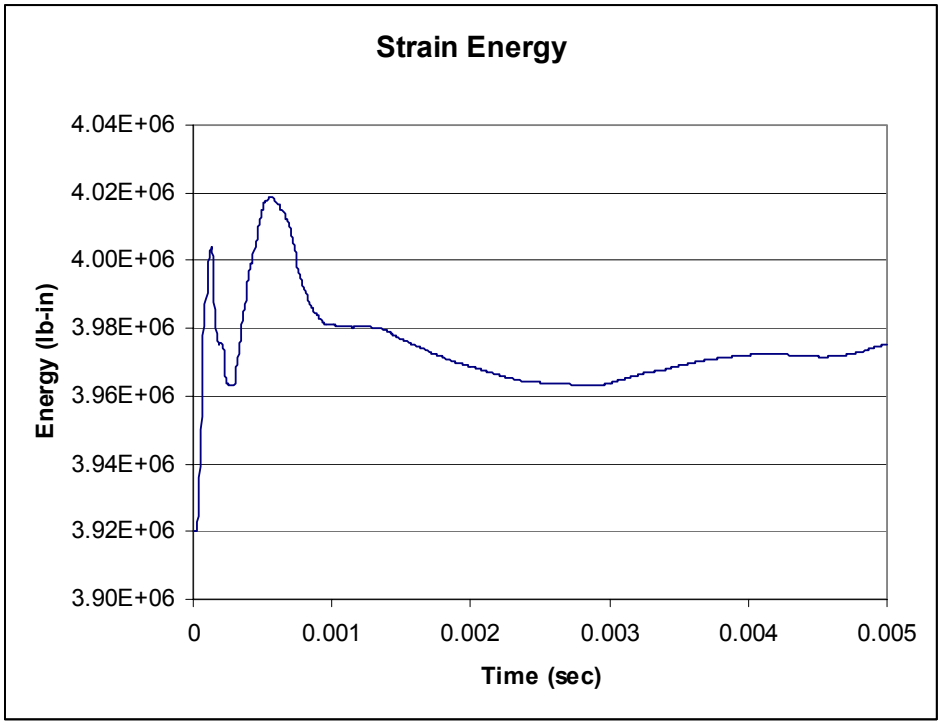
Strain Energy
4.04E+06
4.02E+06
4.00E+06
3.98E+06
3.96E+06
3.94E+06
3.92E+06
3.90E+06
Energy (lb-in)
0
0.001
0.002
0.003
0.004
0.005
Time (sec)

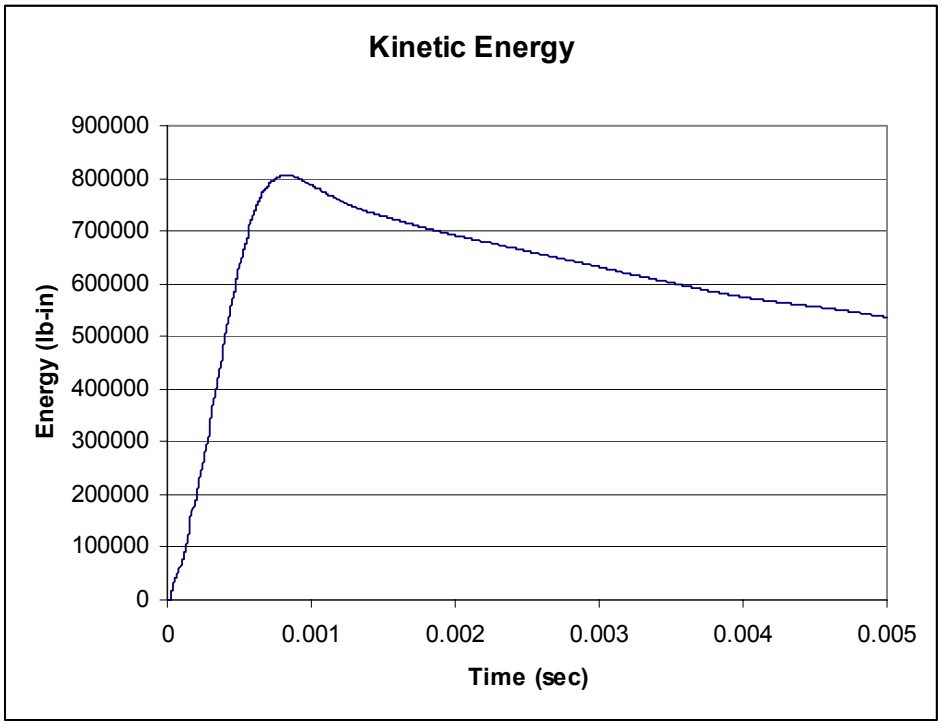
Kinetic Energy
900000
800000
700000
600000
500000
400000
300000
200000
100000
0
Energy (lb-in)
0
0.001
0.002
0.003
0.004
0.005
Time (sec)

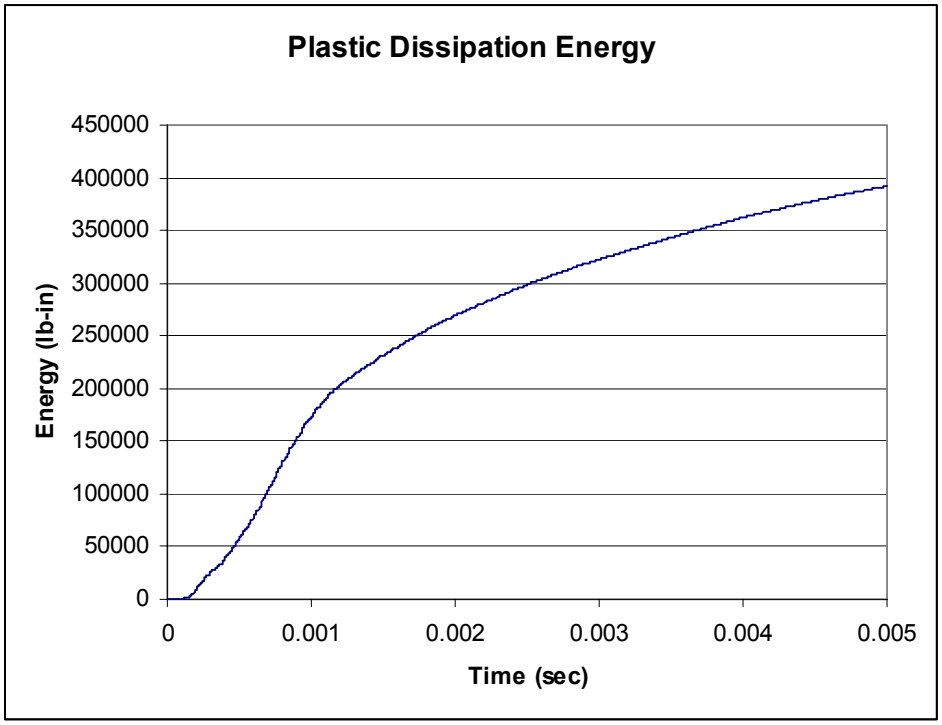
Plastic Dissipation Energy
Energy (lb-in)
450000
400000
350000
300000
250000
200000
150000
100000
50000
0
0
0.001
0.002
0.003
0.004
0.005
Time (sec)

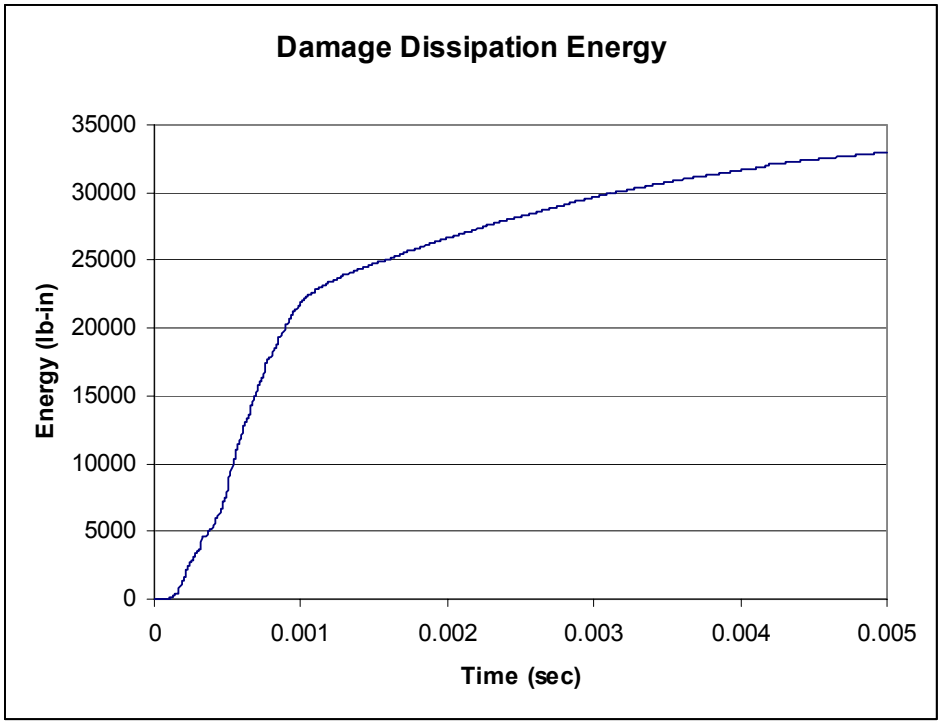
Damage Dissipation Energy
Energy (lb-in)
35000
30000
25000
20000
15000
10000
5000
0
0
0.001
0.002
0.003
0.004
0.005
Time (sec)

D.5: BLAST BELOW, BETWEEN GIRDERS

D.5.1. MAXIMUM PRINCIPAL PLASTIC STRAIN

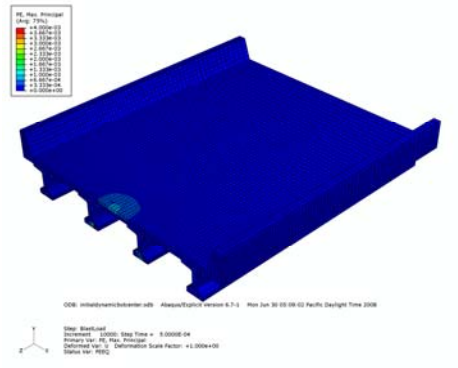

0.5 Milliseconds

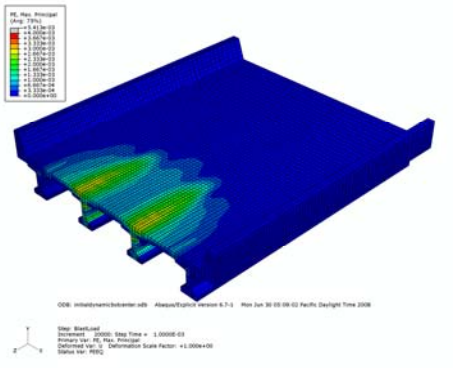

1.0 Milliseconds

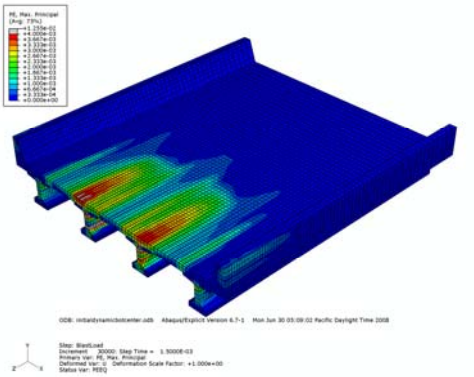

1.5 Milliseconds

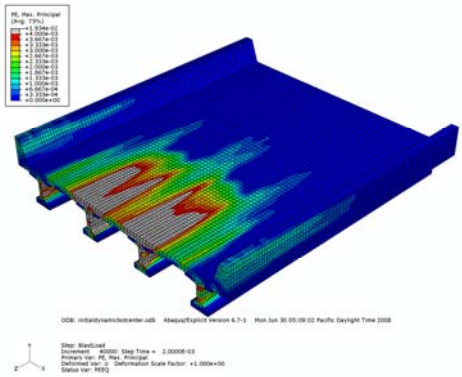

2.0 Milliseconds

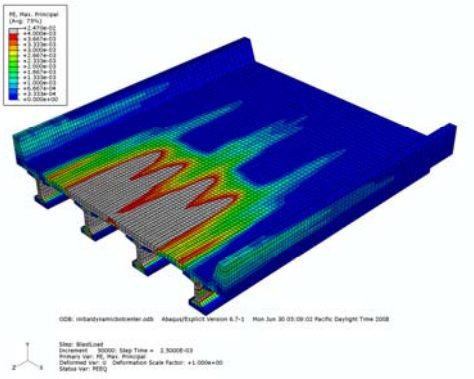

2.5 Milliseconds

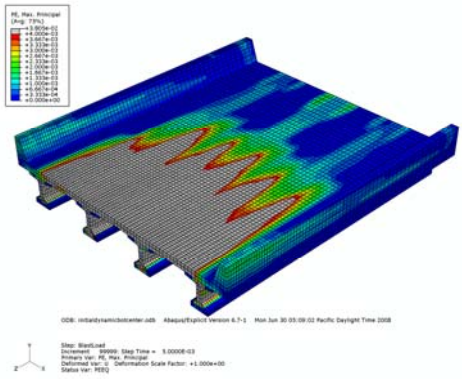

5.0 Milliseconds

D.5.2. STRAND STRESS, GIRDER ADJACENT TO BLAST

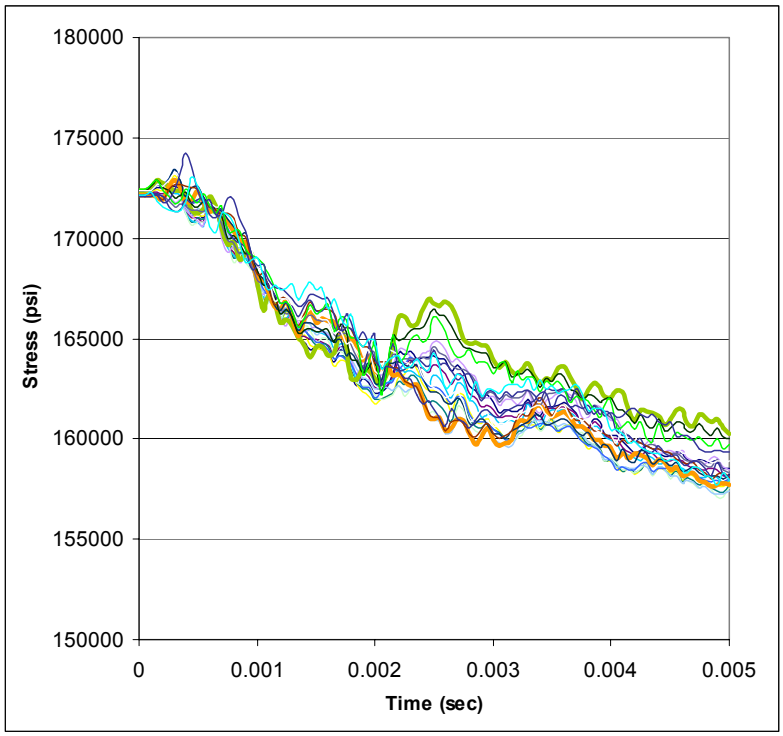

D.5.3. MODEL PARAMETERS

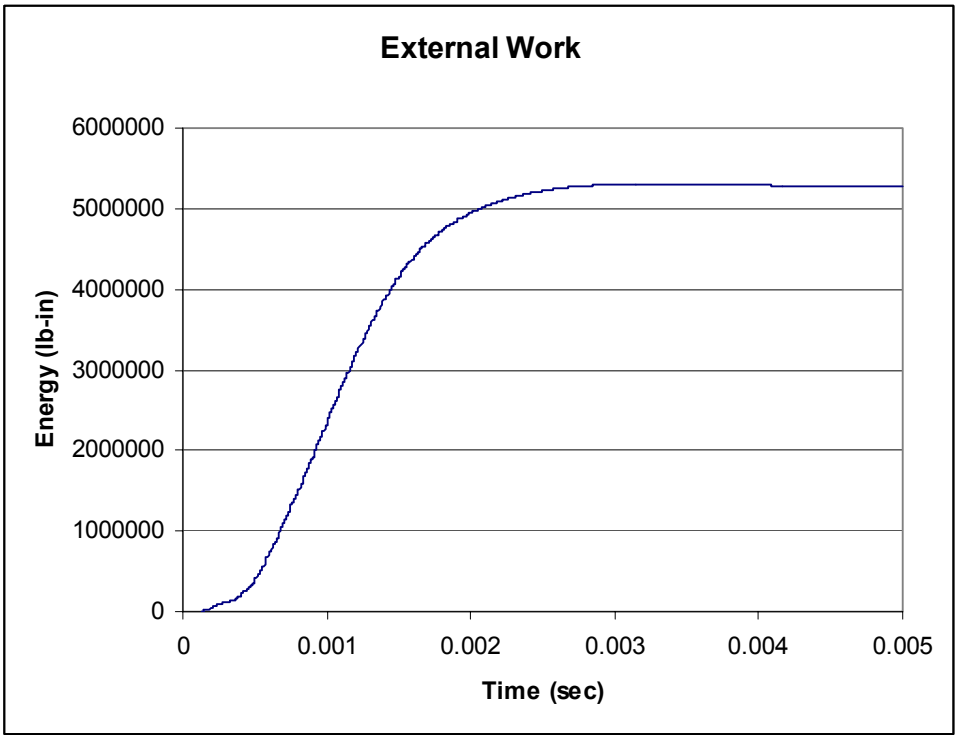

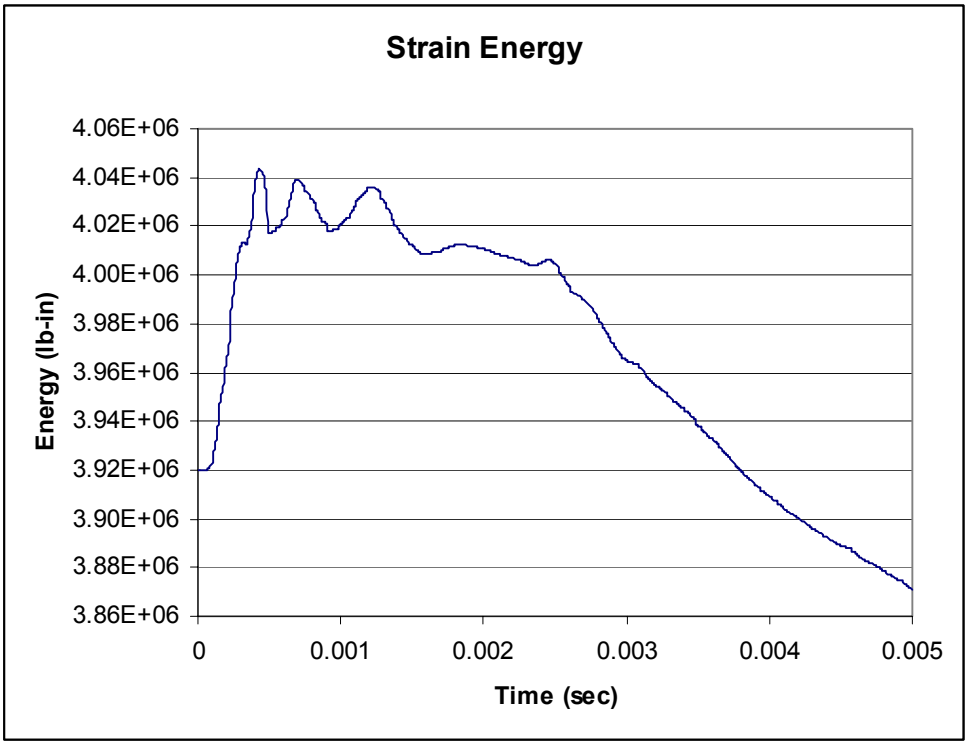
Strain Energy
4.06E+06
4.04E+06
4.02E+06
4.00E+06
3.98E+06
3.96E+06
3.94E+06
3.92E+06
3.90E+06
3.88E+06
3.86E+06
Energy (lb-in)
0
0.001
0.002
0.003
0.004
0.005
Time (sec)

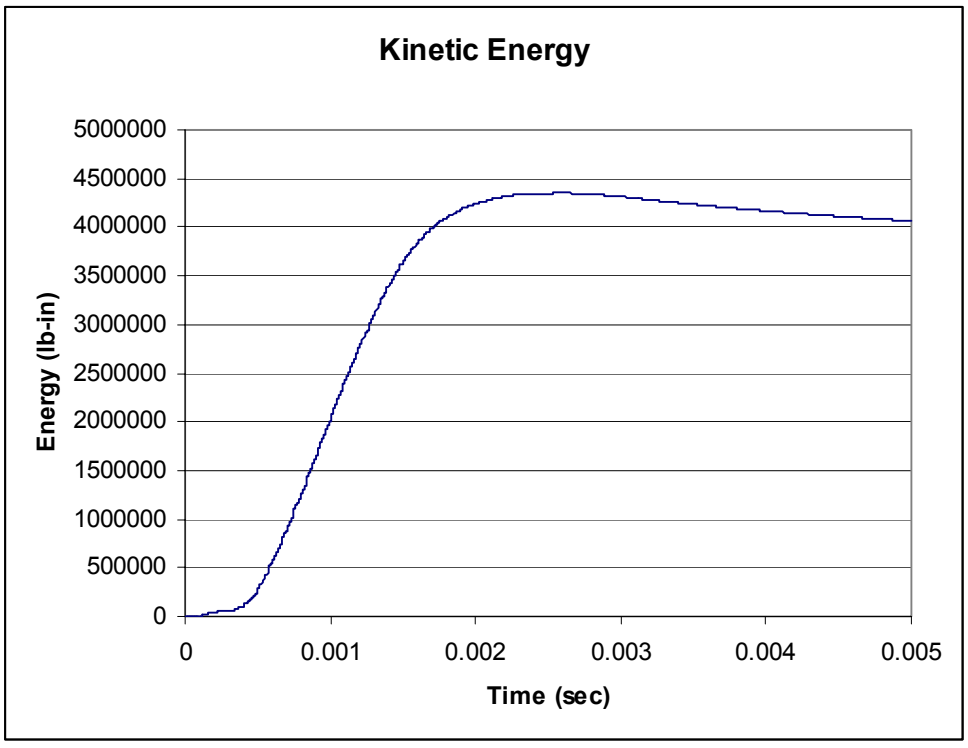
Kinetic Energy
5000000
4500000
4000000
3500000
3000000
2500000
2000000
1500000
1000000
500000
0
Energy (lb-in)
0
0.001
0.002
0.003
0.004
0.005
Time (sec)

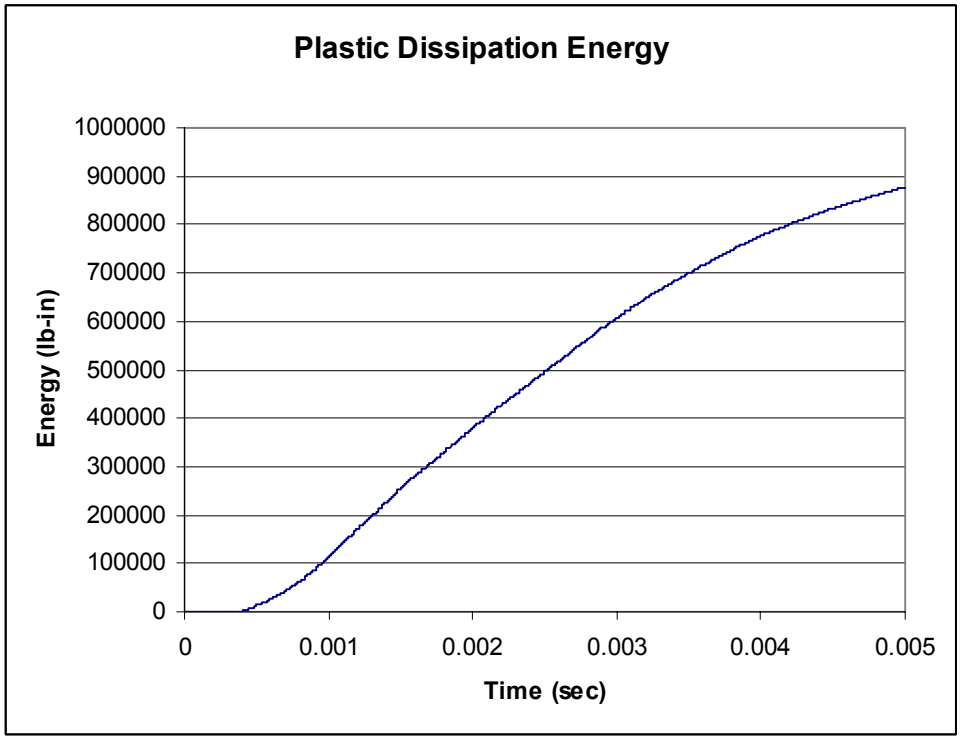
Plastic Dissipation Energy
Energy (lb-in)
1000000
900000
800000
700000
600000
500000
400000
300000
200000
100000
0
0
0.001
0.002
0.003
0.004
0.005
Time (sec)

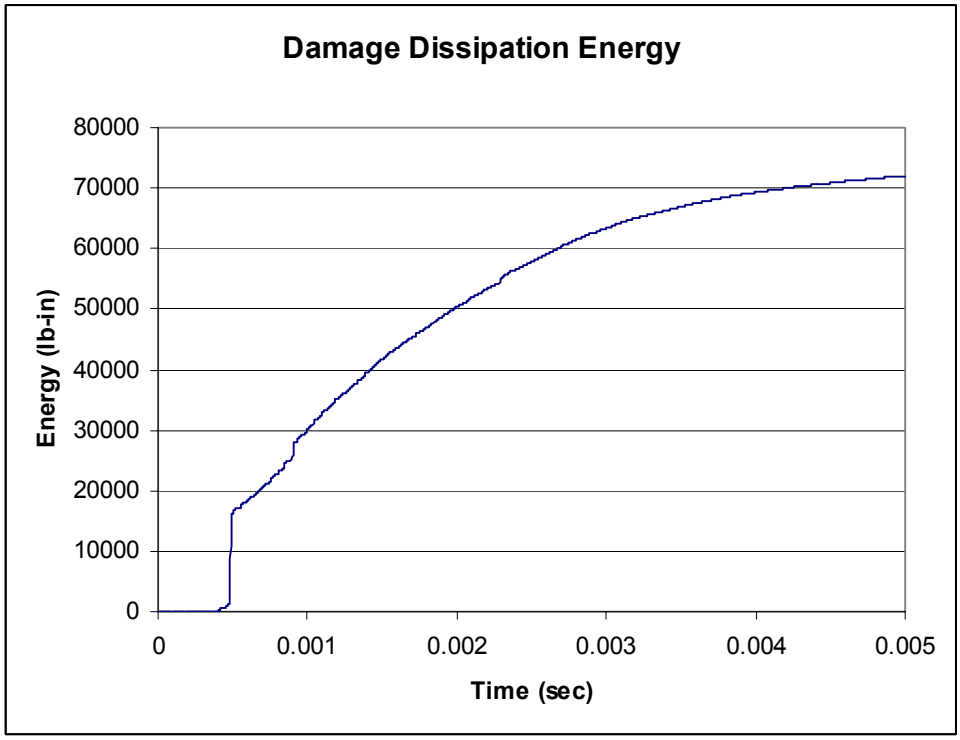
Damage Dissipation Energy
Energy (lb-in)
80000
70000
60000
50000
40000
30000
20000
10000
0
0
0.001
0.002
0.003
0.004
0.005
Time (sec)

D.6: BLAST BELOW, CENTERED ON GIRDER

D.6.1. MAXIMUM PRINCIPAL PLASTIC STRAIN

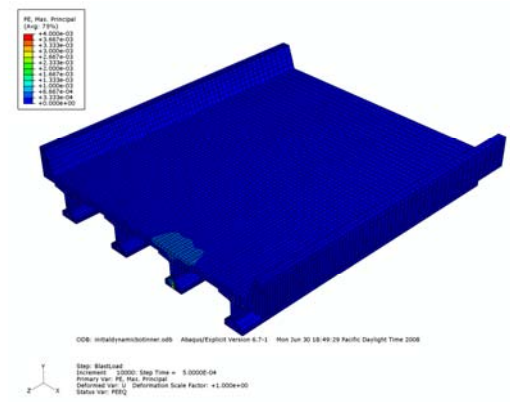

0.5 Milliseconds

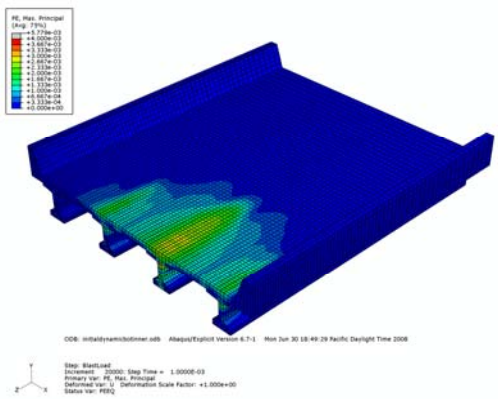

1.0 Milliseconds

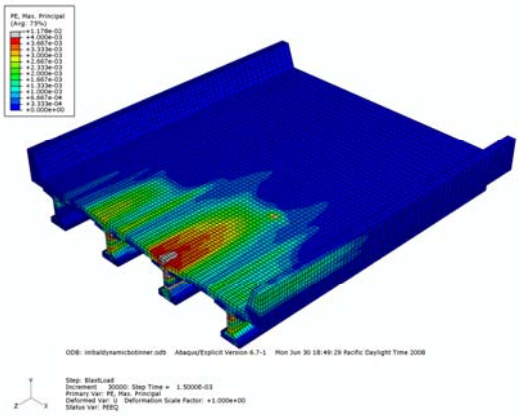

1.5 Milliseconds

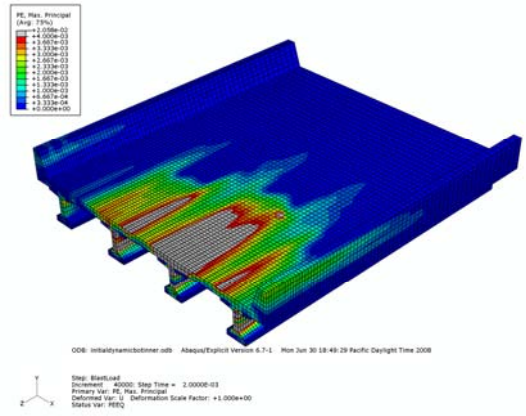

2.0 Milliseconds

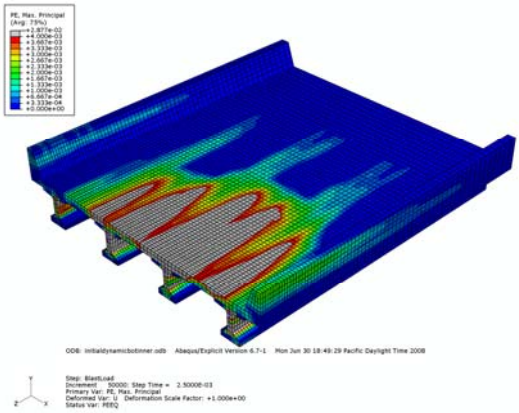

2.5 Milliseconds

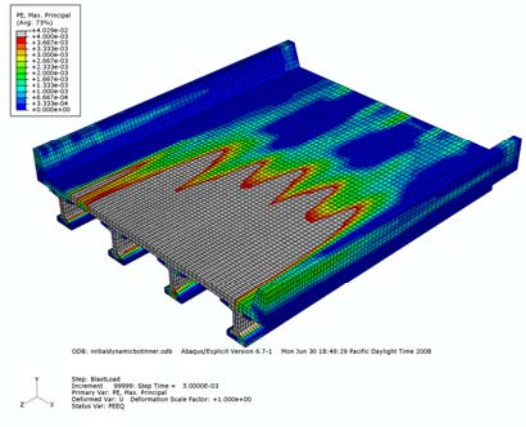

5.0 Milliseconds

D.6.2. STRAND STRESS, GIRDER ADJACENT TO BLAST

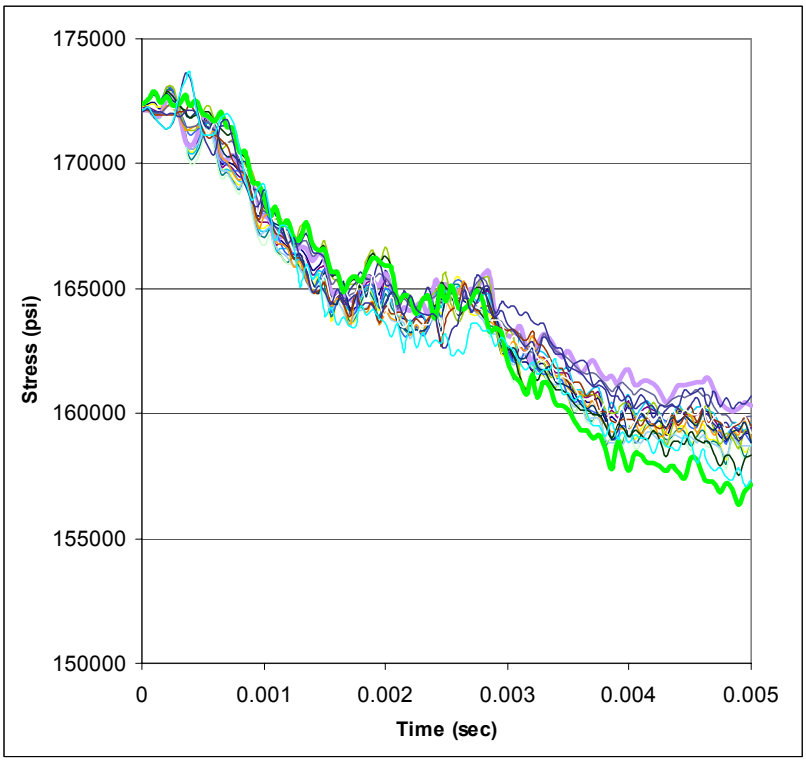

D.6.3. MODEL PARAMETERS

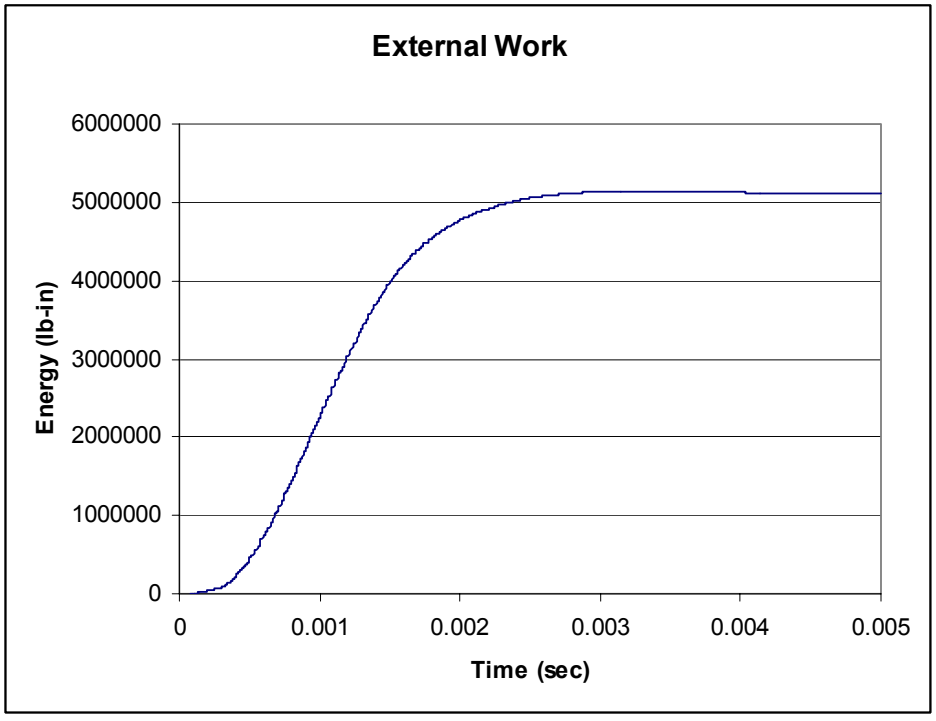

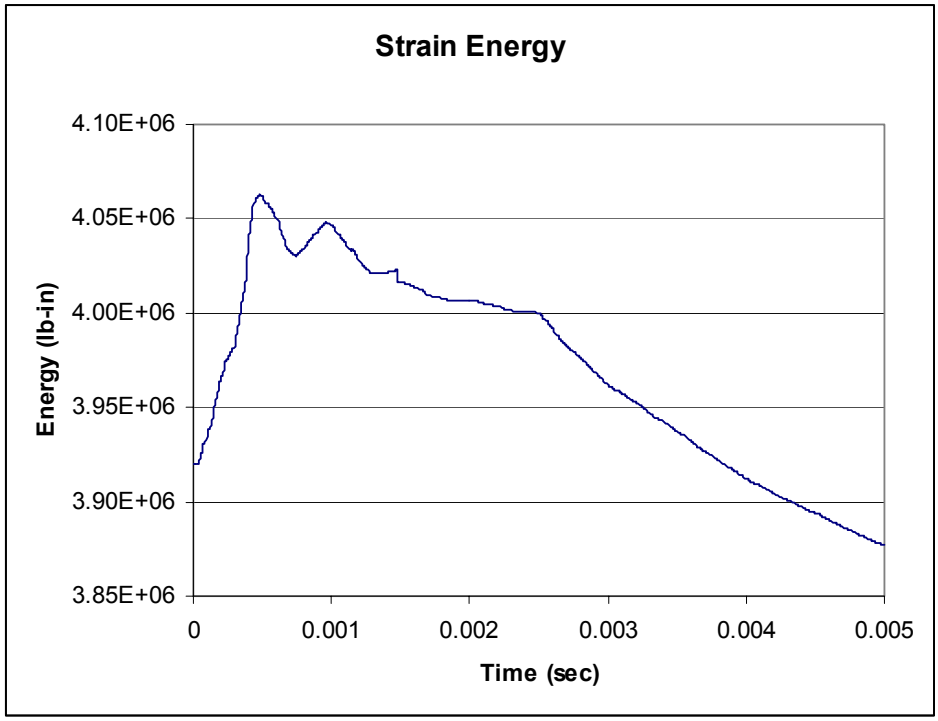
Strain Energy
4.10E+06
4.05E+06
4.00E+06
3.95E+06
3.90E+06
3.85E+06
Energy (lb-in)
0
0.001
0.002
0.003
0.004
0.005
Time (sec)

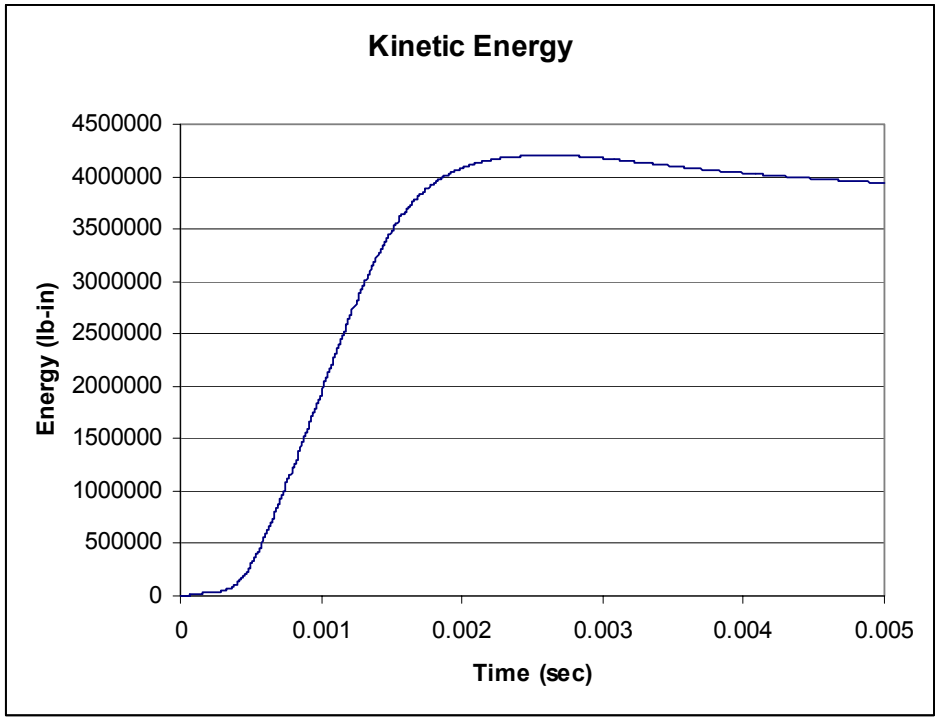
Kinetic Energy
4500000
4000000
3500000
3000000
2500000
2000000
1500000
1000000
500000
0
Energy (lb-in)
0
0.001
0.002
0.003
0.004
0.005
Time (sec)

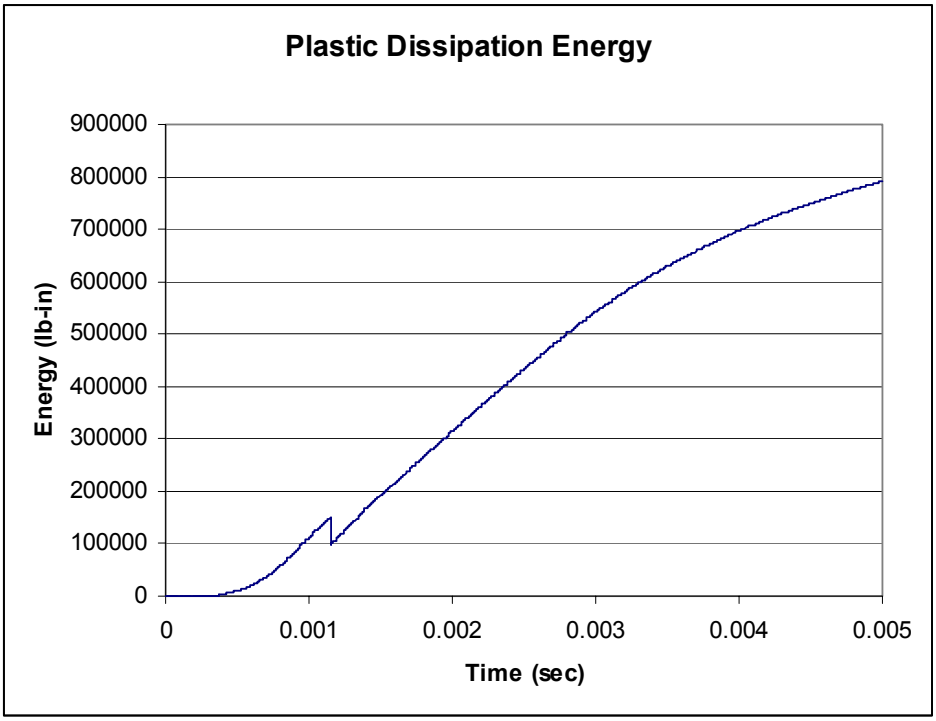
Plastic Dissipation Energy
900000
800000
700000
600000
500000
400000
300000
200000
100000
0
Energy (lb-in)
0
0.001
0.002
0.003
0.004
0.005
Time (sec)

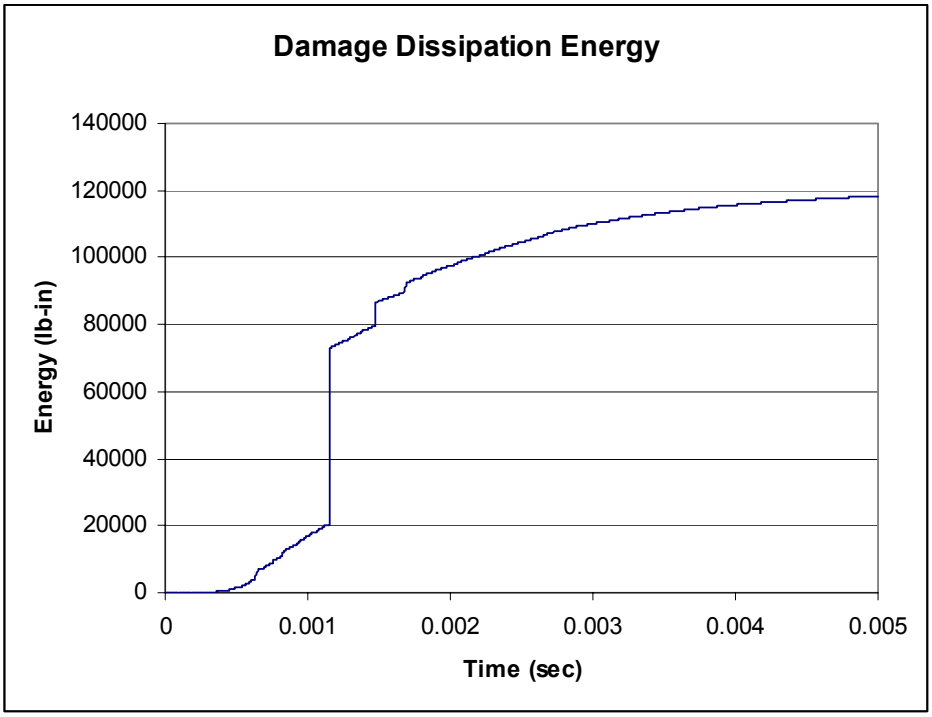
Damage Dissipation Energy
140000
120000
100000
80000
60000
40000
20000
0
Energy (lb-in)
0
0.001
0.002
0.003
0.004
0.005
Time (sec)

REFERENCES

1. Ertle, Chuck, James Ray, Bob Walker, and Sonny Johnson. (2008) "Explosive Tests of Precast, Prestressed Bridge Girders-DRAFT." U.S. Army Corp of Engineers, Vicksburg, MS.
2. Fang, Q., Q-H. Qian, and Y-L. Shi. (1996) "A Rate-Sensitive Analysis of R/C Beams Subjected to Blast Loads." *Structures Under Shock and Impact IV*, edited by N. Jones, C. A. Brebbia, and A. J. Watson, Computational Mechanics Inc., Billerica, Ma., 221-230.
3. Ishikawa, N., H. Enrin, S. Katsuki, and T. Ohta. (1998) "Dynamic Behavior of Prestressed Concrete Beams Under Rapid Speed Loading." *Structures Under Shock and Impact V*, edited by N. Jones, D. G. Talaslidis, C. A. Brebbia, and G. D. Manolis, Computational Mechanics Inc., Billerica, Ma., 717-726.
4. Ishikawa, N., S. Katsuki, and K. Takemoto. (2000) "Dynamic Analysis of Prestressed Concrete Beams Under Impact and High Speed Loadings." *Structures Under Shock and Impact VI*, edited by N. Jones and C. A. Brebbia, Computational Mechanics Inc., Billerica, Ma., 247-256.
5. Ishikawa, N., S. Katsuki, and K. Takemoto. (2002) "Incremental Impact Test and Simulation of Prestressed Concrete Beam." *Structures Under Shock and Impact VII*, edited by N. Jones, C. A. Brebbia, and A. M. Rajendran, Computational Mechanics Inc., Billerica, Ma., 489-498.
6. Magnusson, J. and M. Hallgren. (2004) "Reinforced High Strength Concrete Beams Subjected to Air Blast Loading." *Structures Under Shock and Impact VIII*, edited by N. Jones and C. A. Brebbia, Computational Mechanics Inc., Billerica, Ma., 53-62.
7. Marchand, K., E. B. Williamson, and D.G. Winget. (2004) "Analysis of Blast Loads on

Bridge Substructures." *Structures Under Shock and Impact VIII*, edited by N. Jones and C. A. Brebbia, Computational Mechanics Inc., Billerica, Ma., 151-160.

8. Stevens, David J. and Theodor Krauthammer. (1989) "Nonlinear Finite Element Analysis of Impulse Loaded RC Beams." *Structures Under Shock and Impact*, edited by P. S. Bulson, Elsevier Science Publishing Company Inc., New York, N.Y., 41-53.
9. Van Wees, R. M. M. and J. Weerheijm. (1989) "Simulation of Concrete Beams Under Explosive Loading with the Finite Element Method." *Structures Under Shock and Impact*, edited by P. S. Bulson, Elsevier Science Publishing Company Inc., New York, N.Y., 97-106.
10. Watson, A. J., B. Hobbs, and S. J. Wright. (1989) "Scaling Explosive Damage to Reinforced Concrete Beams and Slabs." *Structures Under Shock and Impact*, edited by P. S. Bulson, Elsevier Science Publishing Company Inc., New York, N.Y., 15-27.
11. Williamson, E. B. and D. G. Winget. (2005) "Risk Management and Design of Critical Bridges for Terrorist Attacks." *Journal of Bridge Engineering*, 10(1), 96-106.
12. Winget, D. G., K. A. Marchand, and E. B. Williamson. (2005) "Analysis and Design of Critical Bridges Subjected to Blast Loads." *Journal of Structural Engineering*, 131(8), 1243-1255.